# THE INFLUENCE OF WETTABILITY ON SCALING THE CAPILLARY PRESSURE-SATURATION RELATIONSHIP

by

Peter W. Burck

Submitted in partial fulfillment of
the requirements for the degree of
Master of Science in Hydrology

New Mexico Institute of Mining and Technology
Socorro, New Mexico

May 1993

**ABSTRACT**

The wettability of porous media is an important factor influencing groundwater contaminant migration and multiphase flow. To investigate the role of wettability in these situations, column displacement experiments were conducted to determine primary drainage and spontaneous imbibition curves for water-air, water-Soltrol 130, Soltrol 130-air systems.

Experiments using these fluid combinations were performed with clean, 50 $\mu$m soda-lime glass beads. The experiments were conducted using hydrophilic (untreated), hydrophobic (treated with Glassclad 18; GC-18) and intermediate-wet (treated with methyltrimethoxysilane; MTMS) glass beads.

Surface and interfacial tension measurements were made for the three fluid combinations. The water-air surface tension was 70.7 dynes/cm. The Soltrol 130-air surface tension was 22.6 dynes/cm. The interfacial tension between water and Soltrol 130 was 36.9 dynes/cm.

Advancing and receding contact angles were determined for the three fluid pairs using hydrophilic, hydrophobic, and intermediate-wet glass microscope slides. Advancing contact angles ranged from 6.5° for water and air on an untreated slide to 147.7° for water and Soltrol 130 (measured through the water) on a slide treated with GC-18. Receding contact angles ranged from 4.5° for water and air on an untreated slide to 112.3° for water and Soltrol 130

(measured through the water) on a slide treated with GC-18.

Using the capillary tube model, the drainage and imbibition curves were scaled according to the surface or interfacial tension and the contact angle of the fluids used. Except for problems attributed to experimental errors, the scaled curves for low (<50°) contact angle systems generally could be superimposed satisfactorily.

The results indicate that for low contact angle systems simple scaling gives reasonable prediction of the effects of wetting alteration on capillary pressure-saturation curves. However, the curves for intermediate and high contact angle systems did not scale well. This may indicate that the measured contact angle is not the effective angle for intermediate-wet and oil-wet systems. Furthermore the geometric features of the porous media (such as converging and diverging pores) are probably not adequately modelled by the capillary tube model. Therefore, using the capillary tube model to scale capillary pressure-saturation curves is flawed and should be avoided.

Scaling the capillary pressure-saturation function was also investigated using classical geometric corrections, including Melrose's (1965) curvature correction factor.

*Z* factors were calculated for the nine systems investigated.

**ACKNOWLEDGEMENTS**

Many people helped me with this thesis, and I thank them. In particular, I am indebted to my advisors, Drs. Robert Bowman, John Wilson, and Norman Morrow. Their guidance and generous sharing of knowledge and ideas benefitted me greatly.

I also wish to thank the various agencies who made this research possible for me by offering funding. The first year of this project was funded by the New Mexico Water Resources Research Institute and by the USGS under grant number 14-08-0001-G1657. Frank Wobber of The Department of Energy - Subsurface Science Program funded me during the second year under the project "Small scale laboratory studies of flow and transport phenomena in pores and fractures," under grant number DE-FG04-89ER 60829.

Drs. Kay Brower of the Chemistry Department and Jill Buckley of the Petroleum Resource Recovery Center assisted me with some of the chemistry and wettability issues.

I appreciate all of the students who offered advise, assistance, or showed me how to work some piece of equipment in the lab. I am grateful to Mike Wei, Grace Haggerty, Jiamin Wan, Paul Hofmann, Robert Mace, Anil Bagri, Susan Hoines and other Blob Lab personnel.

Thanks to Felix Barreras and John Reiche for their help in maintaining lab equipment. Thanks to Edith Montoya, Loretta Murillo, and Pat Mills for their assistance.

Finally, thanks to my family for their support.

## TABLE OF CONTENTS

## LIST OF ILLUSTRATIONS

## LIST OF TABLES

## LIST OF NOTATION

| | |
|---|---|
| $P_c$ | capillary pressure |
| $r$ | radius of capillary tube or mean particle radius |
| $R$ | average radius of meniscus |
| $Z$ | curvature correction factor |

Greek Symbols

| | |
|---|---|
| $\rho$ | density |
| $\sigma$ | surface and interfacial tension |
| $\Theta$ | contact angle |
| $\mu$ | micro- |

# CHAPTER 1

# INTRODUCTION AND BACKGROUND

## 1.1 INTRODUCTION AND OBJECTIVES

Wettability is an important consideration in multiphase flow, groundwater contaminant migration, and hazardous waste site remediation. The motivation for this research was to gain a better understanding of the role of wettability in these situations (Bowman and Wilson, 1988).

Wettability refers to the affinity of one fluid for a solid surface in the presence of another immiscible fluid. For instance, pure water spreads on or wets a clean hydrophilic surface such as glass, but tends to "bead up" on a nonwetting or hydrophobic surface. Generally most subsurface porous materials are assumed to be water-wet. However, a range of wettabilities are possible in situations such as spill sites where polar organic compounds have adsorbed to the porous medium or where surfactants are present.

One of the fundamental relationships governing the distribution of fluids in porous media is the capillary pressure-saturation relationship. Capillary forces separate fluids into distinct locations in a porous material, typically moving wetting phases through the smaller pores, while causing nonwetting phases to pass through the larger pores. Thus, the capillary pressure-saturation relationship is important for modelling and remediation purposes. The capillary pressure-saturation relationship varies

considerably for systems with different fluids, pore sizes, and for systems with different wettability. Unfortunately, determining the capillary pressure-saturation relationship for different systems by conventional column methods often is time-consuming because of the potential for long equilibration times between measurements. Therefore, it would be desirable to have a method of predicting the capillary pressure-saturation relationship for different fluids and porous materials. A promising method of estimating one capillary pressure-saturation relationship from another is through scaling.

The primary objective of this research was to determine whether simple scaling of capillary pressure-saturation curves can be accomplished using the capillary tube model. The idea of scaling capillary pressure-saturation functions was originally investigated by Leverett (1941). Our hypothesis was that scaled capillary pressure-saturation curves are identical (ie. they match well when superimposed) for different fluids and different wetting properties of the porous medium. Thus the goal of this research was to select a grain size and conduct a total of nine types of column displacement experiments.

The experiments involved three fluid pairs:

- water - air
- water - Soltrol 130
- Soltrol 130 - air

Soltrol 130 is a common laboratory fluid consisting of a mixture of $C_{10}$ to $C_{13}$ isoparaffins and is manufactured by Phillips Petroleum Inc., Bartlesville, OK. Soltrol is less dense than water (0.753 g/cc), has a low volatility, and is essentially immiscible in water. The water used in the experiments was purified and is described in detail in the next chapter. The column experiments were performed using hydrophilic (untreated), hydrophobic (treated with Glassclad 18; GC-18), and intermediate-wet (treated with methyltrimethoxysilane; MTMS) glass beads. To support the column experiments, surface tension, interfacial tension, and contact angle measurements were performed. Finally, the capillary pressure-saturation curves were scaled using the capillary tube model.

The Young-Laplace equation is one of the solutions to the Laplace equation for capillarity. The Young-Laplace equation is given by (Adamson, 1982):

$$P_c = \sigma_{L_1 L_2} \left( \frac{1}{R_1} + \frac{1}{R_2} \right) \qquad (1)$$

where $P_c$ is the capillary pressure or the difference between the wetting and nonwetting fluids,

$\sigma L_1 L_2$ is the interfacial tension between the wetting and nonwetting fluids, and

$R_1$ *and* $R_2$ are the principal radii of curvature of the meniscus.

When this equation is related to the capillary tube model,

the meniscus is spherical and the principal radii of curvature, $R_1$ and $R_2$, are equal. The radius of curvature of the meniscus $R$ is equal to $r/cos\ \theta$, where $r$ is the radius of the capillary tube and $\theta$ is the contact angle between the fluid and the tube. Incorporating these relationships yields the capillary tube model (Equation 2), which relates the capillary pressure to the interfacial tension of the fluids, the contact angle of the system and the radius of the capillary tube.

$$P_c = \frac{2\ \sigma\ \cos\ \theta}{r} \qquad (2)$$

where $\theta$ is the contact angle of the system, and

$r$ is the radius of the capillary tube.

This equation has been used to model capillary pressure in porous media by treating the porous media as a bundle of capillary tubes. Our goal was to determine whether this model is appropriate for scaling the capillary pressure-saturation curves of systems with a range of wettabilities.

Scaling of the capillary pressure-saturation function was investigated using different particle sizes and classical geometric corrections, including Melrose's (1965) $Z(\theta)$ curvature correction factor. $Z$ factors were calculated for the nine systems investigated.

## 1.2 BACKGROUND

This section provides brief background on wettability

measurement and classification, surface and interfacial tension and capillary pressure-saturation measurements.

What is Wettability?

In hydrology and the petroleum industry the wettability of an object or surface refers to its tendency to be wetted by or repel a fluid. As the terms indicate, water-wet or hydrophilic surfaces are wetted by water. For example, in air a drop of water spreads out on a clean hydrophilic surface such as glass. In this case the water is the wetting fluid, and the air is the nonwetting fluid. Oil-wet or hydrophobic surfaces such as polytetrafluoroethylene (Teflon) are wetted by oil. When a drop of oil is placed on Teflon in air, the oil is the wetting fluid, and the air is the nonwetting fluid again. Surfaces that display no particular preference for water or oil are neutral or intermediate-wet. Clean steel is typically intermediate-wet (Koorevaar, et al., 1983). Photographs of low, intermediate, and high contact angles are shown in Figures 3.1 through 3.6.

Aquifer materials encountered in hydrology are normally hydrophilic. Most of these materials contain significant amounts of silicates and carbonates which are generally water-wet. In some cases aquifer materials may be rendered hydrophobic. This may occur when surfactants are present or when polar organic molecules such as resins or asphaltenes are bonded to or adsorbed onto subsurface materials. Soils

encountered in agriculture are typically hydrophilic. However, sometimes soils near the ground surface are rendered water repellent. This hydrophobicity occurs as the result of fire, microbes, fungi, algae, humic coatings, or plant remnants (Wilson, 1988; Dekker, 1992). The water-repellency of agricultural soils generally decreases with depth until the soils are water-wet again.

Petroleum reservoir materials are often characterized by mixed wettability. This means that some reservoir materials are hydrophilic, others are hydrophobic and the remainder are somewhere in between the extremes. The wettability state of such materials often is controversial.

The wettability of a surface can be altered artificially in a laboratory using compounds such as organosilanes. This alteration can be conducted either in the aqueous phase (eg., Wei, et al., 1993) or the vapor phase (Fenimore, et al., 1976 and Takach, et al., 1988). The stability of organosilane-altered surfaces varies considerably, from surfaces that degrade almost immediately (especially by hydrolysis in water) to those that remain relatively stable for at least 1000 hours (Wei, et al., 1993).

Measuring Wettability

The common method of characterizing the wettability of flat smooth solid surfaces is through the contact angle. Both advancing and receding contact angles can be

determined. The difference between these two values is known as the contact angle hysteresis.

Contact angles can be measured using several methods. Among these are the static and dynamic sessile drop methods, the Wilhelmy plate method, and the axisymmetric drop shape method (ADSM). In their simplest forms the sessile drop methods can be used to measure directly the contact angle made by a drop of fluid such as water on a flat surface. The dynamic sessile drop method was used in this research and is described in further detail in the next chapter.

The Wilhelmy plate method involves partially submerging a flat surface such as a glass slide into a fluid and measuring the angle between the slide and fluid. Both advancing and receding angles can be determined.

The axisymmetric drop shape method uses video equipment to photograph sessile drops and pendant drops of a fluid (Rotenberg, et al., 1983). The image is analyzed by a computer program which selects several points on the outside edge of the drop. The data are used to calculate the surface tension and contact angle through numerical integration of the Laplace equation of capillarity.

Contact angles are larger when a fluid is advancing against a solid, and are smaller when the fluid is receding. As mentioned earlier, the difference is known as the contact angle hysteresis. Contact angles and contact angle hysteresis are affected by several factors including surface

roughness and surface heterogeneities. Some surfaces on which contact angles can be measured are not completely smooth. The surface roughness will alter the apparent contact angle. Angles greater than 90° will appear somewhat larger, whereas angles less than 90° will seem smaller.

Surface heterogeneities refer to such features as imperfections in the material, compounds adsorbed onto the surface and the presence of other contaminants. These conditions also influence the contact angle. For instance, a hydrophilic slide will show an increase in the water-air contact angle when organic compounds are adsorbed onto it.

The average or bulk wettability of a porous medium such as sand or glass beads also can be measured in several ways. One method is the water drop penetration time test (Dekker, 1992). This simple procedure involves the placement of three drops of water on a sample. The length of time required for the drops to penetrate the sample is recorded. In some cases, the drops may penetrate in less than five seconds, indicating the sample is strongly water-wet. At the other extreme, the drops of water may not have penetrated a strongly hydrophobic sample after 3600 seconds or more.

Other tests for average wettability of porous materials are the alcohol percentage (Dekker, 1992), the Amott (Amott, 1959) and USBM (Donaldson, et al., 1969) tests.

Wettability Classifications

When the contact angle between a surface and a fluid (measured through the fluid) is low (near 0°), the surface is wetted by the fluid. High angles (those close to 180°) indicate the fluid is non-wetting. Angles near 90° are neutral or intermediate-wet. Several wettability classifications have been proposed. Anderson's (1986b) summary of wettability classifications is given below in Table 1.1.

Table 1.1 Wettability Classification (After Anderson, 1986b)

| CONTACT ANGLE IN DEGREES | HYDROPHILIC | INTERMEDIATE | HYDROPHOBIC |
|---|---|---|---|
| LOWEST | 0° | 60-75° | 105-120° |
| HIGHEST | 60-75° | 105-120° | 180° |

Surface and Interfacial Tension

In this research the surface or interfacial tension refers to fluid-fluid properties such as those at vapor-liquid or liquid-liquid interfaces. These values are relatively easy to measure. However, the term interfacial tension also applies to fluid-solid interfaces, the values for which are more difficult to measure directly. Interfacial tension and contact angles are related through Young's equation (Hillel, 1980).

$$\sigma_{gs} = \sigma_{sl} + \sigma_{lg}\cos\theta \qquad (3)$$

where $\sigma_{gs}$ is the interfacial tension between the gas and

solid,

$\sigma_{sl}$ is the interfacial tension between the solid and liquid,

$\sigma_{lg}$ is the surface tension between the liquid and gas, and

$\Theta$ is the contact angle.

Several methods are available to determine surface and interfacial tension. One of the commonly used methods, the pendant drop, was developed by Andreas, et al., (1938). The pendant drop method uses the shape of a drop to determine the interfacial tension.

Another method involves the ring tensiometer (du Nouy, 1919), which was used to determine surface and interfacial tensions in this research. The method involves placing a ring of known dimensions in a fluid and measuring the force needed to pull the ring through an interface with another fluid.

Capillary Pressure-Saturation Relationship

Considerable research has been conducted in the past to determine capillary pressure-saturation relationships. One of the early works on the topic was conducted by Haines (1930). Figure 1.1 shows a typical drainage-imbibition curve, as well as some of the scanning curves between them. The figure shows the main features of the capillary pressure-saturation relationship. Initially the experiments are 100% saturated with the wetting fluid and are at zero

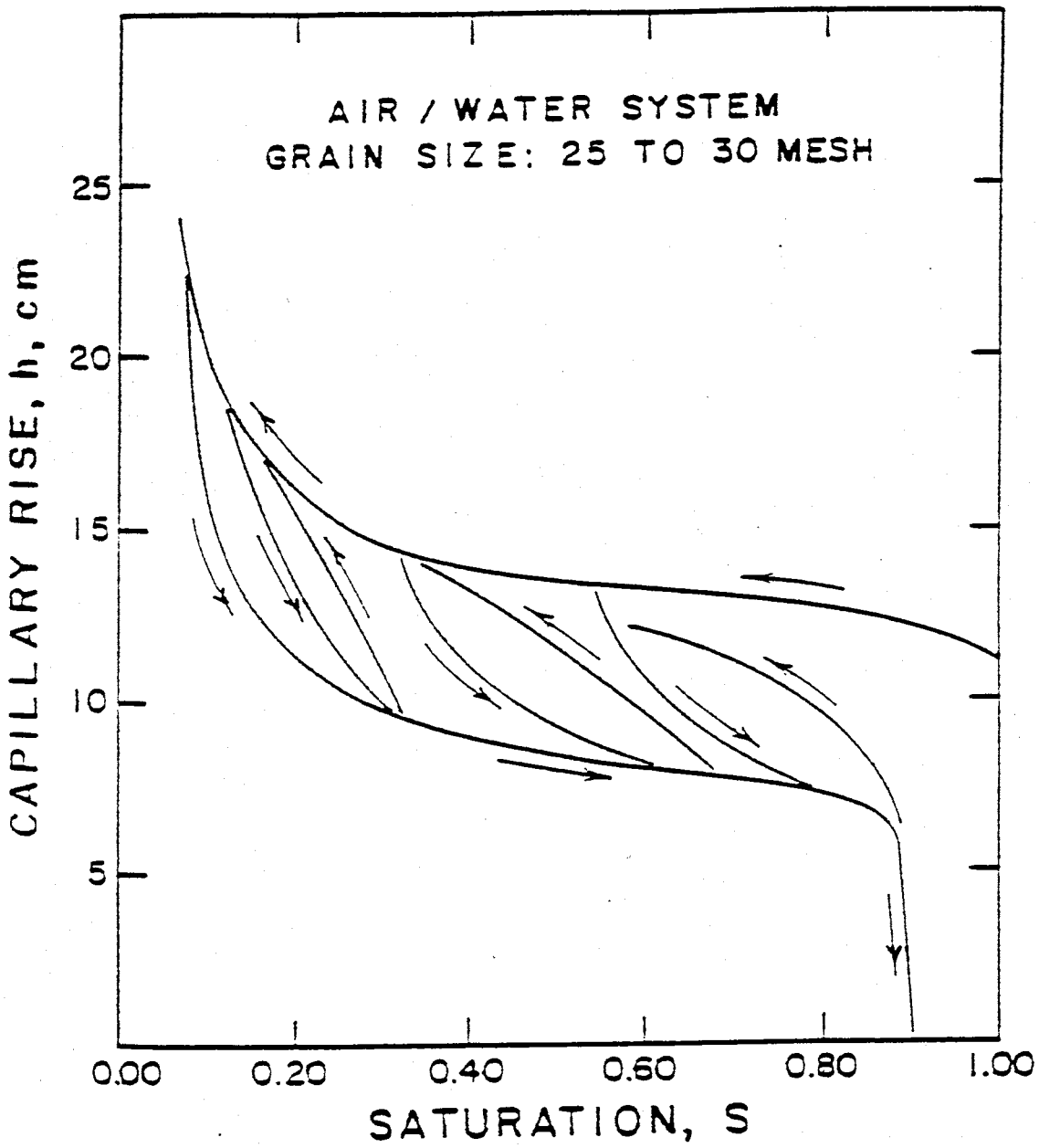


Figure 1.1: A typical capillary pressure-saturation curve (after Haines, 1930, from Melrose, 1965)

pressure. The pressure increases without much of a reduction in saturation until the non-wetting fluid entry pressure of the system is reached. Then the porous medium begins to drain and generally drains steadily until a residual wetting phase saturation is reached. This is typically in the range of 5 to 10%. At this point as the pressure continues to increase, there is no longer any appreciable loss of wetting fluid. This is the end of the drainage curve. To obtain the imbibition curve, the pressure is lowered. At first as the pressure decreases there is no substantial increase in saturation. Then gradually, the pressure reaches a level where the wetting fluid reenters the porous material. This process continues until no more wetting fluid can enter the porous material. Then for each additional decrease in the capillary pressure, no more wetting fluid can move into the porous material. This typically occurs at 85 to 90% saturation. The remaining 10 to 15% of the pore space is taken up by the nonwetting phase that has become trapped by capillary forces. If desired, the drainage procedure can be repeated from the end of the imbibition process. As the pressure is increased a second time, a secondary drainage curve can be obtained.

When they are plotted together, there is a difference between the location of the drainage curve and the imbibition curve, which is caused by the hysteretic

properties of the porous medium. The drainage curve is above the imbibition curve.

Other work involving the capillary pressure-saturation relationship has been done by Wilson et al., (1990), Bowman, et al., (1992), Mace (1990), Wei (1991), Wei, et al., (1993), Lenhard and Parker (1987), Demond (1988), Demond and Roberts (1991), Morrow and McCaffery (1978), Purcell (1949), Purcell (1950), Melrose (1965) and numerous others.

# CHAPTER 2

# PROCEDURES AND MATERIALS

This chapter presents the methods and materials used to alter the wettability of glass surfaces, measure contact angles on glass slides, determine surface and interfacial tension, perform capillary pressure-saturation experiments, and scale capillary pressure-saturation curves with the capillary tube model.

The water used in the following experiments was purified by a two-step process. First, water from the municipal system was purified by reverse osmosis (RO) using a Millipore Milli-RO Plus system (Millipore, Bedford, MA). This water was purified further by a Millipore Milli-Q Plus water purification system to produce deionized, Type I, reagent-grade water (hereafter referred to as "water"). The resistivity of this ultrapure water was 18 megohm/cm.

In some situations such as rinsing procedures, RO water was used in place of the ultrapure water.

## 2.1 Wettability Alteration Techniques

This section describes the methods used to prepare glass slides for contact angle measurements and glass beads for capillary pressure-saturation experiments.

### Cleaning glass slides

The first step in characterizing the wettability of a glass slide was to clean the surface. Corning soda-lime

glass microscope slides (Micro Slides No. 2947) were used as the substrates. The chemical composition of the slides is provided in Appendix A. To prepare clean slides, we followed procedures developed by Menawat, et al., (1984) and modified by Wei, et al., (1993). These procedures are summarized here.

Several slides were cut in half with a glass cutter to a size of approximately 1" x 1.5" and positioned in a machined Teflon block. The Teflon block was placed in a beaker with enough 2-butanone (methyl ethyl ketone, MEK) to cover the slides, and the slides were cleaned for 20 minutes in an ultrasonic bath. This procedure was intended to dissolve any organic contaminants on the glass surface. The 2-butanone was decanted to a waste bottle.

The residual 2-butanone was rinsed off the glass with deionized water. This was accomplished by adding water to the beaker and placing the beaker in the ultrasonic bath for several minutes. The rinse procedure was repeated five times.

To remove any inorganic contaminants from the slides, they were soaked in hot (70° C) nitric acid ($HNO_3$) for 20 minutes. The nitric acid was decanted, and the water rinsing procedure described above was repeated to remove residual nitric acid from the slides.

In earlier experiments the slides were dried for several hours or overnight in an oven set at 100° to 110° C.

However, in later experiments slides were allowed to air-dry. The oven drying procedure was discontinued when it became evident that the low contact angle (< 20°) normally associated with a clean, untreated, water-wet slide was not being obtained. This discovery led to the hypothesis that the slides were adsorbing contaminants during the oven-drying step. So far, however, this hypothesis has not been verified.

These clean glass slides were used in the hydrophilic contact angle experiments.

Preparing hydrophobic glass slides

Clean glass slides were rendered hydrophobic by applying a solution of GC-18, a 20% active octadecylsilane derivative (an 18 carbon alkoxysilane) in a t-butanol solution and diacetone alcohol. GC-18 is manufactured by Hüls America (formerly Petrarch). The application procedure was the same as Wei, et al., (1993) and was from the Hüls America catalog entitled Silicon Compounds Register and Review (1991). A 1% solution by volume was prepared using 2 mL of GC-18 in 198 mL of water. This solution was mixed with a Teflon stirbar for about 2.5 minutes before being poured over the slides. The whole beaker was placed in an ultrasonic bath for another 2.5 minutes. The GC-18 solution was decanted, and the procedure was repeated a total of ten times to ensure complete surface coverage. Finally, the slides were placed in an oven at about 100° C for several

minutes to cure.

To determine the appropriate number of GC-18 treatments, an experiment was performed in which the contact angle was measured after each of ten treatments with GC-18. The results of this experiment, CAM08, are included in section 3.1 and illustrate the increase in contact angle with each successive treatment up to about the fifth treatment whereafter the contact angle remained relatively stable.

The precise chemical composition of GC-18 is a trade secret, so the exact reaction mechanism is not known. However, the general reaction mechanism for an alkoxysilane with glass involves an initial hydrolysis of the alkoxysilane to yield alcohol (methanol) and highly reactive intermediate silanol products (Arkles, et al., 1991).

$RSi(OCH_3)_3 + 3\ H_2O \rightarrow Rsi(OH)_3 + 3\ CH_3OH$ (hydrolysis)

The silanol condenses and releases water.

$2RSi(OH)_3 \rightarrow 2\ H_2O +$

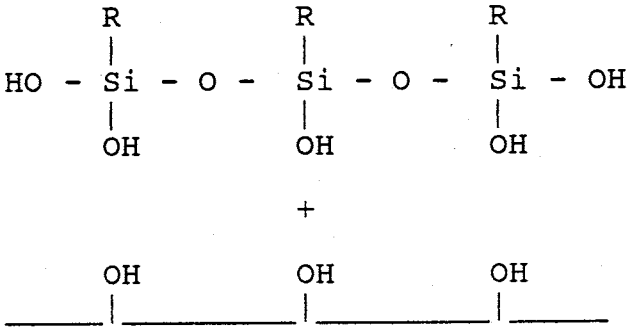


Next hydrogen bonding occurs between the OH groups on the

condensation product and the glass substrate.

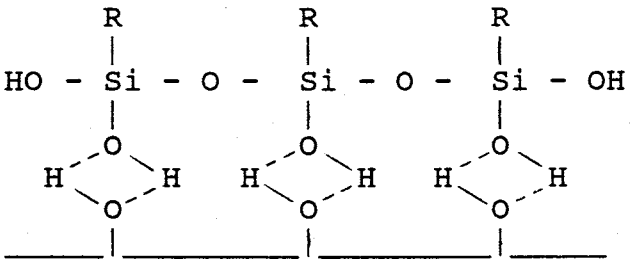

Heating completes the bond formation and releases water.

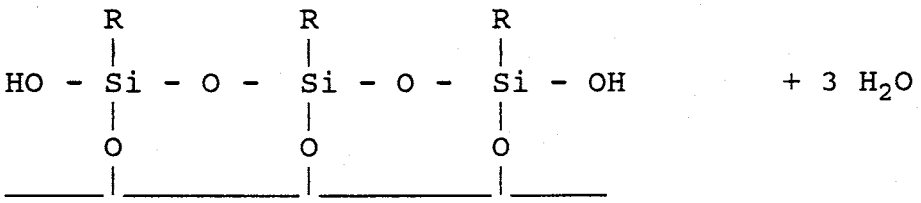

In general, longer carbon chain functional groups (-R) impart more hydrophobic properties to a treated surface.

Preparing intermediate-wet glass slides

The surface of clean glass slides was altered to intermediate-wet by applying a 1% by volume aqueous solution of methyltrimethoxysilane (MTMS). MTMS was obtained from Hüls America and is used commercially to restore marble and to render paperboard water repellant. The chemical formula of MTMS is $C_4H_{12}O_3Si$, and its molecular weight is 136.22. The reaction was performed in a glove bag under a nitrogen atmosphere. The slides were inserted in a machined Teflon block, placed in a Teflon beaker, covered with the MTMS solution and placed in an ultrasonic bath for five minutes. Curing was accomplished by placing the slides overnight in an oven at 100° C.

The intermediate-wet reaction mechanism

The MTMS-glass reaction mechanism was presented by Arkles, et al., (1991). Initially, the MTMS reacts with water to form a highly reactive intermediate silanol molecule and methanol.

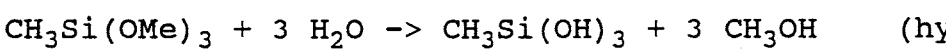


The second step is a condensation in which the silanol reacts with other silanol molecules, and water is released.

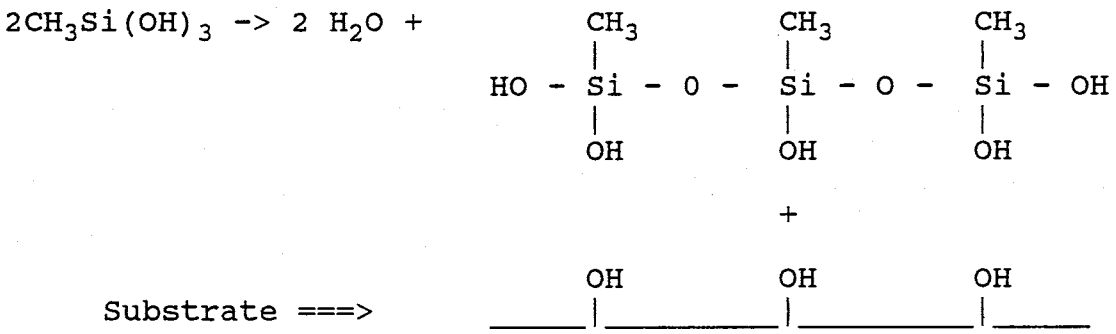


In the next portion of the reaction, hydrogen bonding occurs between the OH groups on the condensation product and the substrate.

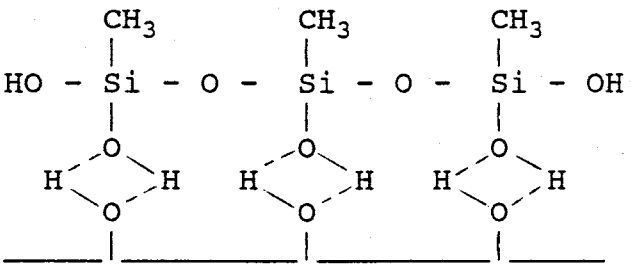


Finally, the bond is completed by heating which liberates water.

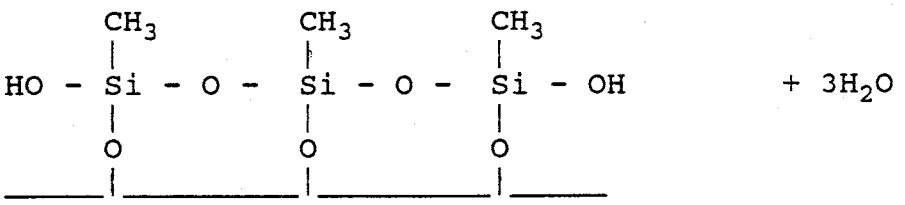

The methyl group ($-CH_3$) is the functional group that imparts the intermediate-wet character to the substrate.

Cleaning glass beads

The procedures for cleaning glass beads were essentially the same as those used for cleaning glass slides (Menawat, et al., 1984 and Wei, et al., 1993). The glass beads used in the experiments were 53-63 $\mu$m diameter (230-270 mesh) Class V Close Sized Uni-spheres and were manufactured by Cataphote, Inc. of Jackson, MS. The glass used to make glass beads is remelted soda-lime plate glass. The chemical composition of the beads is provided in Appendix A.

About 120 to 150 g of glass beads were poured into an Erlenmeyer flask with a Teflon stirbar. Enough 2-butanone was added to cover the beads, and the flask was placed on a stir plate and stirred for about 20 minutes. The 2-butanone was removed, and the beads were rinsed five times for about five minutes with deionized water.

To remove inorganic contaminants, enough nitric acid was added to cover the beads. Again the beads were stirred for about 20 minutes. The nitric acid was decanted, and the beads were rinsed five times with deionized water. Finally,

the beads were placed in a beaker and dried overnight in an oven at 100° to 110° C.

In some cases the beads became fused together during the drying procedure. To remove any large aggregates, the beads were passed through a clean 75-$\mu$m sieve. The clean glass beads were used in the hydrophilic column experiments.

Preparing hydrophobic glass beads

Clean glass beads were rendered oil-wet using GC-18. The procedures were modified slightly from those used to silylate the glass slides. A 1% aqueous solution by volume was prepared using 2 mL of GC-18 in 198 mL of water. This solution was mixed with a Teflon stirbar for about 2.5 minutes. Then the solution was poured over the beads. The entire Erlenmeyer flask was placed in the ultrasonic bath for another 2.5 minutes. The procedure was repeated ten times to ensure complete treatment of the beads. Finally, the beads were left to cure overnight in an oven at about 100° C.

Preparing intermediate-wet glass beads

Glass beads were made intermediate-wet by applying a 1% by volume aqueous solution of MTMS. The reaction was performed in a glove bag under a nitrogen atmosphere to prevent premature hydrolysis of the alkoxysilane to the less stable silanol. The reaction was encouraged by placing the Teflon beaker containing the beads and solution in an ultrasonic bath for five minutes. Curing was accomplished

by placing the beads overnight in an oven at about 100° C.

## 2.2 Contact Angle Measurements

Advancing and receding contact angles for three fluid pairs were measured on hydrophilic, hydrophobic and intermediate-wet soda-lime glass slides with the dynamic sessile drop method. The three fluid pairs used were:

- water - air
- water - Soltrol 130
- Soltrol 130 - air.

As mentioned earlier the aqueous phase was deionized water from a Millipore Milli-Q water purification system. Soltrol 130 was chosen as the organic phase for the contact angle, interfacial tension, and capillary pressure-saturation experiments for several reasons.

First, the physical properties of Soltrol 130 make it favorable for use in studying light nonaqueous phase liquids. Soltrol 130 is a mixture of $C_{10}$ to $C_{13}$ isoparaffins manufactured by Phillips Petroleum Inc., Bartlesville, OK. Soltrol is less dense than water (0.753 g/cc) and is essentially immiscible in water. The volatility of Soltrol 130 is low. Second, because Soltrol is used frequently in laboratory studies such as this one, these results can be compared to previous work.

Slides were placed on an adjustable stage and viewed through a Zeiss microscope equipped with a Tiyoda

goniometer. When a water-air contact angle was desired, water was placed in a clean Gilmont 2-mL microliter buret which was positioned above and normal to the plane of the slide. A drop of water was formed at the buret tip. The stage was raised until the drop and slide touched. To find the advancing angle, the drop was enlarged slightly by turning the knob on the microliter buret. The crosshair of the goniometer was aligned tangent with the angle formed between the slide and the drop. Measurements were taken on both the left and the right side of each drop, and drops were measured in five different locations on each slide. The measurements from all five trials were averaged together.

Receding angles were measured on each drop by turning the knob on top of the microliter buret the other direction to make the drop smaller. Again, the left and right sides of drops at five different locations on each slide were measured and averaged.

The measurement of Soltrol 130-air contact angles was accomplished by thoroughly cleaning the glass portion of the microliter buret with acetone and deionized water and placing Soltrol 130 in the buret. Then the contact angles were measured in the same way as the water-air angles.

Water-Soltrol 130 contact angles were determined by submerging the slide to be measured into a small transparent container filled with Soltrol 130. The microliter buret was

cleaned and filled with water and placed into the Soltrol 130. A drop of water was formed, and the platform was raised until the drop and the slide made contact. Again both advancing and receding contact angles were determined in five locations.

Photographing contact angles through the microscope

In order to document and illustrate the different types of contact angles measured in these experiments, photographs of selected contact angles were taken using the 35-mm camera attachment to the Zeiss microscope. These photos are shown in Chapter 3 (Figures 3.1 through 3.6).

## 2.3 Surface and Interfacial Tension Measurements

A Fisher Model 20 Ring Tensiometer (Fisher Scientific, Pittsburgh, PA) was used to determine surface and interfacial tensions for the three fluid pairs. The measurements were performed following the procedure outlined in the instrument manual.

Prior to a surface or interfacial tension measurement, the tensiometer ring was cleaned by dipping the ring into benzene. This was followed by an acetone rinse, and finally the ring was held in the flame of a bunsen burner until it glowed.

The surface tension between deionized water and air was determined by placing about 40 mL of water in a clean 100-mL beaker. The platinum-iridium tensiometer ring was submerged

into the water. The surface tension was found by gradually moving the ring to the surface of the water and noting the tension required to pull the ring through the surface of the water. All measurements were in dynes/cm. The surface tension between Soltrol 130 and air was found in a similar manner.

The interfacial tension between water and Soltrol 130 was found using the following procedure. A beaker with water only was placed on the tensiometer stage, and the ring was submerged in the water. Soltrol 130 was added to the beaker to a thickness of about 1 cm. The interfacial tension between the water and Soltrol 130 was found by measuring the force needed to pull the ring through the interface between the two fluids.

Surface and interfacial tension values read off the dial of the tensiometer were "apparent" surface tensions. A correction had to be applied to convert these values to absolute surface tensions. The correction factor was found using the formula provided in the tensiometer instruction manual:

$$F = 0.7250 + \sqrt{\frac{0.01452\ P}{C^2\ (D-d)} + 0.04534 - \frac{1.679\ r}{R}} \qquad (4)$$

where $F$ is the correction factor,

$P$ is the apparent or dial reading,

$C$ is the circumference of the ring,

$D$ is the density of the lower phase,

$d$ is the density of the upper phase,

$r$ is the radius of the wire of the ring, and

$R$ is the radius of the ring.

A series of surface and interfacial tension measurements were performed. The primary results are summarized and discussed in Chapter 3, and the data are provided in Appendix C.

The surface tension between water and air was found for ultrapure water at room temperature, 21.5° C (Experiment STM 101). To determine the effect of degassing the water, Experiment STM 102 was conducted with ultrapure, degassed water. To investigate the influence of solutes on the water-air surface tension, Experiment STM 103 was performed using ultrapure, degassed water with 1000 mg/L $NaN_3$ as a bactericide. To determine the influence of a small increase in temperature, Experiment STM 109 was done to measure the water-air surface tension of ultrapure water at 26° C.

Experiment STM 104 was conducted to determine the surface tension between Soltrol 130 and air at room temperature. The experiment was repeated for degassed Soltrol (Experiment STM 105).

Each of the surface tension experiments (those for water-air and Soltrol-air) consisted of ten separate measurements. As with the contact angles, these measurements were averaged, and the sample standard deviation was determined.

The interfacial tension between water and Soltrol 130 was measured in triplicate (Experiments STM 106 through STM 108).

## 2.4 Capillary Pressure-Saturation Measurements

The following section describes the materials and procedures used to construct the columns and the procedures used to conduct the drainage and imbibition experiments.

Materials

A 5 cm-long, 5-cm diameter glass chromatography column (short column) was used to determine capillary pressure-saturation curves following procedures modified from Wei (1991) and Wilson, et al., (1990). The columns were manufactured by Ace Glass of Vineland, NJ.

The short column procedures involved packing soda-lime glass beads into the column. As mentioned earlier the glass beads used in the experiments were 53-63 $\mu$m in diameter (Class V Close Sized Uni-spheres, 230-270 mesh) and were manufactured by Cataphote, Inc. of Jackson, MS. In the U.S. Department of Agriculture (USDA) classification of soil fractions, this particle diameter falls at the border between silt and very fine sand. The beads were held in the columns with Teflon endcaps (also from Ace Glass) equipped with o-rings, valves and appropriate selective membranes (filters) to allow only the desired fluid to pass. The o-rings were obtained from Ace Glass and were made of FETFE®,

a fluoroelastomer with special TFE additives. The valves were purchased from Cole-Parmer Instrument Company (Chicago, IL), and were made of clear polycarbonate and white polypropylene.

Water-wet nylon filters (MSI, Westboro, MA) were used to allow water to pass but not oil or air. The openings in the nylon filters were 0.22 $\mu$m. Hydrophobic Teflon filters (Gelman Sciences, Ann Arbor, MI) were used to allow oil to pass, but not water or air. The openings in the Teflon filters were 0.5 $\mu$m. Polypropylene filters with 10 $\mu$m openings (Gelman Sciences, Ann Arbor, MI) were used on some top endcaps to keep the beads in place in the column.

Three different experiments were performed using water-wet beads. They were done using the fluid pairs water-air, water-Soltrol 130, and Soltrol 130-air. The same experiments were repeated for hydrophobic and intermediate-wet glass beads.

The aqueous phase was deionized, degassed water. The water was degassed by boiling two liters in an Erlenmeyer flask on a hot plate for about ten minutes. The boiling water was transferred to a holding flask which was attached to the laboratory vacuum line to keep gasses from redissolving in the water. In column experiments expected to last more than two or three days, 1000 mg/L sodium azide ($NaN_3$) was added to the water as a bactericide.

The light non-aqueous phase liquid, Soltrol 130, was

degassed by placing it in a flask connected to the laboratory vacuum line for a minimum of several hours prior to use. To enhance the action of the vacuum to remove gasses from the Soltrol 130, a Teflon stirbar was rotated slowly in the flask.

Preparing conventional short column experiments

In conventional water-air short column experiments, a nylon filter was glued with 2 Ton Clear Epoxy (Devcon Corporation, Danvers, MA) onto the fritted glass disc (filter and packing support) of a bottom Teflon endcap. Once the glue was dry (typically overnight), the endcap was fitted with an o-ring and a valve. Then the endcap was weighed, and the integrity of the filter was tested as follows. The o-ring was temporarily removed, and the endcap was submerged in degassed water. Water was pulled through the endcap to saturate it using a small vacuum pump. A suction of about 10 to 12 inches of mercury was applied for about 3 minutes. This amount of time was about two or three times the amount normally needed to remove any air from the endcap. Another 3 minute period was used to observe the filter under suction in air. If any air leaked through the filter during the test, air bubbles would be visible in the tubing between the endcap and the pump. Only the endcaps that passed the test with no leakage of air were used in the column experiments. The bottom endcap was screwed onto a glass chromatography column, along with a top endcap

equipped with an o-ring and a valve (but initially no filter, scrim or glue). This mass was recorded. The point to which the top endcap was screwed on was marked. Next a buret filled with degassed water was connected to the valve of the bottom endcap via tubing. The valves were opened and the buret raised such that water would flow into the column from below. The valve on the top endcap was left open to allow air to escape. Usually some air bubbles were trapped inside as the column was filled. Most of the time these bubbles could be removed by rotating the column until the bubbles reached the center of the endcap and were forced out. The column was often allowed to stand overnight to allow any air bubbles to dissolve.

The mass of the water-filled column was recorded. The difference in mass between the empty and water-filled column was used to determine the total column volume, $V_{total}$.

$$CM_{H_2O} - CM_{Empty} = Mass_{H_2O} \quad (5)$$

where $CM_{H2O}$ is the mass of the water-filled column,

$CM_{Empty}$ is the mass of the empty column, and

$Mass_{H2O}$ is the mass of the water added.

$$V_{Total} = \frac{Mass_{H_2O}}{\rho_{H_2O}} \quad (6)$$

where $\rho_{H2O}$ is the density of water, taken as one g/cm$^3$.

After the top endcap was removed, dried and a polypropylene scrim was glued on with epoxy, the column was

ready for packing. Clean glass beads were packed in the column which remained full of water. Generally, a layer of beads 10-mm thick was added to the column at a time. A hand-held massager/vibrator was used to vibrate the column to remove any trapped air bubbles and to obtain a uniform pack. This procedure of adding beads followed by vibration of the column was repeated until the column was filled. Then the complete top endcap was screwed onto the column. In almost every case, the column was either over or underpacked and the seal between the o-ring and the column was not established properly. If the column was underpacked, more beads were added. If the column was overpacked, beads were removed. This procedure was repeated until a proper seal was obtained. A proper seal was confirmed by attaching a water-filled buret to the bottom endcap valve, closing the top endcap valve, and raising the buret to apply a positive hydraulic head. If the seal was good, no water would leak out of the top endcap threads.

The mass of the beads added to the column was recorded, along with the final mass of the column. The mass of the beads allowed the calculation of the pore volume in the column. First, the bead volume was found using the equation:

$$V_{Beads} = \frac{Mass_{Beads}}{\rho_{Beads}} \qquad (7)$$

where $\rho_{Beads}$, the density of the beads, was 2.47 g/cm$^3$. This

density was reported by the manufacturer and was confirmed using a pycnometer. Second, the pore volume, *PV*, was found by subtracting the bead volume from the total volume.

$$PV = V_{Total} - V_{Beads} \tag{8}$$

In order to ensure that the column was completely saturated when started, about 100 mL of degassed water was passed through the bottom of the column and out the top. If the mass of the column increased after this flushing with degassed water, the procedure was repeated until the mass reached a maximum and stabilized. If the mass of the column decreased or remained constant, degassing was suspended.

Porosity, $n$, was found using the equation:

$$n = 1 - \frac{Mass_{Beads}}{\rho_{Beads} * V_{Total}} \tag{9}$$

Bulk density was calculated using the following relationship:

$$\rho_{Bulk} = \frac{Mass_{Beads}}{V_{Total}} \tag{10}$$

where $\rho_{Bulk}$ is the bulk density.

Procedures for the other fluid combinations and the other types of beads were analogous. There were only a few significant differences that need to be mentioned.

First, in the Soltrol-air experiments, the bottom endcap was equipped with a Teflon filter. Water-Soltrol experiments used either just a nylon filter on the bottom

endcap or, in the case of "dual filter" experiments, a nylon filter on the bottom endcap and a Teflon filter on the top endcap.

Second, the hydrophobic and intermediate-wet beads float when packed in water using the procedures outlined above. To alleviate this problem, the bottom endcap was saturated with water as usual. Then instead of packing the beads in the column with water, the column was filled with about 1 or 2 cm of ethanol. The surface tension of ethanol is about 22 dynes/cm, so it facilitates the packing of the beads as above. However, before the experiment could begin, the ethanol had to be flushed out completely and replaced with water. This flushing procedure was often very lengthy, requiring a minimum of several days. Flushing was done in one or a combination of methods, including using a syringe pump to flush the column with water and a 100 mL buret hooked up to the bottom endcap.

To monitor the progress of the flushing procedure and to determine when the procedure was completed, about 40 mL of effluent from the flushing procedure was collected at least once a day. The surface tension of the effluent was measured using the ring tensiometer as described in the previous section. The flushing procedure was stopped when the true surface tension of the effluent was that of pure water (72 dynes per cm), thus indicating that all of the ethanol had been removed.

Alternate procedure for preparing short columns

Conventional short column experiments are fairly time-consuming. The amount of time needed to conduct each experiment is controlled by several factors including the amount of time needed for the column to reach equilibrium (or near equilibrium) between each measurement. In addition, longer columns take longer to equilibrate than shorter columns. Therefore, some experiments were conducted using the usual 5-cm long column, but with a bed of beads only about 1 cm thick. The validity of this procedure was confirmed by Larson and Morrow (1981). Drainage curves determined using this method were consistent with those obtained in the conventional manner. However, the imbibition curves were not as good. Often the column would imbibe 50% more fluid than was originally inside. In other words, the imbibition curve would pass the 100% saturation point by a large margin before any fluid could be seen above the surface of the bead pack. Therefore, the imbibition results must be viewed with skepticism.

Procedures for measuring capillary pressure-saturation curves

Once the column was prepared as described above, it was moved to a constant temperature cabinet where the temperature was held at 26.0° C ± 0.5° C. Figures 2.1 through 2.3 show the experimental setups for water and air, water and Soltrol 130, and Soltrol 130 and air systems,

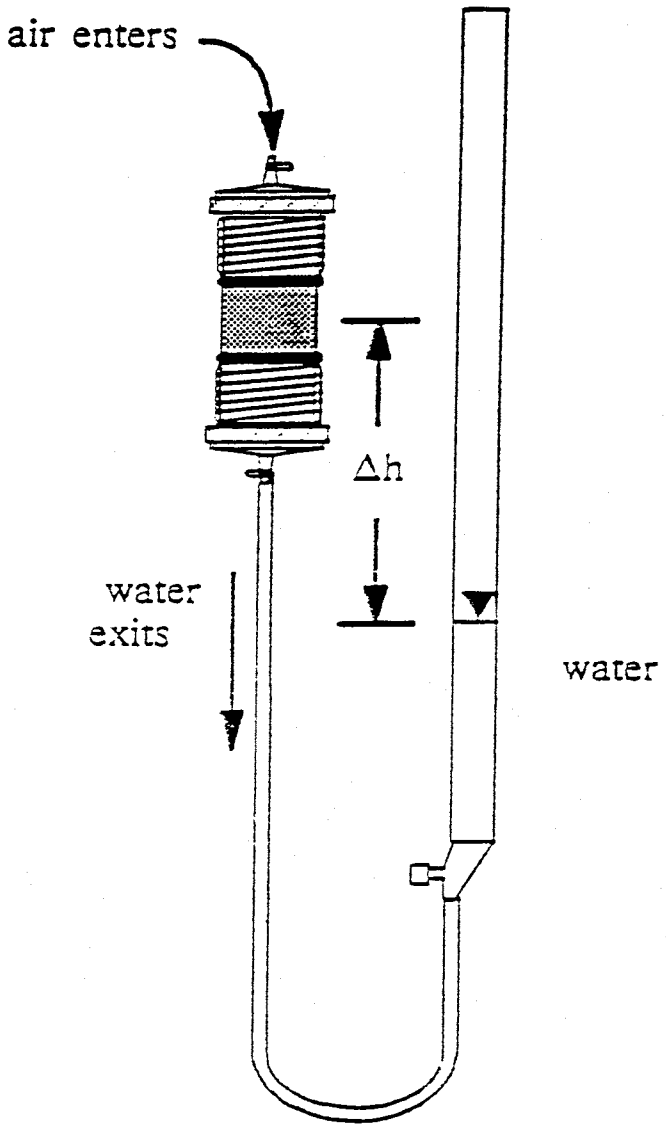


Figure 2.1: Short column experimental setup for water and air systems (from Wilson, et al.,1990)

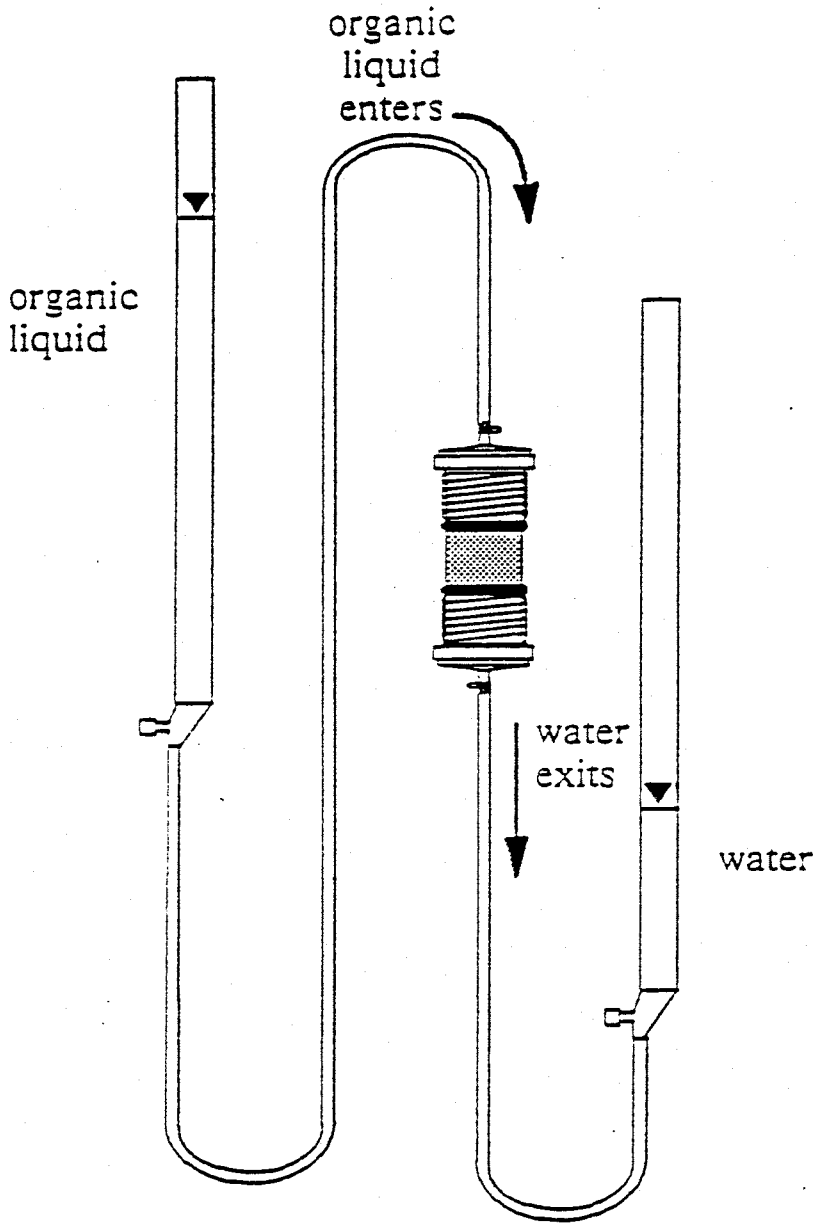


Figure 2.2: Short column experimental setup for water and organic liquid systems (from Wilson, et al.,1990)

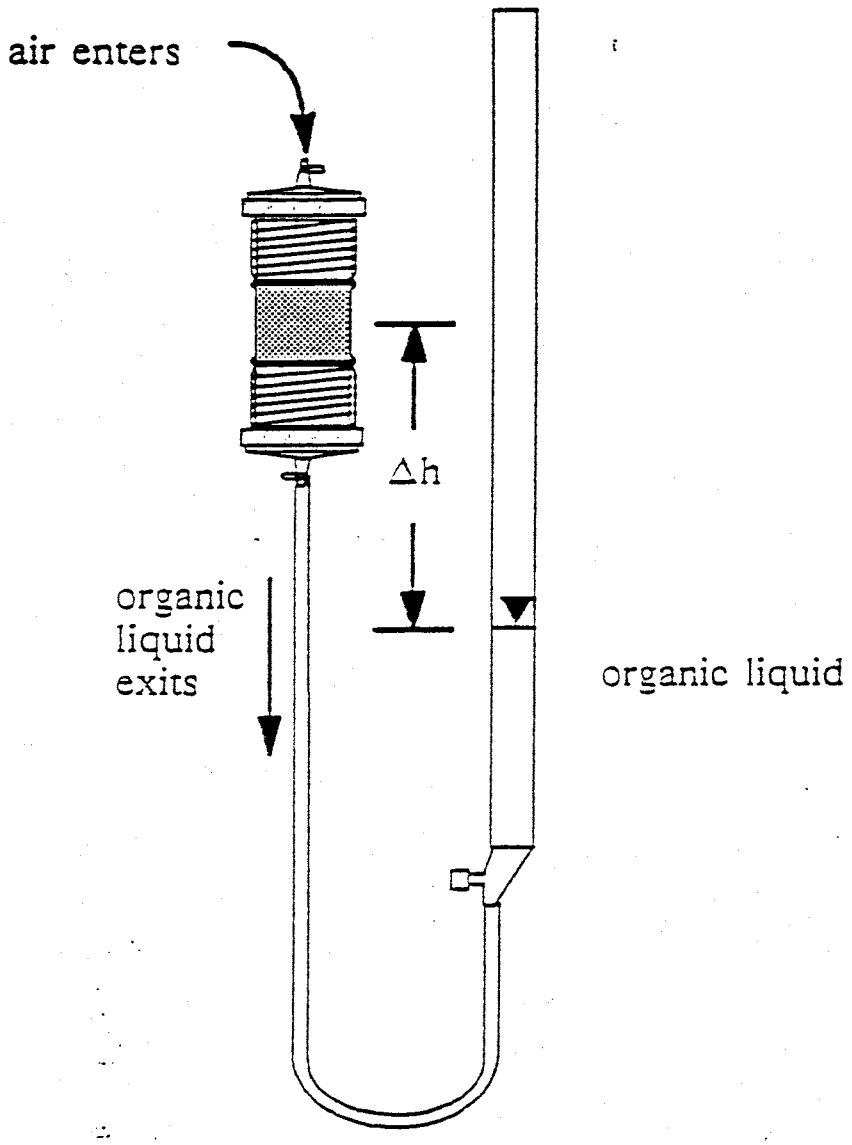


Figure 2.3: Short column experimental setup for organic liquid and air systems (from Wilson, et al.,1990)

respectively. The column was secured to a stand with an appropriate clamp and was hooked up to a buret with (in the case of water and air as the fluids) degassed water. The column was made as plumb as possible with a carpenter's bubble level. The back wall of the cabinet was covered with graph paper with a datum and markings every millimeter. Using this graph paper as the scale and the carpenter's level, the height of the center of the column was recorded to the nearest millimeter along with other information including the date, time, and air temperature. Initially, the water buret was positioned such that the water level was about the same as the center of the column. This situation represented the condition with 100% water saturation in the column at zero capillary pressure. To begin the experiment, the water buret was lowered 5 to 10 cm at a time to apply suction to the water inside the column. The water level was allowed to equilibrate. The difference in the height (as measured using the graph paper scale and the level) between the center of the column and the bottom of the meniscus of the water in the buret was taken as the capillary pressure in centimeters. The general expression used to find the capillary pressure is given below:

$$P_c = \rho_o (h_o - h_c) + \rho_w (h_c - h_w) \qquad (11)$$

where $P_c$ is the capillary pressure,

$\rho_o$ is the density of the organic phase, equal to 0.753 g/cm$^3$ for Soltrol 130,

$h_o$ is the distance from the datum to the organic phase in the buret,

$h_w$ is the distance from the datum to the water in the buret,

$h_c$ is the distance from the datum to the center of the column, and

$\rho_w$ is the density of water, equal to 1.0 g/cm$^3$.

The accuracy of the capillary pressure measurement is estimated to be about one millimeter.

The water saturation was determined in one of two ways, either gravimetrically or volumetrically. The gravimetric method involved closing the valves attached to the top and bottom endcaps, closing the valves on the burets and removing the tubing from the column. The column was then taken to a Mettler balance where it was weighed to the nearest 0.01 g. The percent water saturation ($S_w$) was determined as follows:

$$S_w = 1 - \frac{(M_i - M_c)}{\Delta\rho * PV} \qquad (12)$$

where $M_i$ is the initial mass of the column at the beginning of the experiment,

$M_c$ is the current mass of the column,

$\Delta\rho$ is the density difference between the two fluids being used, and

$PV$ is the pore volume.

The density difference between water and air is about unity.

For water and Soltrol, the difference is 0.247 g/cm$^3$.

To determine the saturation volumetrically, the markings in mL on the burets were used. Theoretically, the fluid draining out of the column will cause a corresponding increase in the fluid level in the buret. Then the saturation can be determined as follows:

$$S_{vol} = \frac{PV - \Delta BV}{PV} \qquad (13)$$

where $S_{vol}$ is the percent saturation,

$PV$ is the original pore volume of the column, and

$\Delta BV$ is the change in fluid volume in the buret.

For each capillary pressure, we determined the saturation. Plotting these data and joining the neighboring points gave the desired drainage and imbibition curves.

## 2.5 Procedures for Scaling Capillary Pressure Curves

Prior to scaling any of our capillary pressure-saturation curves, we compared our hydrophilic (untreated) water-air results with those obtained by Haines (1930). Unfortunately, however, Haines apparently did not tabulate his results (of scaled pressure vs. saturation). In order to make our comparison we measured critical points along Haines' drainage and imbibition curves with a ruler. Haines' results (as we measured them) are tabulated in Table D14 in Appendix D. Haines' results were compared with our Experiment PB6 by converting our pressure values from cm of

water to the dimensionless form: $P*R/\sigma$, where $P$ is the pressure in dynes/cm$^2$, $R$ is the mean particle radius, and $\sigma$ is the interfacial tension of the fluids. In addition the saturation values for both systems were converted to effective saturation using the following equation:

$$S_e = \frac{S_w - S_r}{1 - S_r} \qquad (14)$$

where

$S_e$ is the effective saturation,

$S_w$ is the saturation of the wetting phase, and

$S_r$ is the residual saturation of the wetting phase.

Finally the two sets of results were plotted together on a single figure.

We calculated scaled capillary pressures as follows:

$$P_c\ (cm) = \frac{P_c\ (dynes/cm^2) * R\ (cm)}{\sigma\ (dynes/cm) * \cos\theta} \qquad (15)$$

where $P_c$ is the capillary pressure,

$R$ is the mean particle radius,

$\sigma$ is the interfacial tension of the fluids, and

$\theta$ is the contact angle of the system.

To incorporate the effects of contact angle hysteresis, drainage curves were scaled using the receding contact angle and imbibition curves were scaled using the advancing angle.

The capillary tube model does not include corrections for the geometry of the pore space in a porous material. Therefore, we also used classical corrections to scale the

capillary pressure-saturation function. Work in this area of geometric corrections has been done in the past by other groups including: Leverett (1941), Purcell (1949), Purcell (1950), Melrose (1965), Mason, et al., (1983), Mason and Morrow (1986), Mason and Morrow (1991), Desai, et al., (1992), and Demond, et al., (1992).

One of the promising attempts to scale capillary pressure-saturation relationships was presented by Desai, et al., (1992). They used an air-water-silica-surfactant system and varied the concentration of the surfactant to change the interfacial tension and contact angle of the system. Because they found that they could predict the capillary pressure-saturation relationship fairly well for contact angles up to about 65°, we wanted to try their method on our glass bead systems.

The equation they used to scale the pressure-saturation curves is based on Leverett's function (1941) and is as follows:

$$P_c(S_e)_2 = P_c(S_e)_1 \frac{[\sigma \cos\theta_r Z(\theta)]_2}{[\sigma \cos\theta_r Z(\theta)]_1} \qquad (16)$$

where

$P_c$ is the capillary pressure,

$S_e$ is the effective saturation,

$\sigma$ is the interfacial tension,

$\Theta_r$ is the contact angle corrected for roughness, and

$Z(\Theta)$ is the curvature correction factor.

They also included a contact angle roughness correction published by Morrow (1975). Table 2.1 below gives the roughness corrections.

Table 2.1: Contact Angle Roughness Correction (Morrow, 1975)

| Intrinsic Angle | Operational Angle | |
|---|---|---|
| | Drainage (Receding Angle) | Imbibition (Advancing Angle) |
| $0° < \theta_{INT} < 21.6°$ | $\theta_r = 0°$ | $\theta_r = 0°$ |
| $21.6° < \theta_{INT} < 87.6°$ | $\theta_r = 0.5\exp(0.05\theta_{INT}) - 1.5$ | $\theta_r = 2(\theta_{INT}-21.6)$ |

The subscripts *INT* and *r* stand for intrinsic and corrected for roughness, respectively. The curvature correction factor, $Z(\theta)$ was presented by Melrose (1965), and represents the deviation of the capillary pressure-saturation function from the $cos\theta$ relationship assumed in the capillary tube model. According to Melrose (1965), $Z(\theta)$ can be calculated using the following equation:

$$Z(\theta) = \frac{J(\theta)}{[J(\theta)]_{\theta=0}\cos\theta} \qquad (17)$$

where

$J$ is Leverett's (1941) $J$-function.

This scaling factor was applied to several systems. $Z(\theta)$ was estimated from Figure 7 of Melrose (1965). This figure shows the relationship between the curvature correction factor, $Z(\theta)$, and the contact angle, $\theta$, in

degrees.

We also scaled the capillary pressure-saturation functions using only the interfacial tension and particle size. The equation used is as follows:

$$P_c\ (cm) \rightarrow \frac{P_c\ (dynes/cm^2) * R\ (cm)}{\sigma\ (dynes/cm)} \qquad (18)$$

where the symbols are as previously defined. $Z$ scaling factors were calculated to determine the deviation of this scaling from Haines (1930) results. Because the results of Experiment PB6 were essentially the same as those of Haines, we used the results of PB6 to calculate our $Z$ factors. To accomplish this the capillary pressure of each experiment was estimated at multiples of 10% saturation. $Z$ factors were calculated for 10 through 90% saturation for the drainage curves, and when results were available, the $Z$ factors were found for 10 through 80% saturation for the imbibition curves. $Z$ factors where found using a spreadsheet program that simply divided the capillary pressure for the system in question by the corresponding capillary pressure for the Haines results. In other words $Z$ factors were found as follows:

$$Z = \frac{Capillary\ Pressure_i}{Capillary\ Pressure_{Haines}} \qquad (19)$$

where

$Capillary\ Pressure_i$ is the capillary pressure of the system being examined (at a particular saturation)

and

$Capillary\ Pressure_{Haines}$ is the capillary pressure of the Haines results at the same saturation.

# CHAPTER 3

# RESULTS AND DISCUSSION

This chapter presents the results of the contact angle, interfacial tension, and capillary pressure-saturation experiments. Following each section is a discussion of the results.

## 3.1 Contact Angle Results

Advancing and receding contact angles were measured for three fluid pairs on hydrophilic, hydrophobic and intermediate-wet substrates. In each experiment the substrate was a glass microscope slide. The hydrophilic substrates were untreated slides, and the hydrophobic and intermediate-wet substrates were GC-18-treated and MTMS-treated slides, respectively. Table 3.1 summarizes the contact angle results and standard deviations. The experimental data are provided in Appendix B.

Table 3.1: Initial Advancing and Receding Contact Angle Measurements

| FLUID PAIR | UNTREATED GLASS | MTMS-TREATED GLASS | GC-18-TREATED GLASS |
|---|---|---|---|
| WATER-AIR | ADV 6.7°± 0.7 | ADV 88.0°± 1.6 | ADV 87.6°± 1.9 |
| | REC 4.5°± 1.6 | REC 72.8°± 2.6 | REC 80.2°± 4.1 |
| WATER-SOLTROL | ADV 43.5°± 3.0 | ADV ABOUT 95° | ADV 147.7°± 9.0 |
| | REC 19.9°± 2.5 | REC ABOUT 80° | REC 112.3°± 7.9 |
| SOLTROL -AIR | ADV 7.5°± 2.5 | ADV 10.2°± 2.6 | ADV 8.8°± 1.9 |
| | REC 5.7°± 2.3 | REC 9.3°± 3.0 | REC 6.3°± 1.4 |

ADV = Advancing angle REC = Receding angle

The advancing and receding water-Soltrol contact angles on the MTMS-treated slides are listed as "about" in Table 3.1 because these angles were not as stable over time as the others. Both the advancing and receding contact angles decreased during the first fifty to 100 hours. Thereafter, both angles remained more stable. Therefore, contact angles was chosen that seemed to represent the system after the initial fifty to 100 hour period had passed. This system is discussed in more detail later in this section.

Photographs of selected contact angle experiments are shown in the next six figures (Figures 3.1 through 3.6). The photographs are enlarged about 22 times. The experiments were performed at room temperature which fluctuated between about 19° to 23° C.

In order to test the suitability of a compound as a wettability-altering treatment in capillary pressure-saturation experiments, several contact angle measurements were performed over a period of hundreds of hours to check the stability of the treatment. Treated slides were stored in air, Soltrol, and water to check for deterioration of a treatment in the presence of the fluids to which the glass beads would be exposed. Experiments 33A through 33D and 34A through 34D (Figures 3.7 through 3.10) show that glass slides treated with MTMS remain relatively stable while in contact with most of the fluids over a period of 1000 hours.

Contact angle measurement experiment 33A (CAM33A),

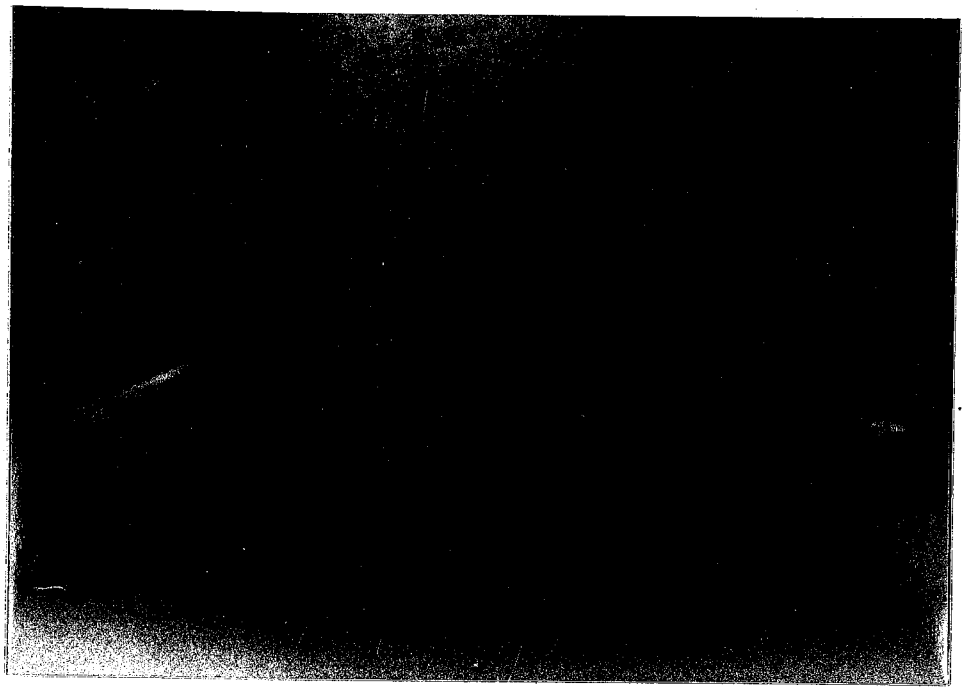

Figure 3.1: Advancing Water-Air Contact Angle on Untreated Surface (22x)

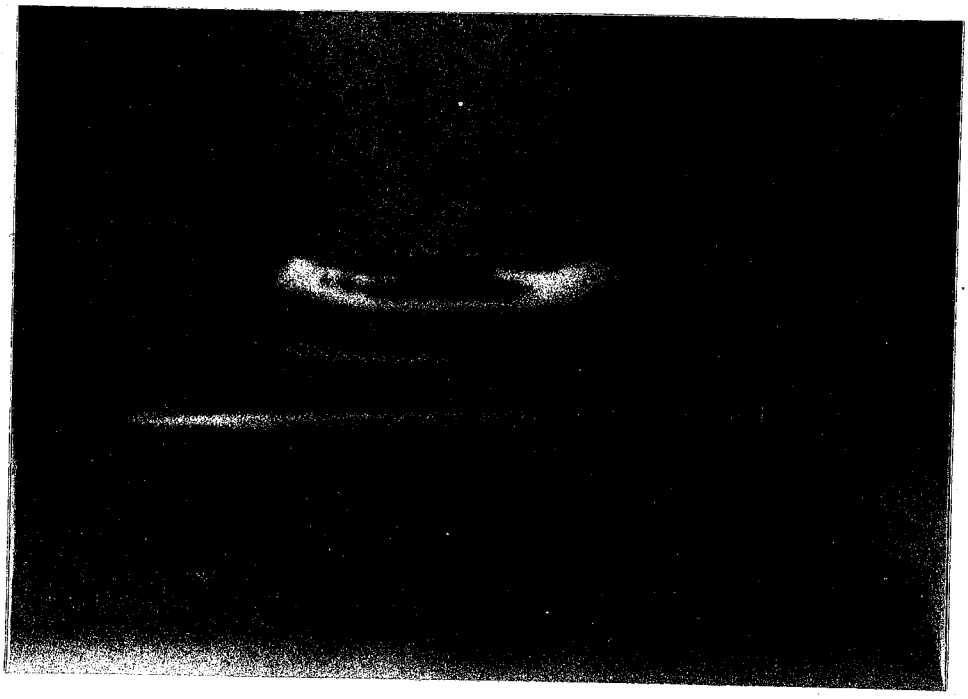

Figure 3.2: Receding Water-Air Contact Angle on Untreated Surface (21x)

Figure 3.3: Advancing Water-Air Contact Angle on MTMS-treated Surface (22x)

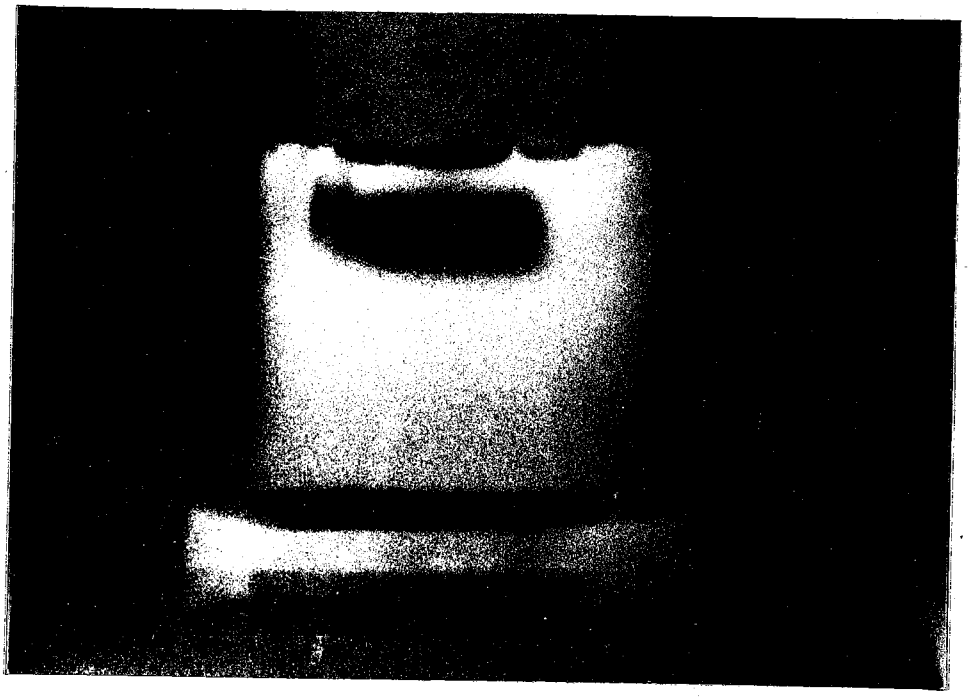

Figure 3.4: Receding Water-Air Contact Angle on MTMS-treated Surface (22x)

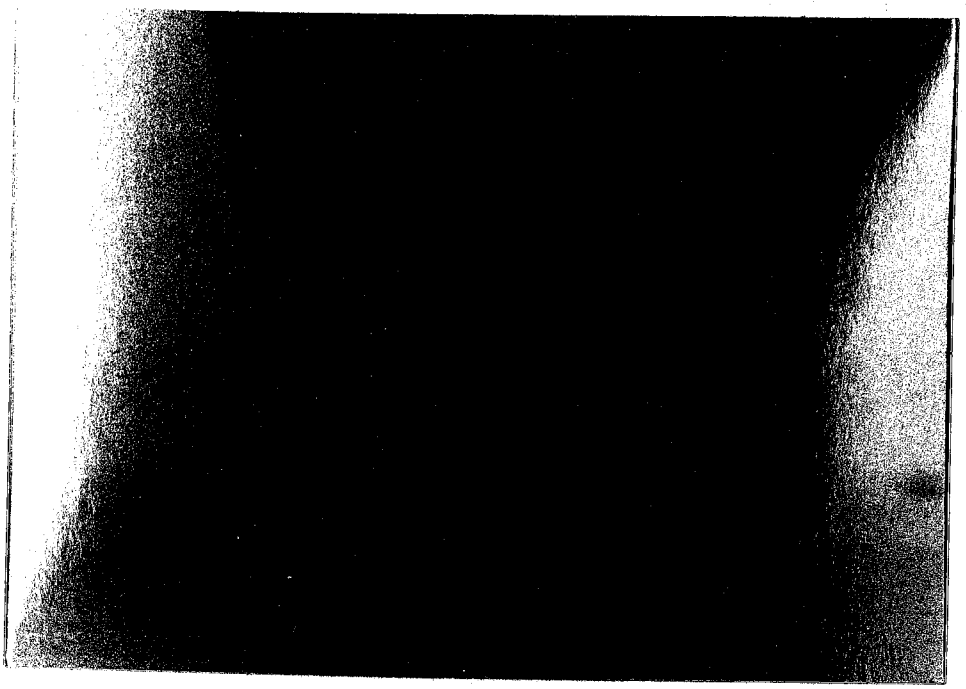

Figure 3.5: Advancing Water-Soltrol Contact Angle on GC-18-treated Surface (22x)

Figure 3.6: Receding Water-Soltrol Contact Angle on GC-18-treated Surface (22x)

FIGURE 3.7: CAM33A AND CAM34A
MTMS-TREATED SLIDE
WATER-AIR STORED IN AIR

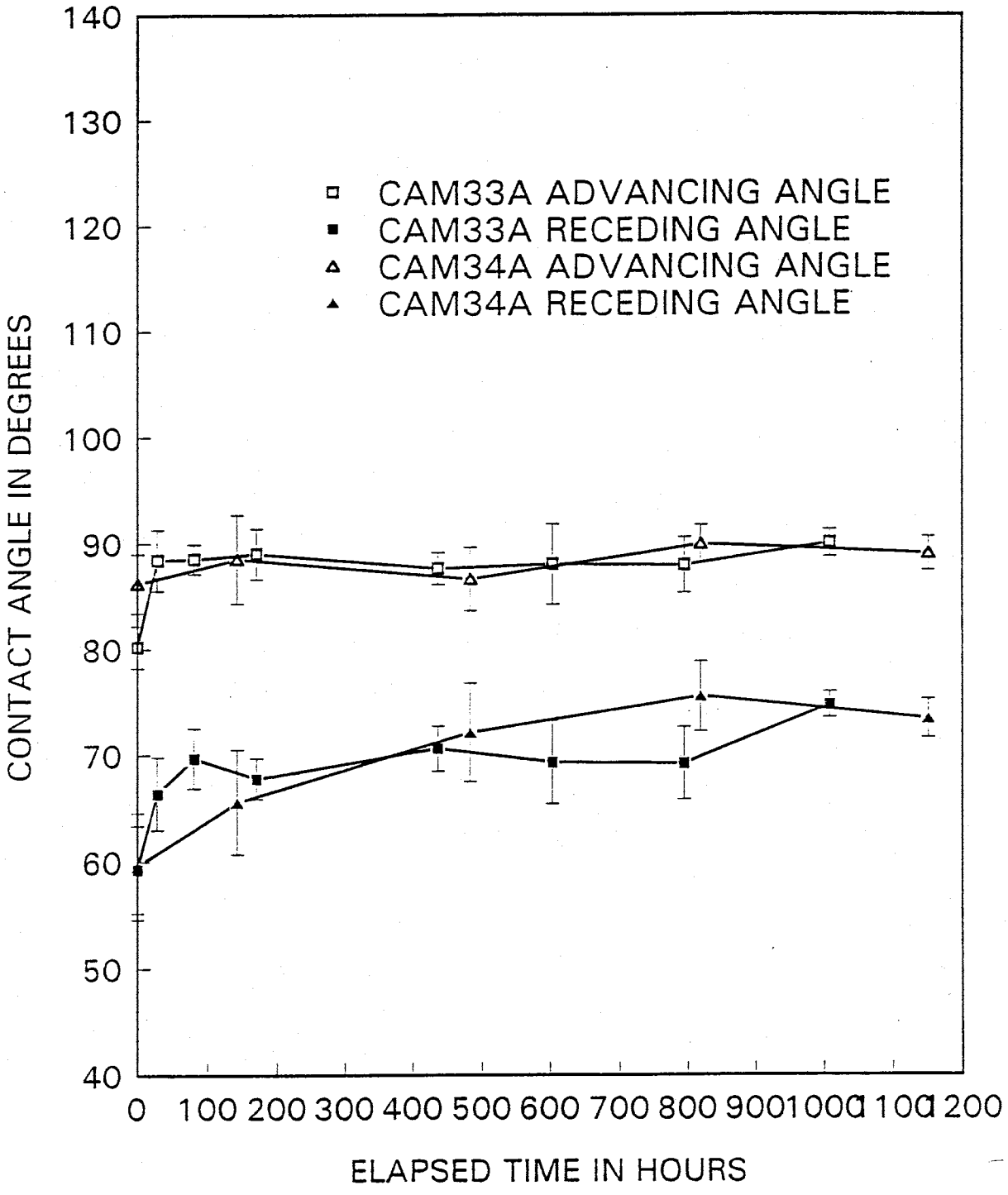

FIGURE 3.8: CAM33B AND CAM34B
MTMS-TREATED SLIDE
WATER-SOLTROL IN NaN3 WATER

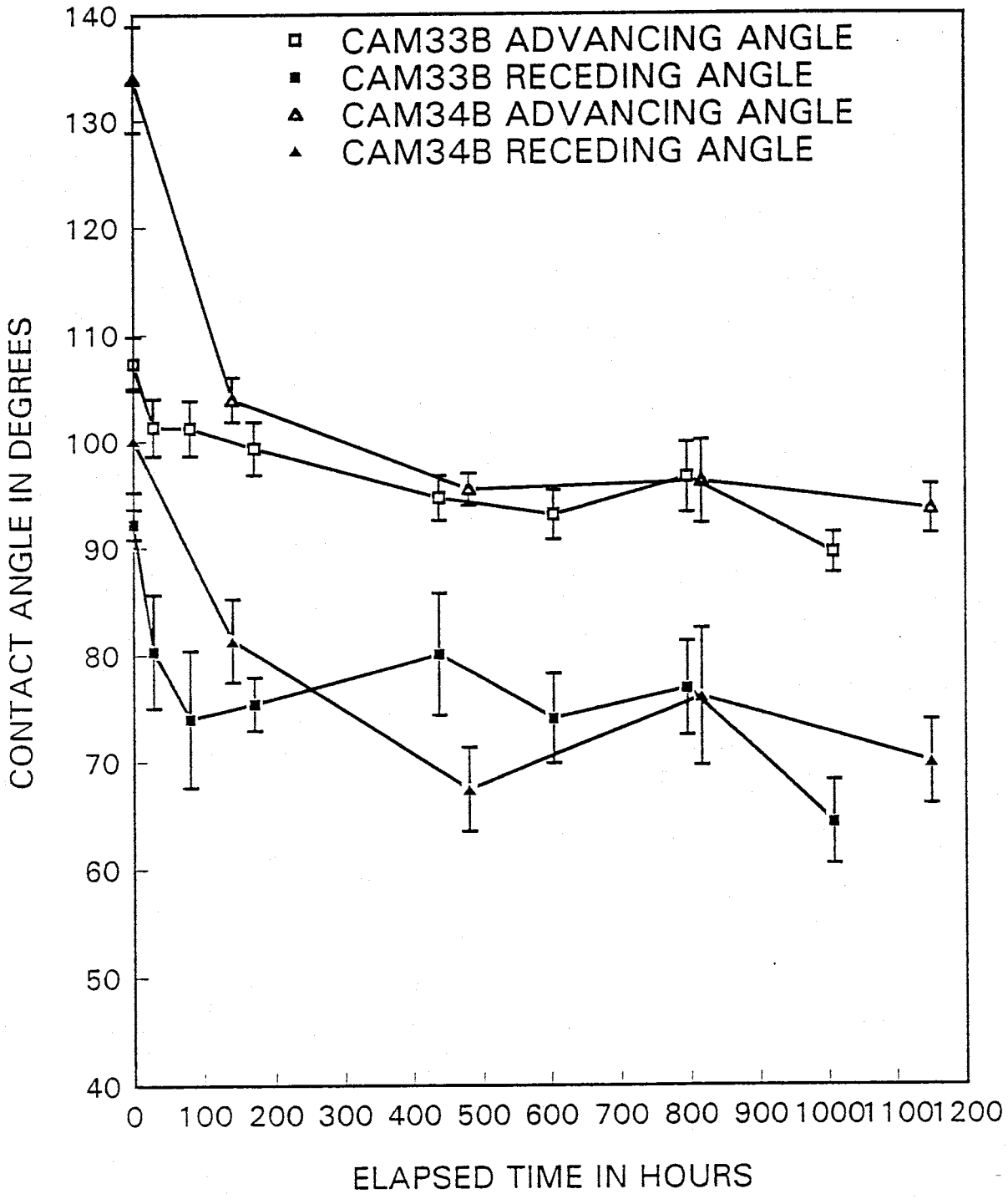

FIGURE 3.9: CAM33C AND CAM34C
MTMS-TREATED SLIDE
WATER-AIR STORED IN SOLTROL

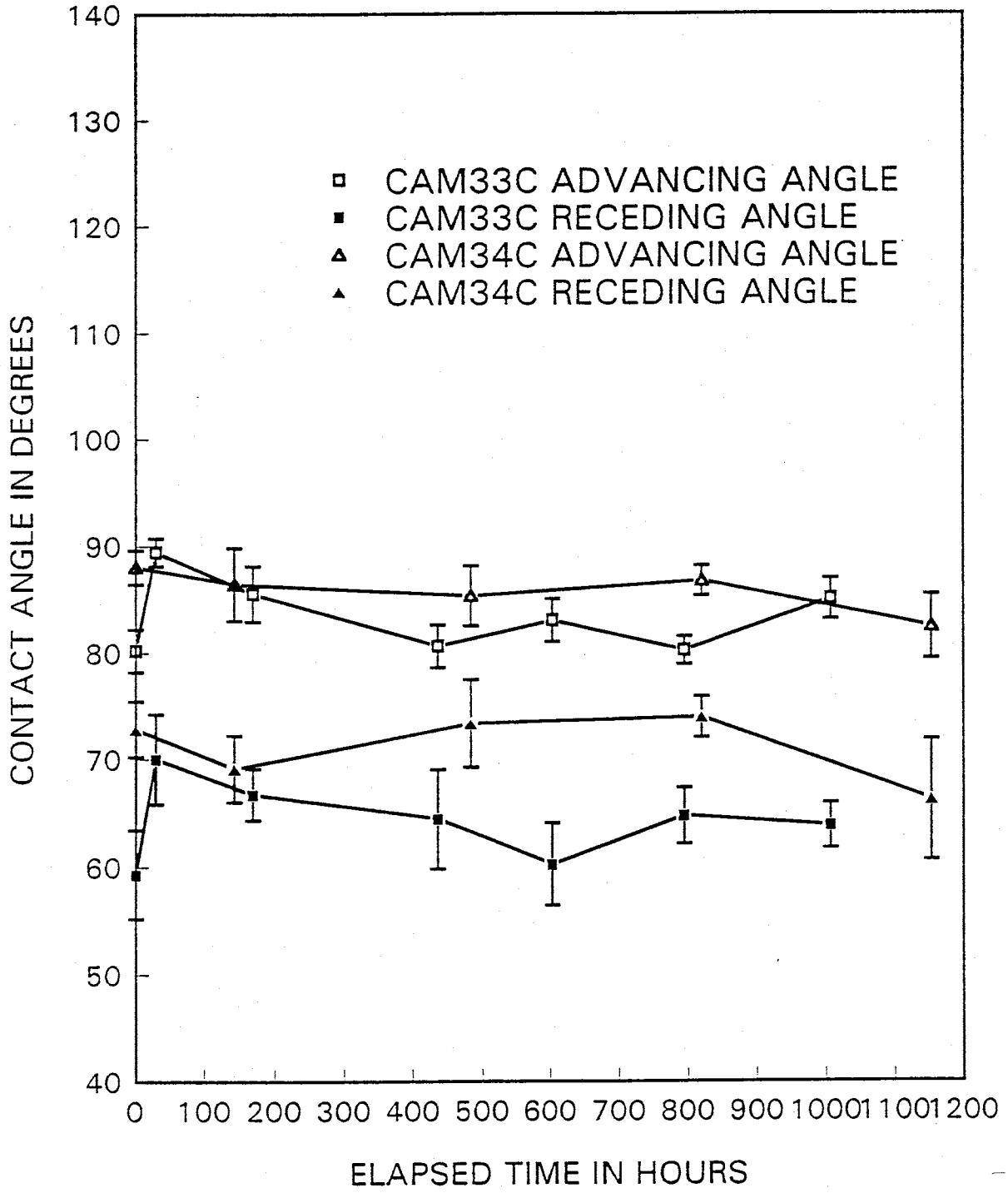

FIGURE 3.10: CAM33D AND CAM34D
MTMS-TREATED SLIDE
WATER-AIR STORED IN NaN3 WATER

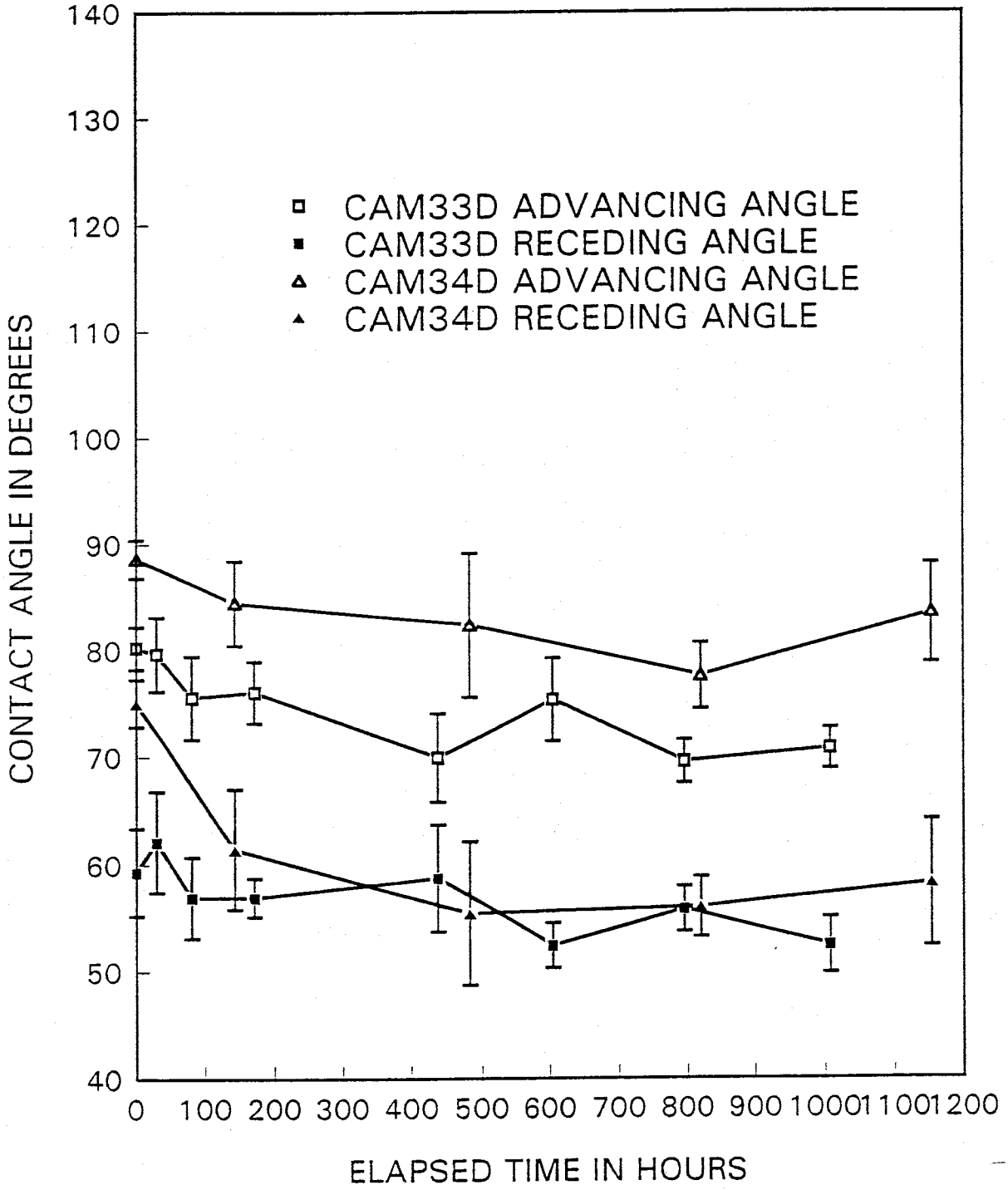

which is a water-air measurement on an MTMS-treated slide stored in air, shows an increase in the advancing angle of about 8° between the first and second measurements (Figure 3.7). However, during the remainder of the experiment, the advancing angle was remarkably stable. The receding angle for this experiment also exhibited this behavior, increasing about 8° after the initial measurement, but remaining fairly stable thereafter.

Experiment CAM34A is a duplicate of CAM33A, with which it is in relatively good agreement (Figure 3.7). The advancing angle is quite stable throughout the experiment and does not show the early increase seen in CAM33A.

Contact angle experiment 33B (CAM33B), which is a water-Soltrol measurement on an MTMS-treated slide stored in water with 1000 mg/L $NaN_3$, shows an initial decrease in the advancing angle of about 10° between the first and second measurements, followed by a gradual decrease of another 10° over the 1000 hours (Figure 3.8). The receding angle decreased by about 10° between the first and second measurements, followed by a relatively stable period of about 700 hours. Then the receding angle decreased by another 10°. The decrease in the contact angle in this experiment is probably the result of deterioration of the MTMS surface by hydrolysis.

Experiment CAM34B (Figure 3.8) is a repeat of CAM33B. The first advancing and receding measurement is

significantly higher in this experiment, after which the results are in good agreement. The higher initial measurement may have been caused by bulk deposition of the silane treatment, which was removed when the slide was stored in water.

Contact angle experiment 33C (CAM33C), which is a water-air measurement on an MTMS-treated slide stored in Soltrol, shows a small decline in both the advancing and receding angles (Figure 3.9). The advancing angle ranges between 80 and 90°, and the receding angle lies between 60 and 70°.

Experiment CAM34C is a duplicate of CAM33C, and the two experiments agree well (Figure 3.9).

Contact angle experiment 33D (CAM33D), which is a water-air measurement on an MTMS-treated slide stored in water with 1000 mg/L $NaN_3$, shows a small decline in both the advancing and receding angles (Figure 3.10). The advancing angle ranges between 70 and 80°, and the receding angle lies between about 52 and 62°.

Experiment CAM34D, a repeat of CAM33D, shows advancing angles about 10° below those in CAM33D (Figure 3.10). The receding angles are fairly close in both experiments.

An experiment (CAM08) was performed to determine how many treatments of GC-18 were needed to obtain complete coverage on the surface of a glass slide (Figure 3.11). Complete coverage was indicated by the contact angles

FIGURE 3.11: CAM08: CHANGE IN CONTACT ANGLE AFTER GC-18 TREATMENTS

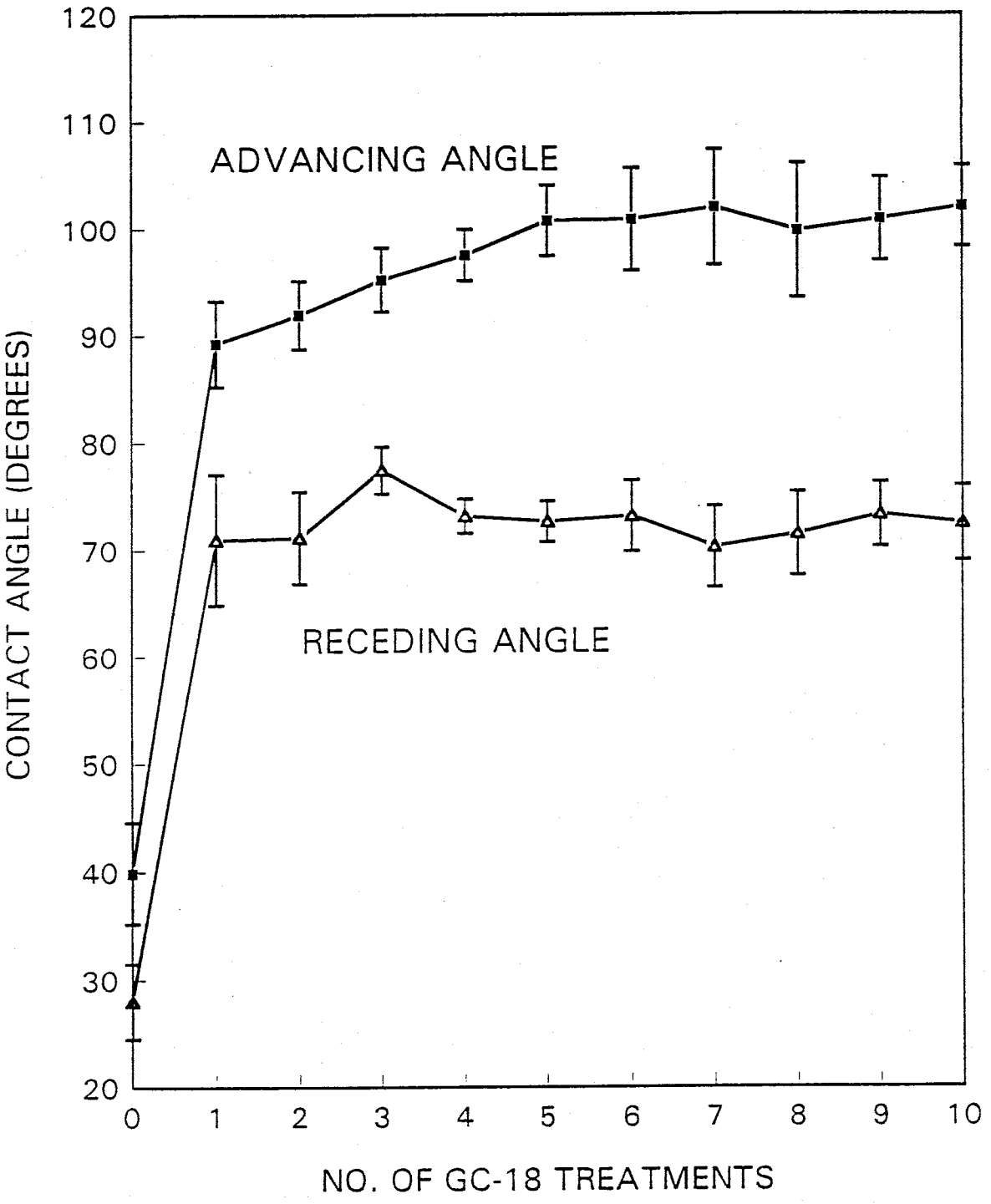

reaching a maximum value that remained essentially unchanged after successive treatments. Figure 3.11 indicates that after about five treatments, the advancing angle remains stable at just above 100°, and the receding angle stabilizes at just above 70°.

Several experiments were conducted to confirm the stability of GC-18 treatments over time. Experiment CAM29A shows that the water-air contact angle on a GC-18-treated slide stored in air remains stable for over 800 hours (Figure 3.12). The advancing angle ranges between 95 and 100°, and the receding angle is between about 73 and 79°.

The second experiment is CAM29, which shows that the water-air contact angle on a GC-18-treated slide stored in water with 1000 mg/L $NaN_3$ remains relatively stable for over 800 hours (Figure 3.13). The advancing angle falls between 90 and 100°, and the receding angle ranges between about 70 and 75°.

Discussion of the contact angle measurements

In all of the contact angle measurements a difference between the advancing and receding angle, known as hysteresis, was observed. Hysteresis ranged from about 1° for the Soltrol-air angle on the MTMS-treated surface to more than 35° for the water-Soltrol angle on the GC-18-treated surface.

*Temperature dependence of contact angle*

According to Adamson (1982), contact angles usually

FIGURE 3.12: CAM29A: GC-18-TREATED WATER-AIR STORED IN AIR

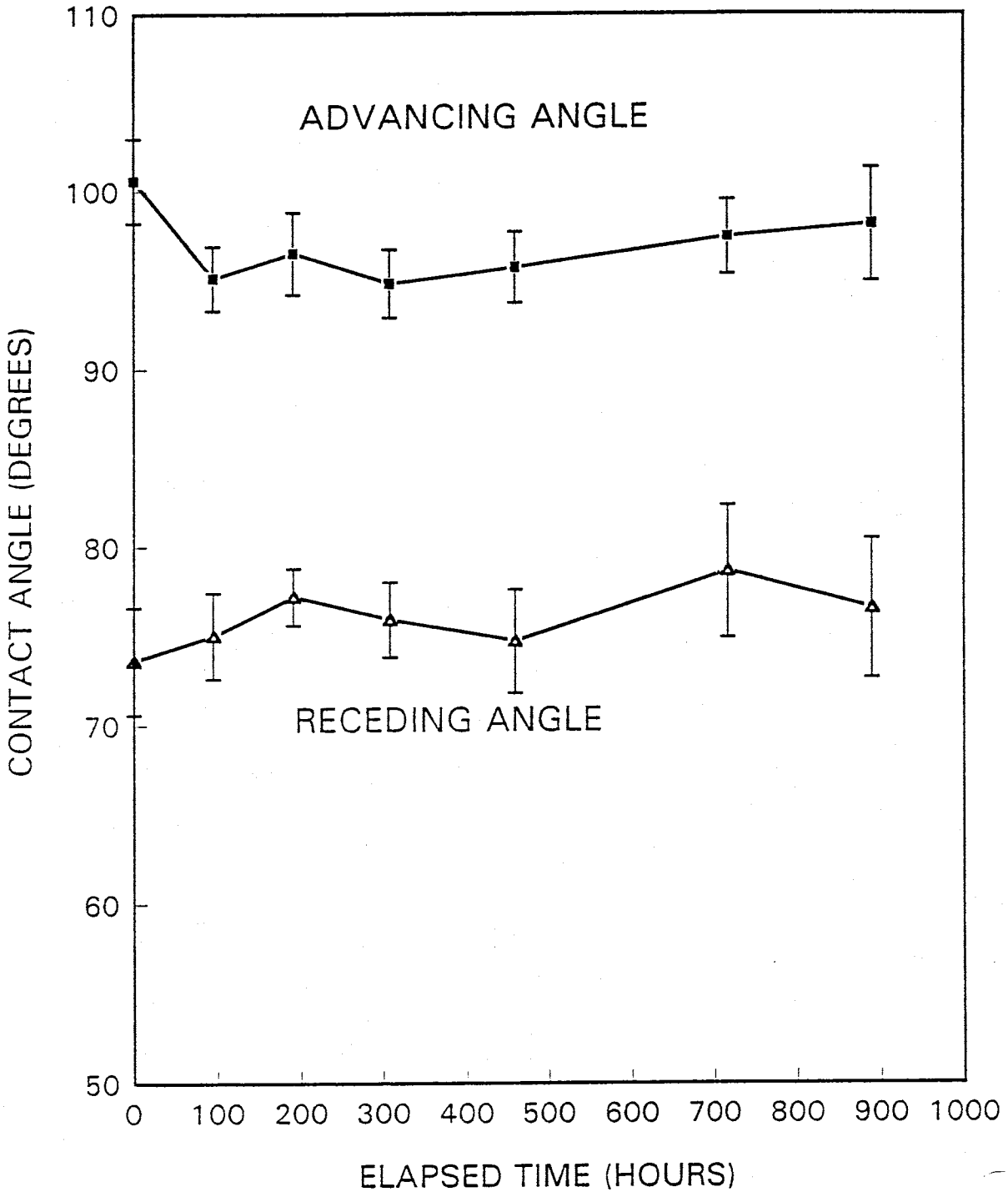

FIGURE 3.13: CAM29: GC-18-TREATED WATER-AIR STORED IN NAN3 WATER

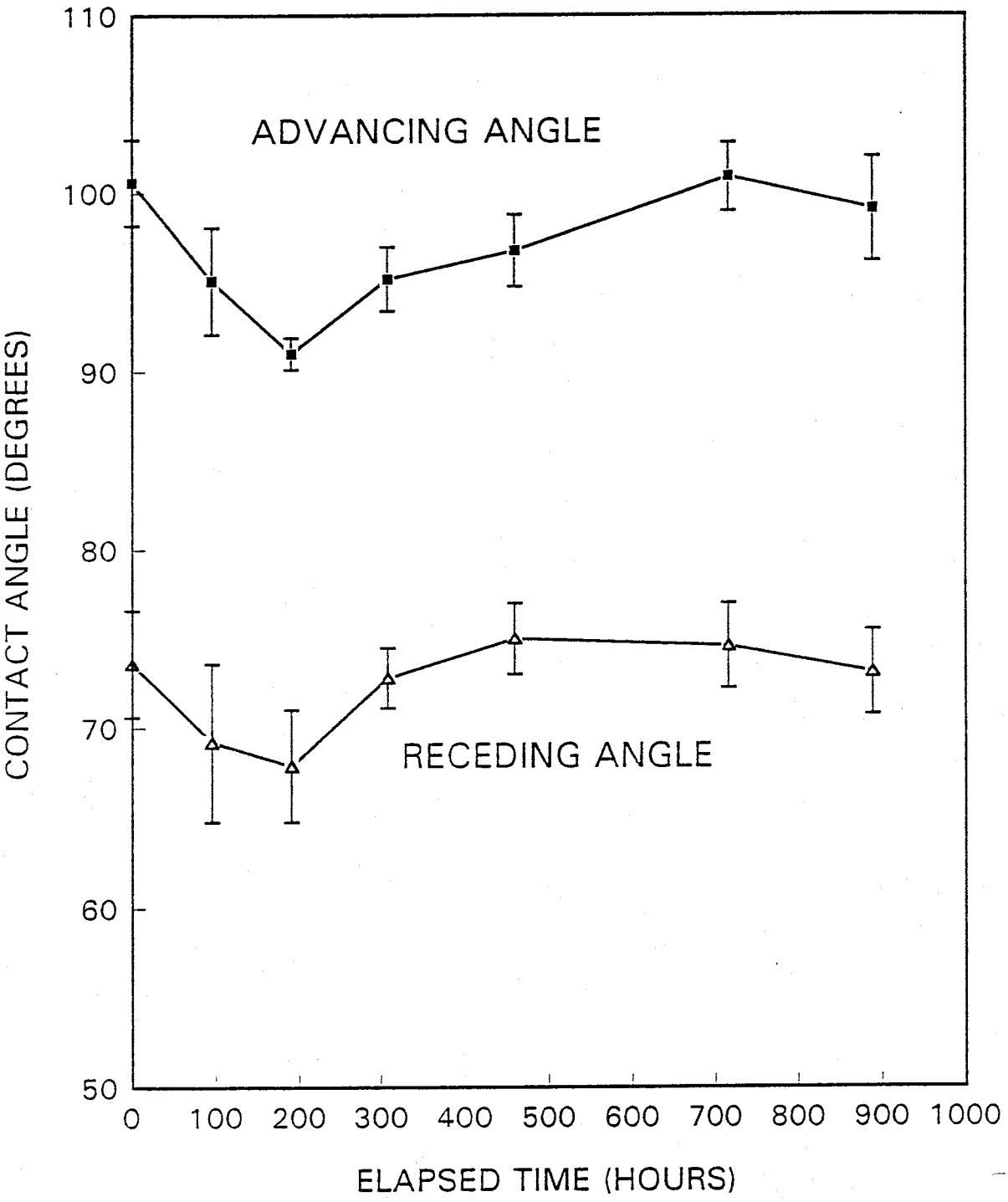

increase with decreasing temperature. The contact angle changes approximately 0.1° per degree Celsius. Therefore the fluctuations in room temperature of a few degrees observed during contact angle measurements are not likely to have introduced any large errors into these results.

*Other sources of error in the contact angle measurements*

During the contact angle measurements the stage and the slide being observed were probably never perfectly plumb. In addition the microscope itself was probably never perfectly level. The microliter buret and the opening at its tip were also probably not ever perfectly plumb. These experimental problems may have introduced some small errors into the contact angle results. One step taken to try to minimize these errors was to average right and left side angles together. This procedure should have averaged out the side to side errors of not having the stage or other equipment perfectly level. The coefficient of variation ranged from 1.0% to 40.4% for the 166 sets of measurements included in Appendix B. However, more than 92% of these sets of measurements had coefficients of variation below 10%.

*Comparison with other available contact angle measurements*

The advancing and receding contact angles between water and air on an untreated glass slide were found to be 6.7° and 4.5°, respectively. These results are in relatively good agreement with theory which suggests that the contact

angles should be zero. The finite contact angles found here indicate there may have been some minor contaminants adsorbed onto the slide surface.

The advancing and receding contact angles between water and air on a GC-18-treated glass slide were measured to be 87.6° and 80.2°, respectively. The results obtained by Wei, et al., (1993) for the same experiment were somewhat higher at 98.9° ± 7.9 for the advancing angle and 79.1° ± 8.6 for the receding angle. This kind of variation may be related to the degree of surface coverage achieved by the treatment.

The advancing and receding contact angles between water and Soltrol on an untreated glass slide were found to be 43.5° and 19.9°, respectively. Wei (1991) measured these to be somewhat higher at 68.8° for the advancing angle and 40.7° for the receding angle. The difference between the two results may be attributed to the difference in slide preparation. The current research omitted an oven drying procedure. Contaminants adsorbed onto the slide during the oven drying procedure could account for the higher contact angles seen by Wei.

The advancing and receding contact angles between water and Soltrol on a GC-18-treated glass slide were measured to be 147.7° and 112.3°, respectively. The results obtained by Wei, et al., (1993) for the same experiment were in good agreement at 151.4° for the advancing angle and 119.8° for the receding angle.

Measuring contact angles using the dynamic sessile drop method is an excellent method to obtain relatively reliable results. Of course, lining up the goniometer crosshair with the tangent line of the angle is subjective, and therefore some minor differences in readings (a few degrees) by different researchers should be expected.

### 3.2 Surface and Interfacial Tension Results

Surface and interfacial tension measurements were made for the three fluid combinations used. The results of these experiments, along with standard deviations, are summarized in Table 3.2, and the experimental data are included in Appendix C.

Table 3.2: Surface and Interfacial Tension Results

| FLUID PAIR | SURFACE OR INTERFACIAL TENSION |
|---|---|
| WATER - AIR | 70.7 ± 0.2 DYNES/CM |
| WATER - SOLTROL 130 | 36.9 ± 0.7 DYNES/CM |
| SOLTROL 130 - AIR | 22.6 ± 0.1 DYNES/CM |

The surface tension between water and air at 21.5° C was 70.7 ± 0.2 dynes/cm (STM 101). When the water was degassed, the surface tension between water and air decreased slightly to 70.1 ± 0.4 dynes/cm (STM 102). Using water that was degassed and spiked with 1000 mg/L $NaN_3$, the surface tension between water and air dropped to 65.3 ± 1.5 dynes/cm (STM 103). When the measurement was performed

inside the constant temperature cabinet to raise the temperature to 26° C, the water-air surface tension dropped slightly to 69.6 ± 0.2 dynes/cm (STM 109).

The Soltrol 130-air surface tension was 22.6 ± 0.1 dynes/cm. The effect of degassing the Soltrol on the Soltrol-air surface tension was minor, with a decrease of only 0.1 dynes/cm for the degassed Soltrol (STM 104 and STM 105).

The interfacial tension between water and Soltrol 130 was 36.9 ± 0.7 dynes/cm (STM 106, 107, and 108).

Discussion of surface and interfacial tension measurements

The value for surface tension between water and air is consistent with the results from previous studies (Table 3.3). Most of these studies found the water-air surface tension was just above 70 dynes/cm.

Table 3.3 Summary of Other Reported Water-Air Surface Tension Measurements (modified from Demond, 1988)

| STUDY | WATER - AIR SURFACE TENSION |
|---|---|
| Calhoun, et al., 1949 | 70 DYNES/CM |
| Demond, 1988 | 71.8 ± 0.6 DYNES/CM |
| Dumore and Schols, 1974 | 71 DYNES/CM |
| Morrow and Mungan, 1971<br>Morrow, 1976<br>Morrow and McCaffery, 1978 | 70.6 DYNES/CM |
| Lenhard and Parker, 1987 | 66.4 DYNES/CM |
| Hillel, 1980 | 72.7 DYNES/CM |

A comparison of the water-Soltrol 130 and Soltrol 130-air interfacial tension results with results obtained by

others is difficult because each lot of Soltrol is different. Wei (1991) reported a water-Soltrol 130 interfacial tension of 40.5 dynes/cm. Corey (1986) reported a Soltrol-air surface tension of about 23 dynes/cm, which is close to our result. Wilson, et al., (1990) reported a Soltrol 130-air surface tension of 19.1 ± 0.3 dynes/cm.

The temperature and pressure dependence of interfacial tension of several water-organic fluid systems was investigated by Jennings (1967). Jennings found that the change in interfacial tension with both temperature and pressure is relatively minor. The change in interfacial tension was approximately 0.1 dyne/cm per degree Celsius (°C) and 0.001 dyne/cm per atmosphere for benzene-water and n-decane-water systems. The interfacial tension decreased with increasing temperature and increased as pressure increased. These trends are typical of most fluid pairs. Thus it is unlikely that temperature fluctuations in the lab introduced any significant errors in the interfacial tension measurements. Perhaps the most likely source of error in these measurements is any contaminants such as surfactants that may be present in the fluids or on the glassware. In an attempt to minimize these problems, careful attention was paid to cleaning the dedicated glassware and to preparing the fluids used in the interfacial tension measurements.

## 3.3 Capillary Pressure-Saturation Results

This section presents the results of the capillary pressure-saturation experiments performed using the techniques and materials described in Chapter 2. The following table (Table 3.4) gives the results of total volume, void volume, porosity and bulk density calculations for columns prepared using the standard method. For the columns prepared using the alternate procedure (ie., without top endcaps), only void volumes were calculated. This was done because the remaining parameters could not be calculated rigorously.

Table 3.4 Short Column Data

| Experiment No. | Total Volume (cc) | Void Volume (cc) | Porosity (-) | Bulk Density (g/cc) |
|---|---|---|---|---|
| 6 | 107.77 | 39.70 | 0.368 | 1.560 |
| 7 | 106.43 | 38.88 | 0.365 | 1.568 |
| 23 | - | 7.2 | - | - |
| 24 | - | 6.6 | - | - |
| 25 | - | 6.0 | - | - |
| 27 | - | 5.7 | - | - |
| 28 | - | 8.4 | - | - |
| 30 | - | 3.5 | - | - |
| 35 | - | 8.8 | - | - |
| 37 | 41.27 | 15.45 | 0.374 | 1.545 |
| 38 | 48.50 | 18.47 | 0.381 | 1.529 |
| 39 | 42.65 | 16.16 | 0.379 | 1.534 |

Untreated Bead Experiments

Column experiment PB6, which is the water-air column

with untreated beads, is shown in Figure 3.14. This column began draining at a capillary pressure of about 150 cm of water and drained to an irreducible water saturation (IWS) of 7.8%. At the end of the imbibition stage, water occupied about 87% of the pore space. Experiment PB7 (Figure 3.14), a duplicate of PB6, agrees well with the previous experiment. This column also began draining at about 150 cm of water. The IWS is 7.7%, and about 87% of the pore volume was filled with water following imbibition.

Figure 3.15 shows the results of experiment PB24 which was a water-saturated column drained with Soltrol packed with untreated beads. This column began to drain at a capillary pressure of about 90 cm of water. The IWS was about 4%, and residual oil saturation (ROS) was about 18%.

Experiment PB23 consisted of a Soltrol-saturated column packed with untreated beads and drained by air (Figure 3.16). Drainage of the column started at about 50 cm of Soltrol. The irreducible Soltrol saturation was about 8%. The imbibition curve for this experiment indicates that about 96% of the pore space was occupied by Soltrol. This is significantly higher than the 80 to 85% saturation normally associated with this kind of experiment. Therefore, the imbibition curve of this experiment should be interpreted with caution.

MTMS Bead Experiments

Experiment PB38 was conducted with MTMS-treated beads

FIGURE 3.14: PRESSURE-SATURATION CURVE
PB6 AND PB7 UNTREATED WATER-AIR

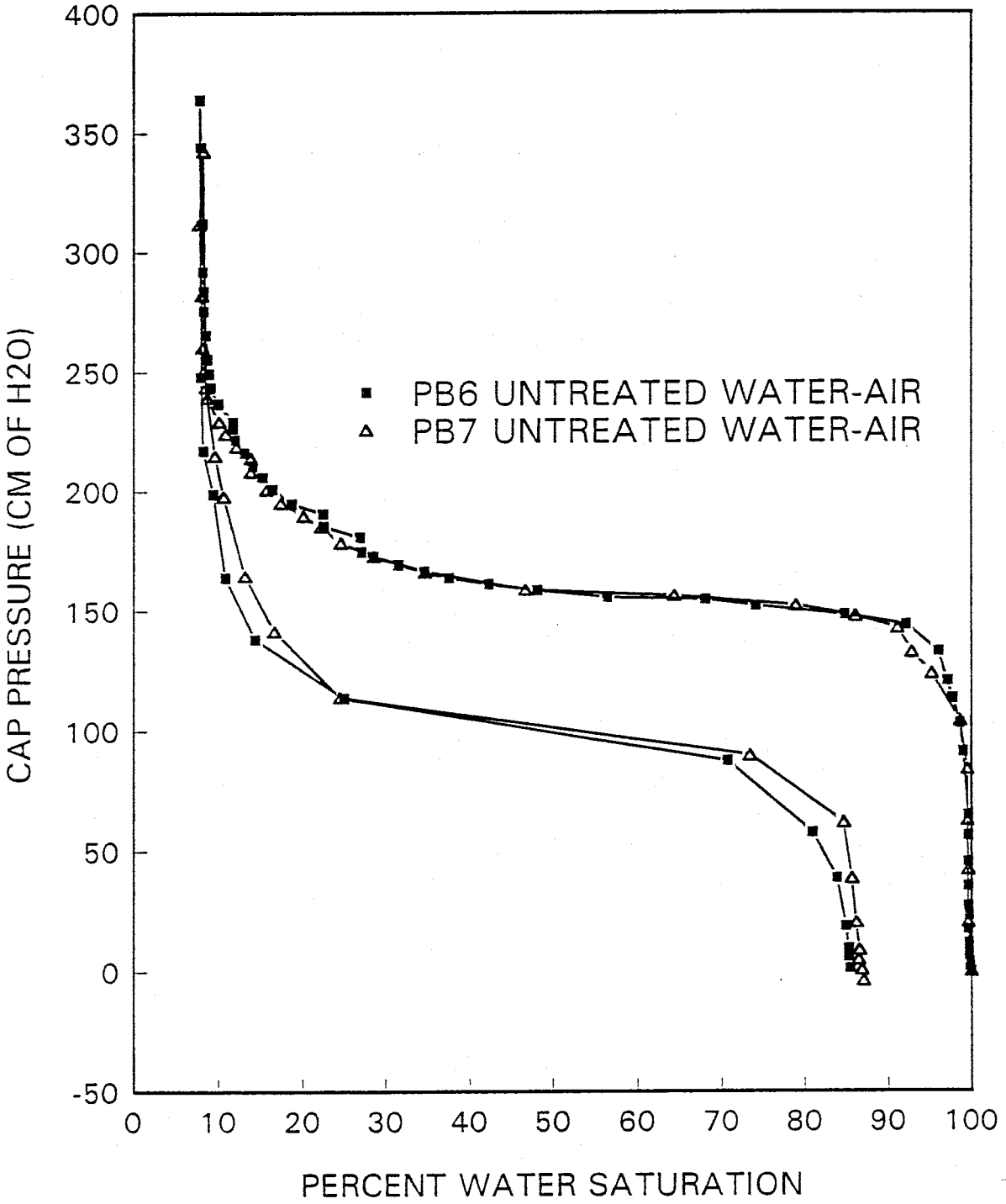

FIGURE 3.15: PRESSURE-SATURATION CURVE
PB24 UNTREATED WATER-SOLTROL

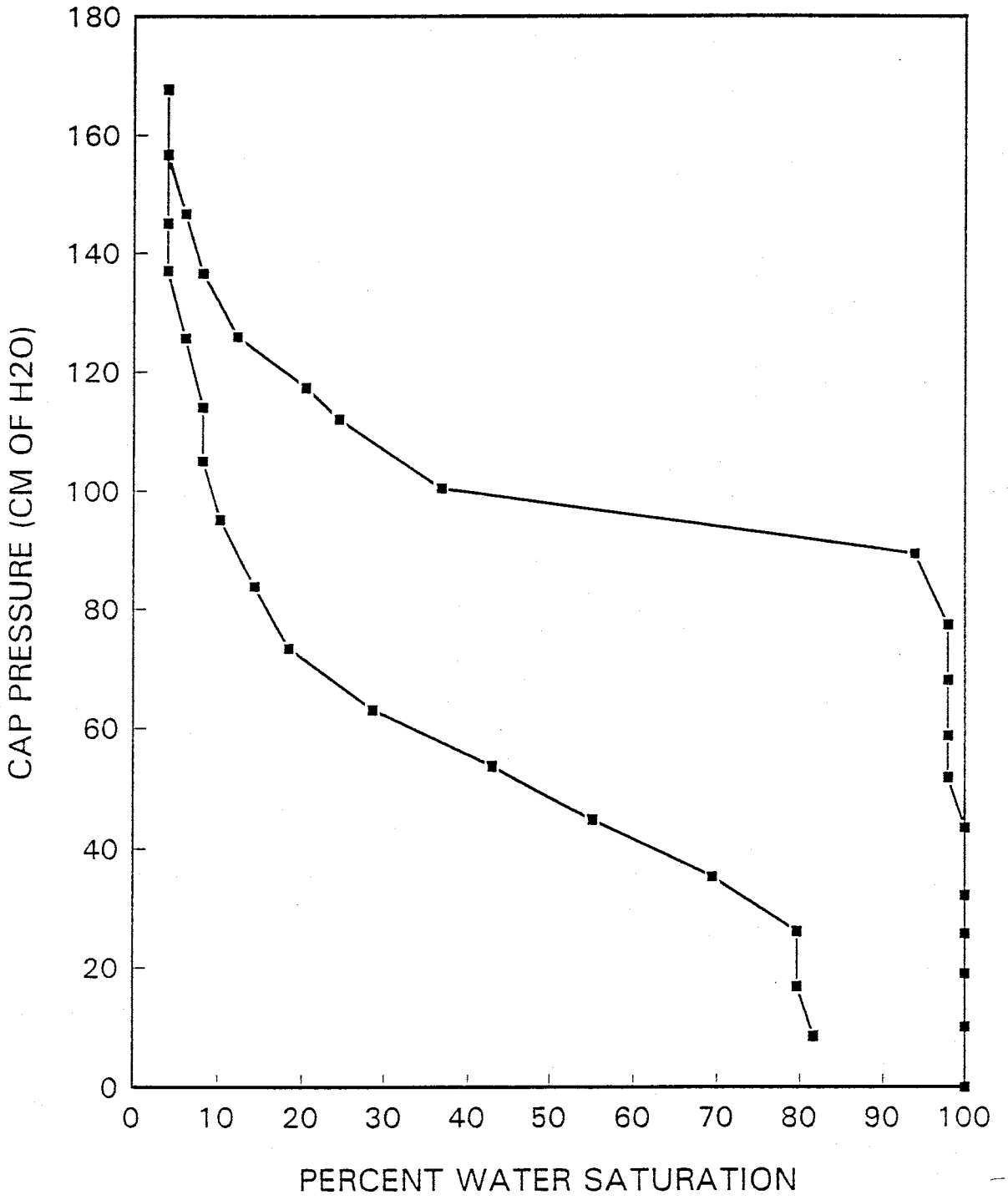

FIGURE 3.16: PRESSURE-SATURATION CURVE
PB23 UNTREATED SOLTROL-AIR

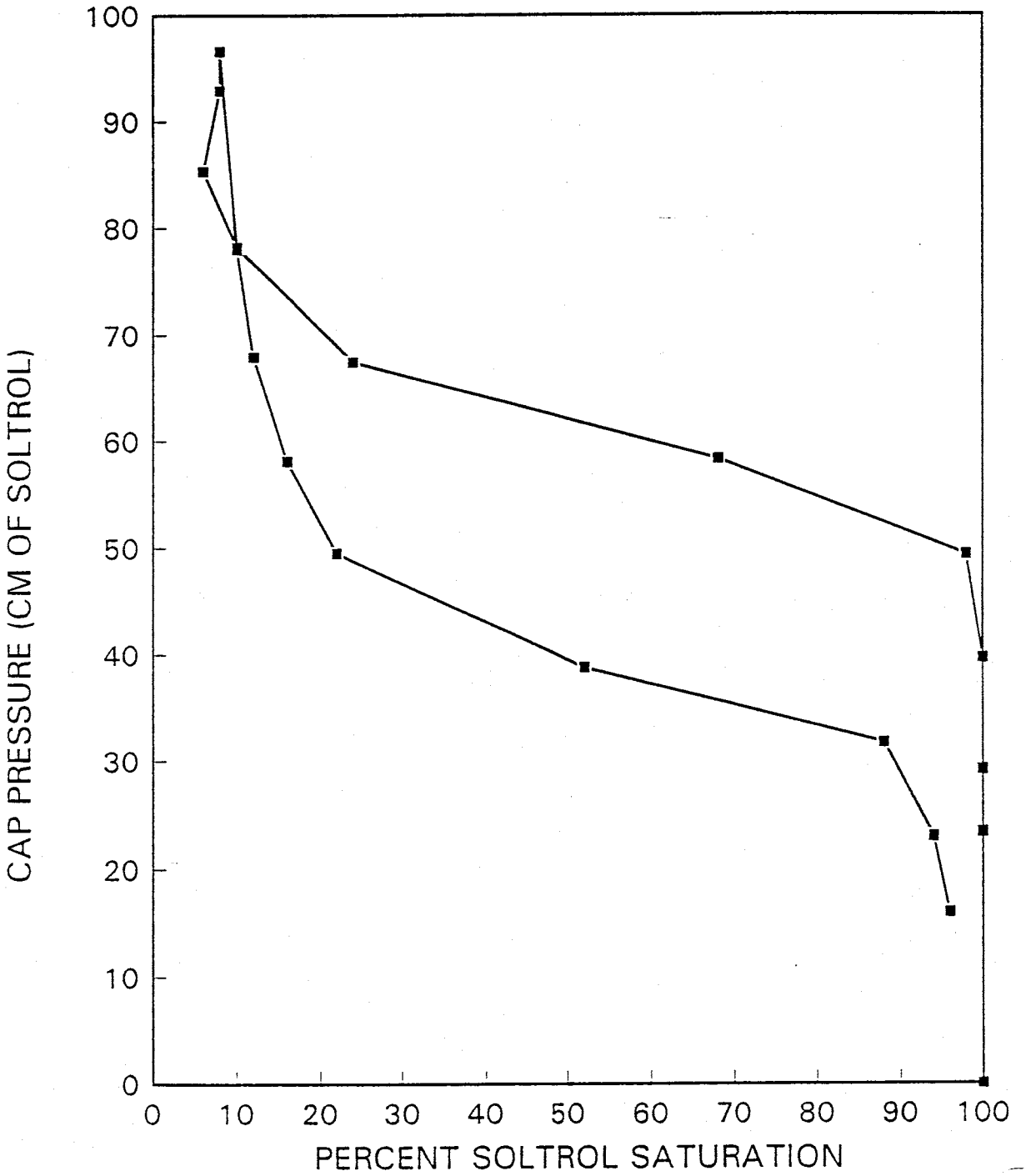

(Figure 3.17). The fluids were water and air. Drainage began at about 40 cm of water. The IWS was about 6%, and the water imbibed to occupy about 72% of the pore space. PB39 (Figure 3.17) was a duplicate of PB38. This experiment had an air entry pressure of about 60 cm of water. The IWS was about 12.5, and the pore volume was about 80% saturated at the end of the imbibition stage.

Experiment PB35 was conducted with MTMS-treated beads (Figure 3.18). The column was initially saturated with Soltrol and was drained with water. Drainage of the Soltrol began at low capillary pressure. The irreducible Soltrol saturation was about 4%. The imbibition curve is nearly vertical with only a small increase in Soltrol saturation.

Experiment PB37 was a Soltrol-air column packed with MTMS-treated beads (Figure 3.19). Drainage began at approximately 50 cm of Soltrol. The irreducible Soltrol saturation was about 3.3%, and Soltrol reimbibed to take up 82% of the pore space.

GC-18 Bead Experiments

Column PB28 was performed with GC-18-treated beads (Figure 3.20). The column was saturated with water and drained with air. Drainage occurred at about 30 cm of water. Drainage stopped at a water saturation of 45%. The imbibition curve was nearly vertical with almost no increase in water saturation.

Experiment PB27 was packed with GC-18-treated beads.

FIGURE 3.17: PRESSURE-SATURATION CURVE
PB38 AND PB39 MTMS-TREATED WATER-AIR

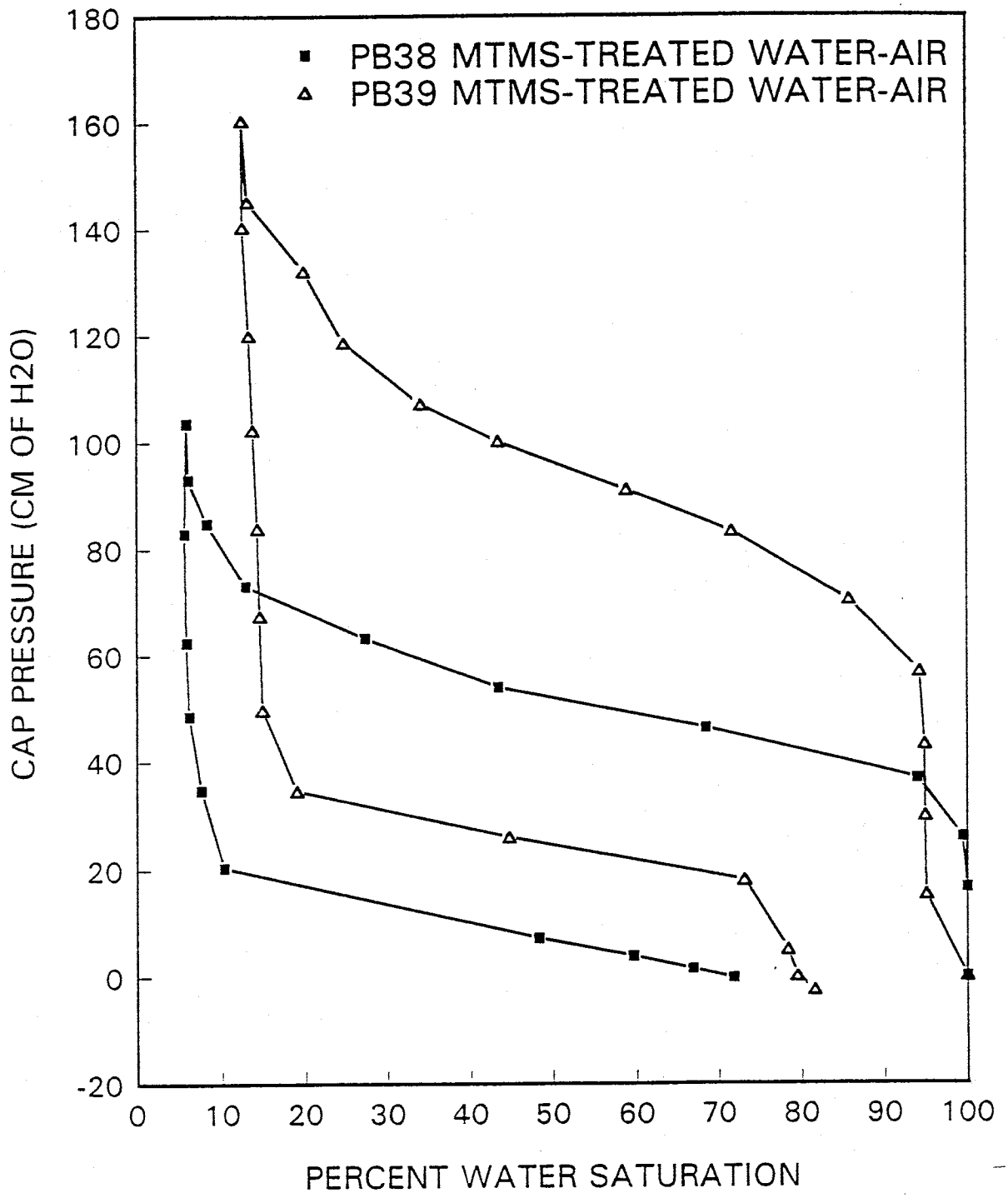

FIGURE 3.18: PRESSURE-SATURATION CURVE
PB35 MTMS-TREATED WATER-SOLTROL

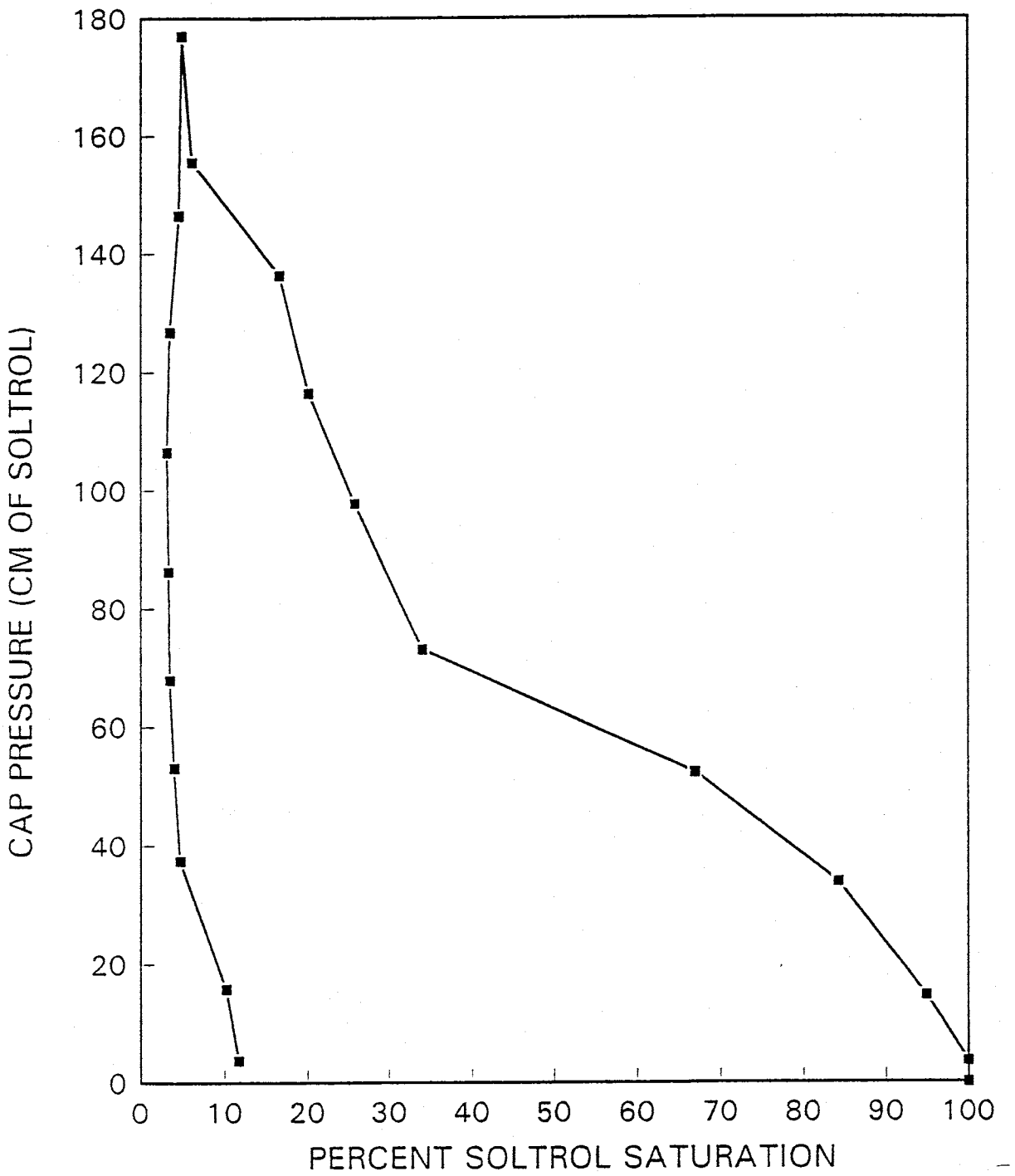

FIGURE 3.19: PRESSURE-SATURATION CURVE
PB37 MTMS-TREATED SOLTROL-AIR

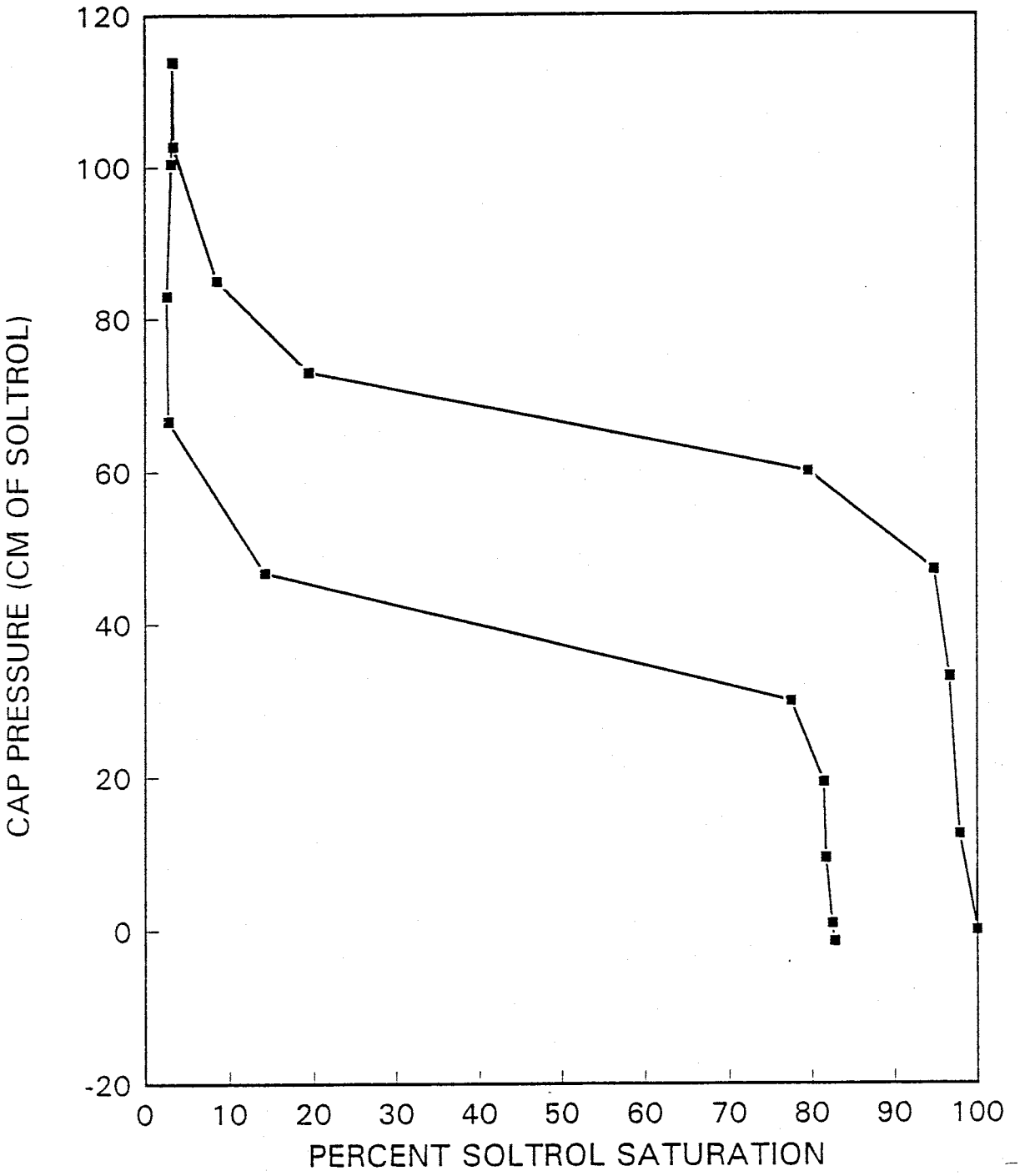

FIGURE 3.20: PRESSURE-SATURATION CURVE
PB28 GC-18-TREATED WATER-AIR

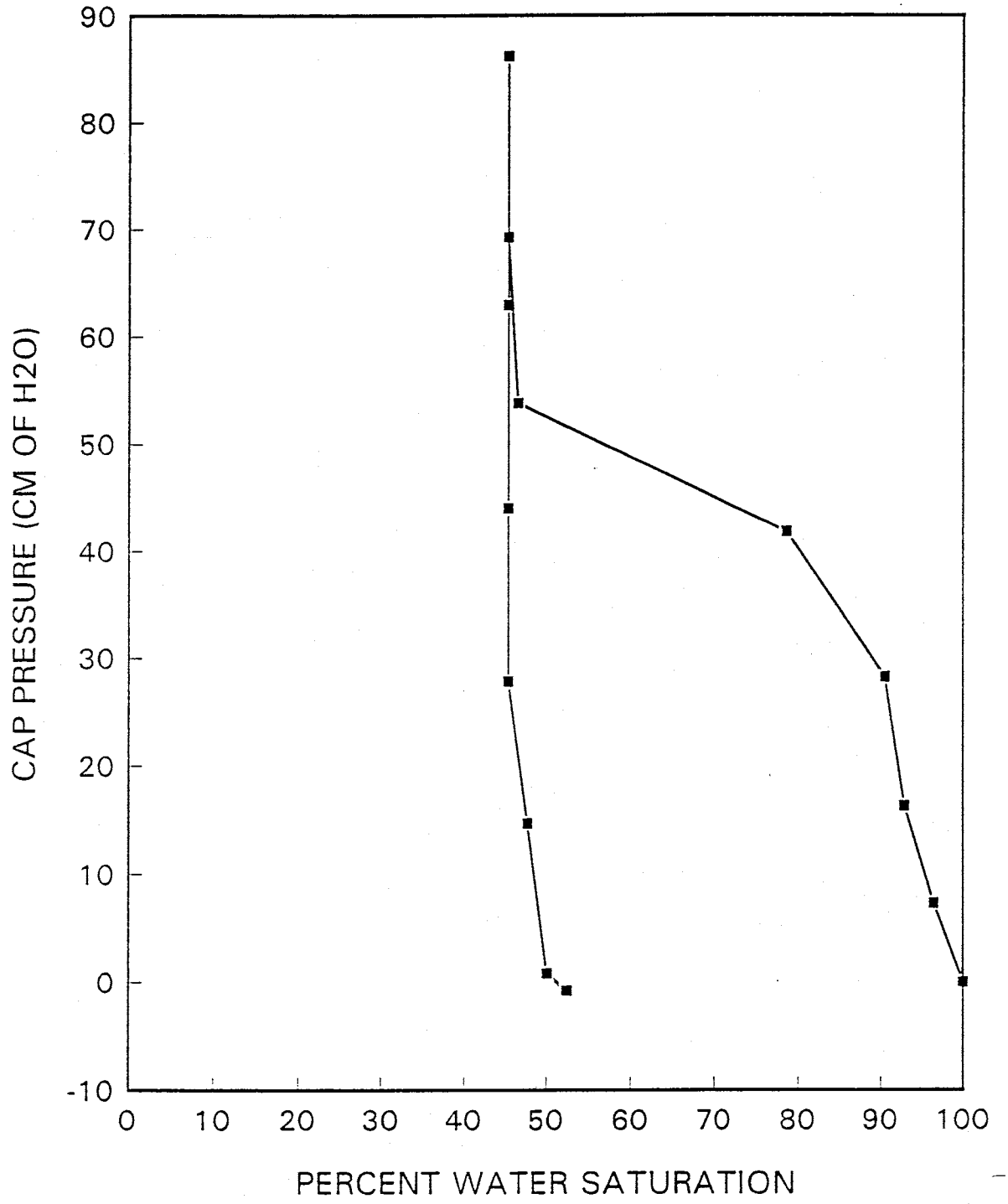

It was saturated with Soltrol and drained with water (Figure 3.21). Drainage began at about 120 cm of Soltrol. Soltrol drained to about 29%. The imbibition portion of the experiment is probably not valid because it indicates that Soltrol occupied 93% of the pore space.

Column PB25 was a Soltrol-air experiment packed with GC-18-treated beads (Figure 3.22). Drainage of Soltrol began at about 60 cm of Soltrol. The irreducible Soltrol saturation was 6%. Again there were experimental problems associated with the imbibition portion of the curve. However, the imbibition curve is probably valid to about 40 cm of Soltrol and about 60% Soltrol saturation.

Experiment PB30 (Figure 3.22) was a duplicate of PB25. Drainage began at about 60 cm of Soltrol. The irreducible Soltrol saturation was about 2%. In this experiment the imbibition curve was somewhat better than the previous experiment, but still failed before it returned to zero capillary pressure.

## 3.4 Scaled Capillary Pressure-Saturation Results

Prior to scaling our capillary pressure-saturation results, we compared our untreated water-air experiment with that of Haines (1930). The two sets of results are plotted together in Figure 3.23. The general agreement between the two systems is good. The match is excellent for the drainage curve and appears reasonable for the imbibition

FIGURE 3.21: PRESSURE-SATURATION CURVE
PB27 GC-18-TREATED WATER-SOLTROL

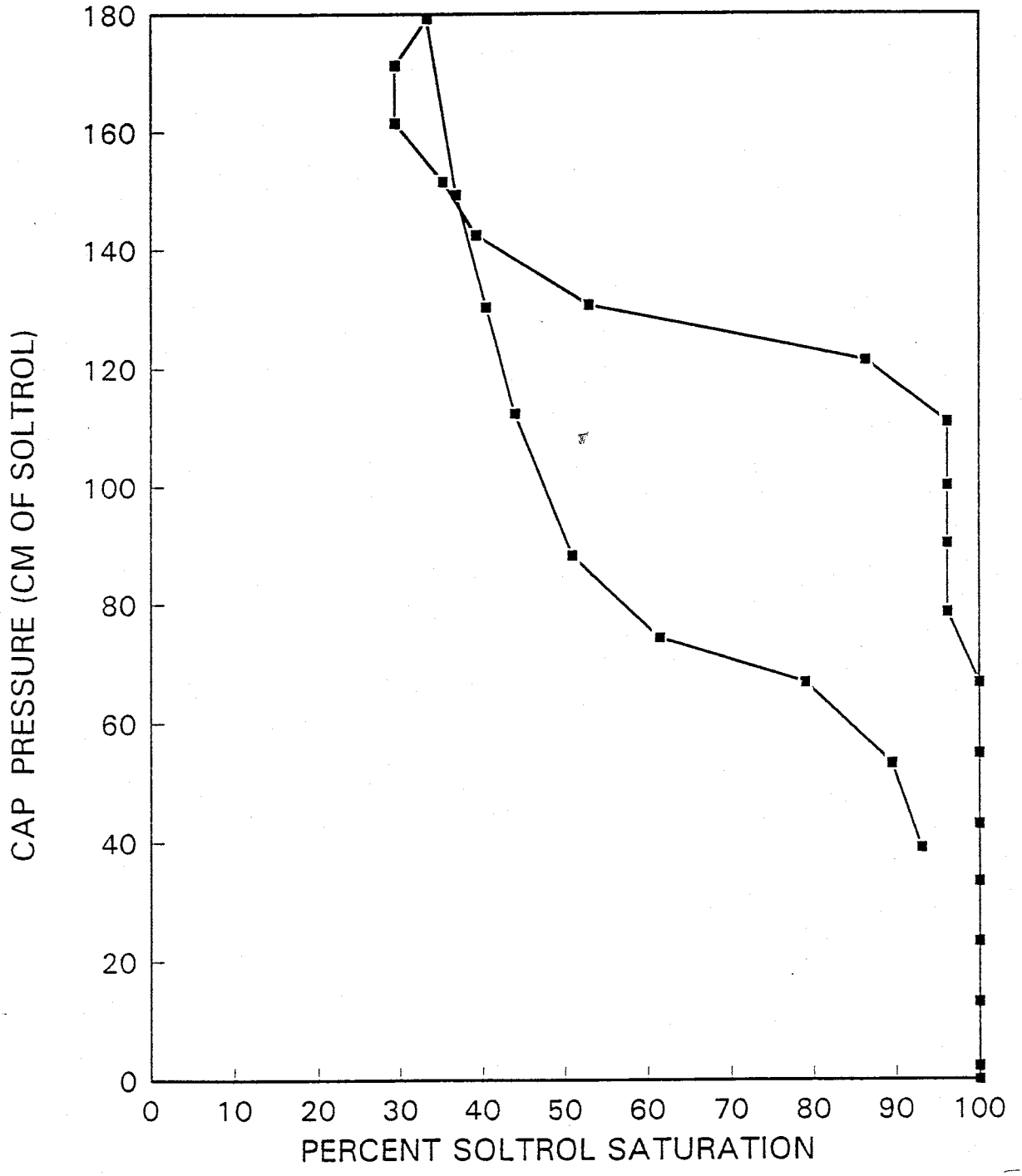

FIGURE 3.22: PRESSURE-SATURATION CURVE
PB25 AND PB30 GC-18-TREATED SOLTROL-AIR

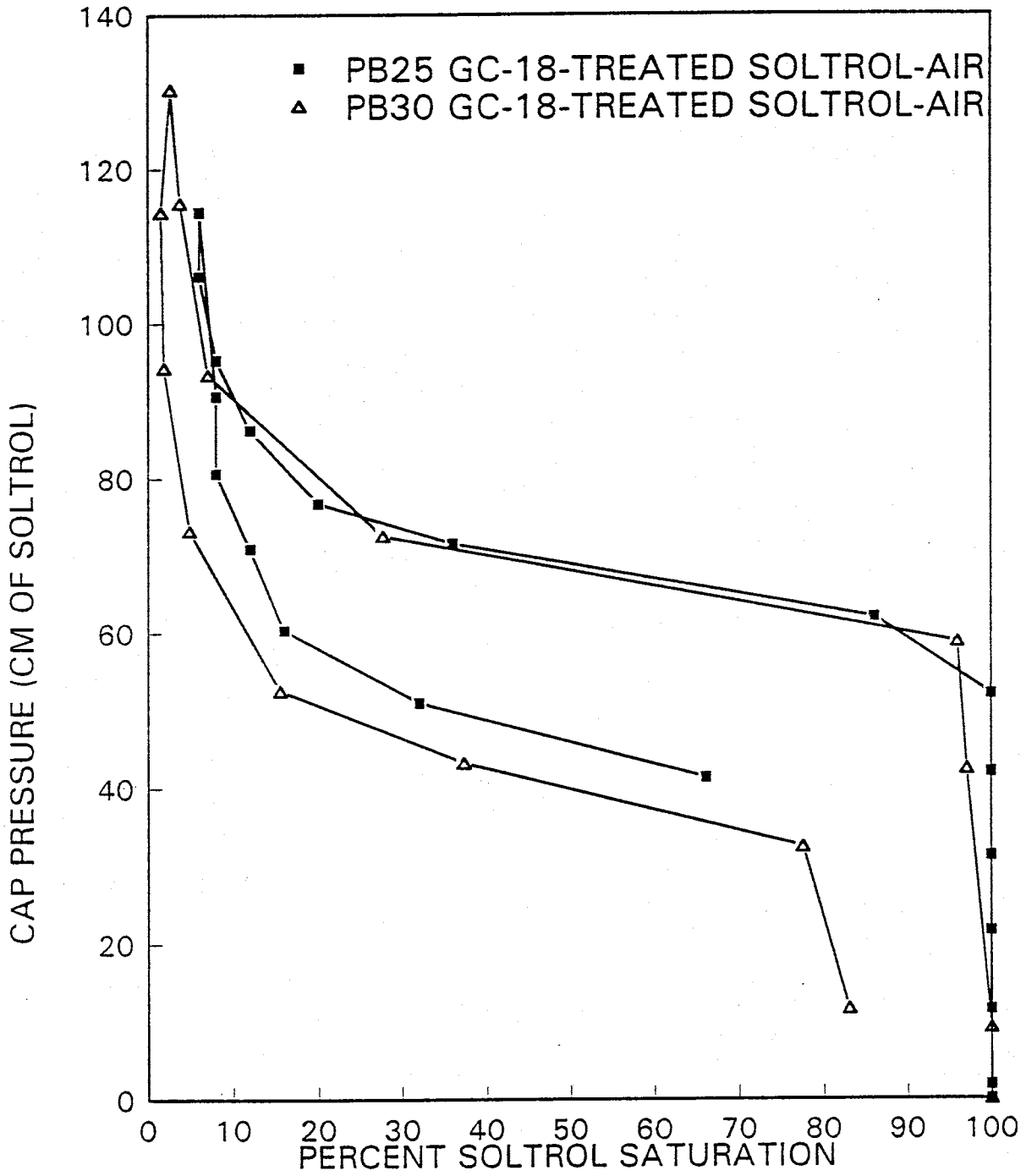

FIGURE 3.23: HAINES UNTREATED WATER-AIR VS. PB6 UNTREATED WATER-AIR

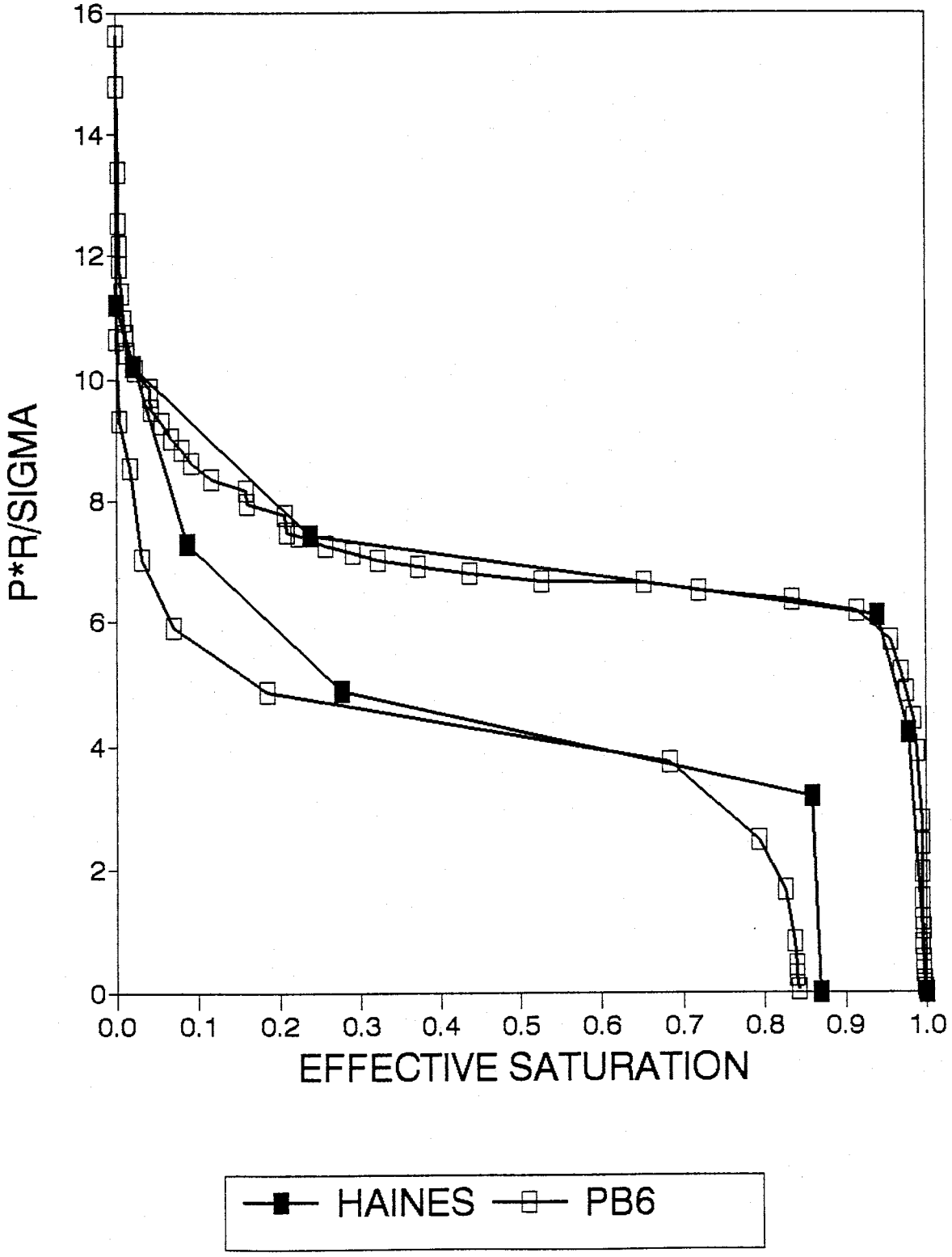

curve.

The following figures show the results of scaling the capillary pressure-saturation curves using the capillary tube model. Figures 3.24 to 3.26 are examples of low contact angle systems for which the scaling procedure worked relatively well. In each of these figures, the scaled curve for the untreated water-air system (Experiment PB6) is used as a control curve for comparison. Figure 3.24 compares the untreated water-air system (PB6) to the untreated water-Soltrol system (PB24). Agreement between the two systems is good, and the curves nearly overlap.

Figure 3.25 shows the results of the untreated water-air system (PB6) and the untreated Soltrol-air system (PB23). Again the curves match fairly well.

The untreated water-air system (PB6) is compared with the MTMS-treated Soltrol-air system (PB37) in Figure 3.26. These curves match well.

The remaining experiments did not scale well. Figure 3.27 shows the results of the GC-18-treated Soltrol-air experiment (PB25). The curves are offset with the GC-18-treated system falling higher on the pressure axis than the untreated system. The GC-18-treated Soltrol-air system has low contact angles, so we might have expected this system to scale better than it did. The discrepancy may be that the geometry in the porous media changes the contact angle operating in the column from that measured on a glass slide.

FIGURE 3.24: SCALED PRESSURE-SATURATION CURVE UNTREATED WATER-AIR VS. UNTREATED WATER-SOLTROL

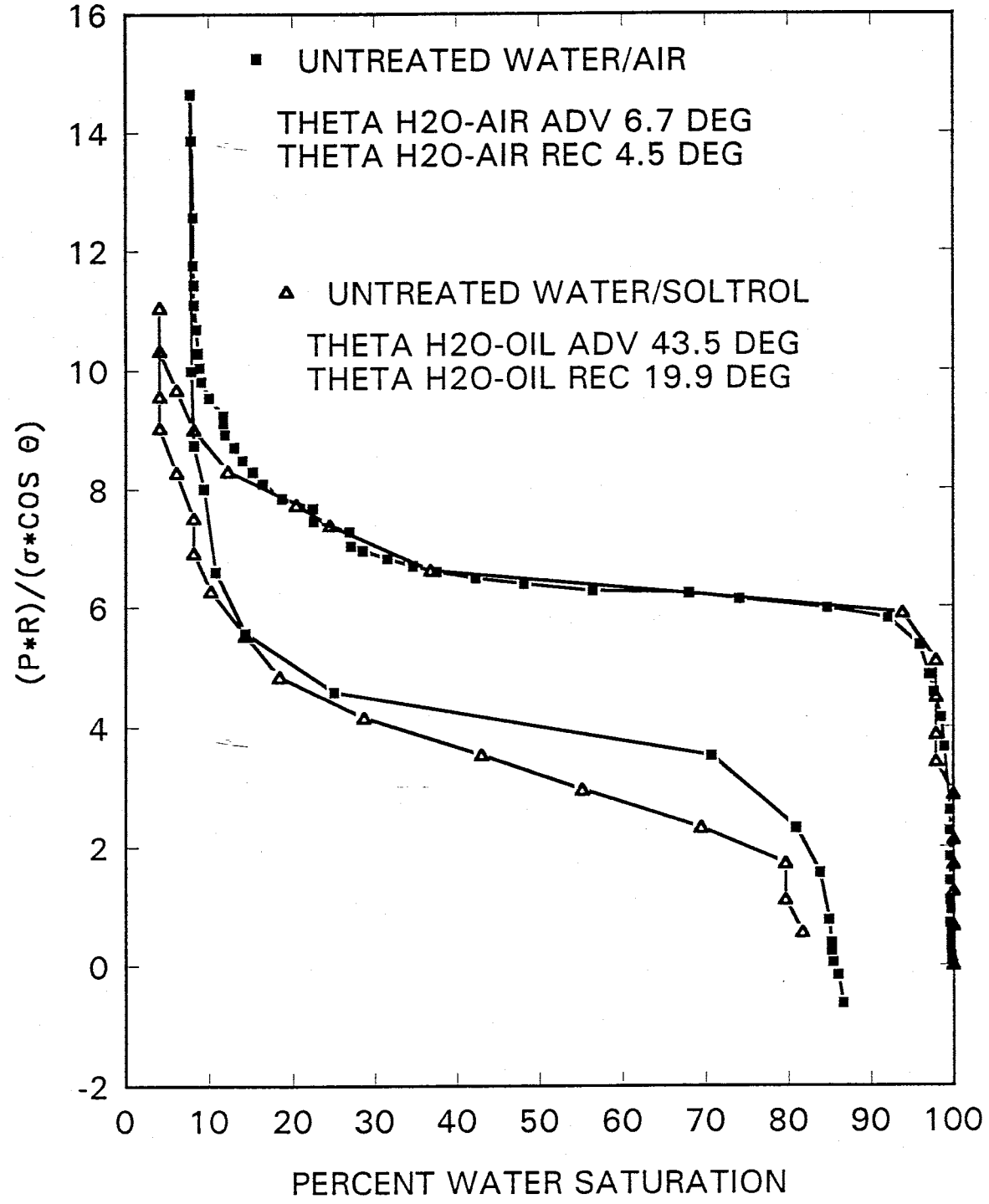

FIGURE 3.25: SCALED PRESSURE-SATURATION CURVE UNTREATED WATER-AIR VS. UNTREATED SOLTROL-AIR

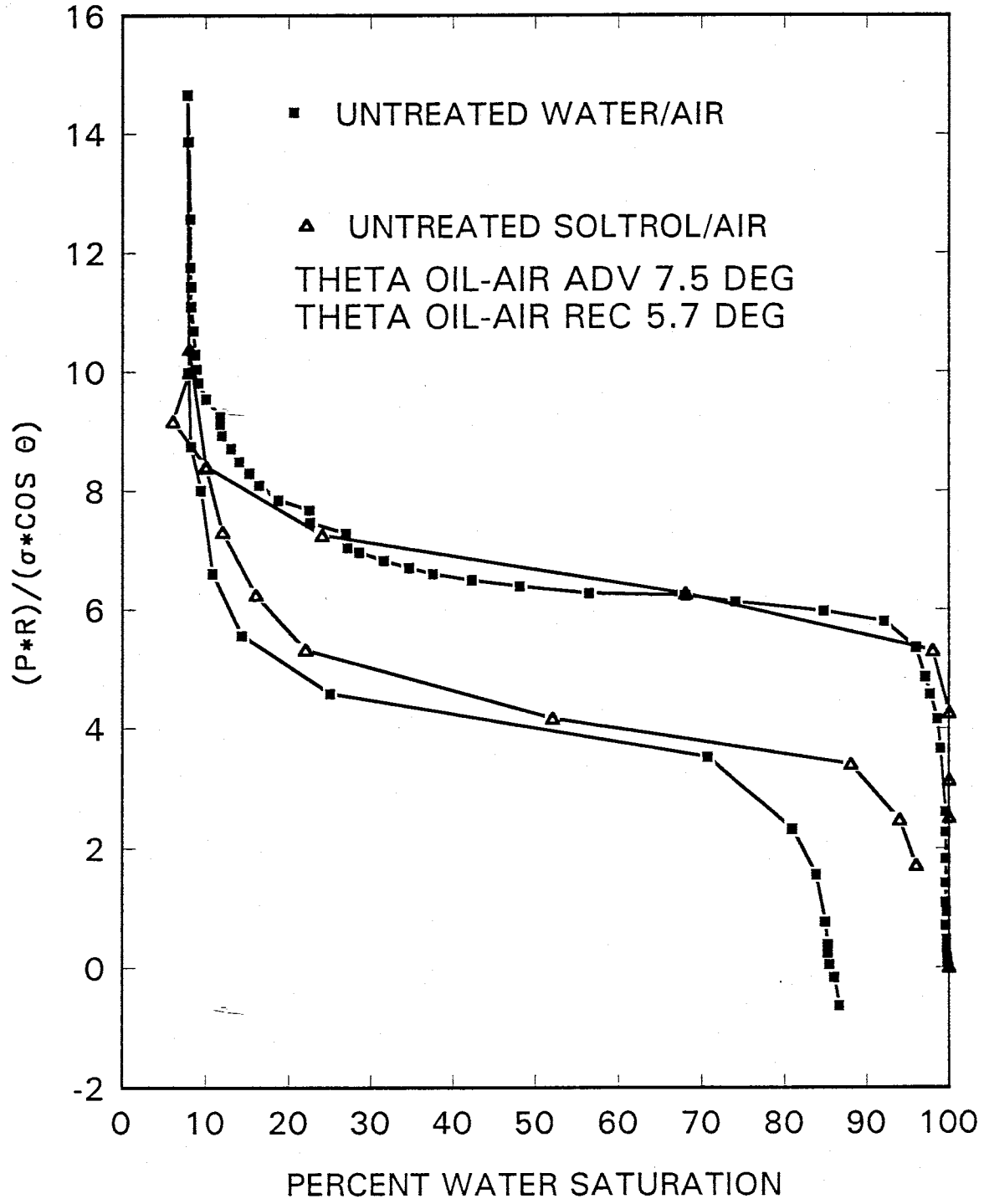

FIGURE 3.26: SCALED PRESSURE-SATURATION CURVE UNTREATED WATER-AIR VS. MTMS-TREATED SOLTROL-AIR

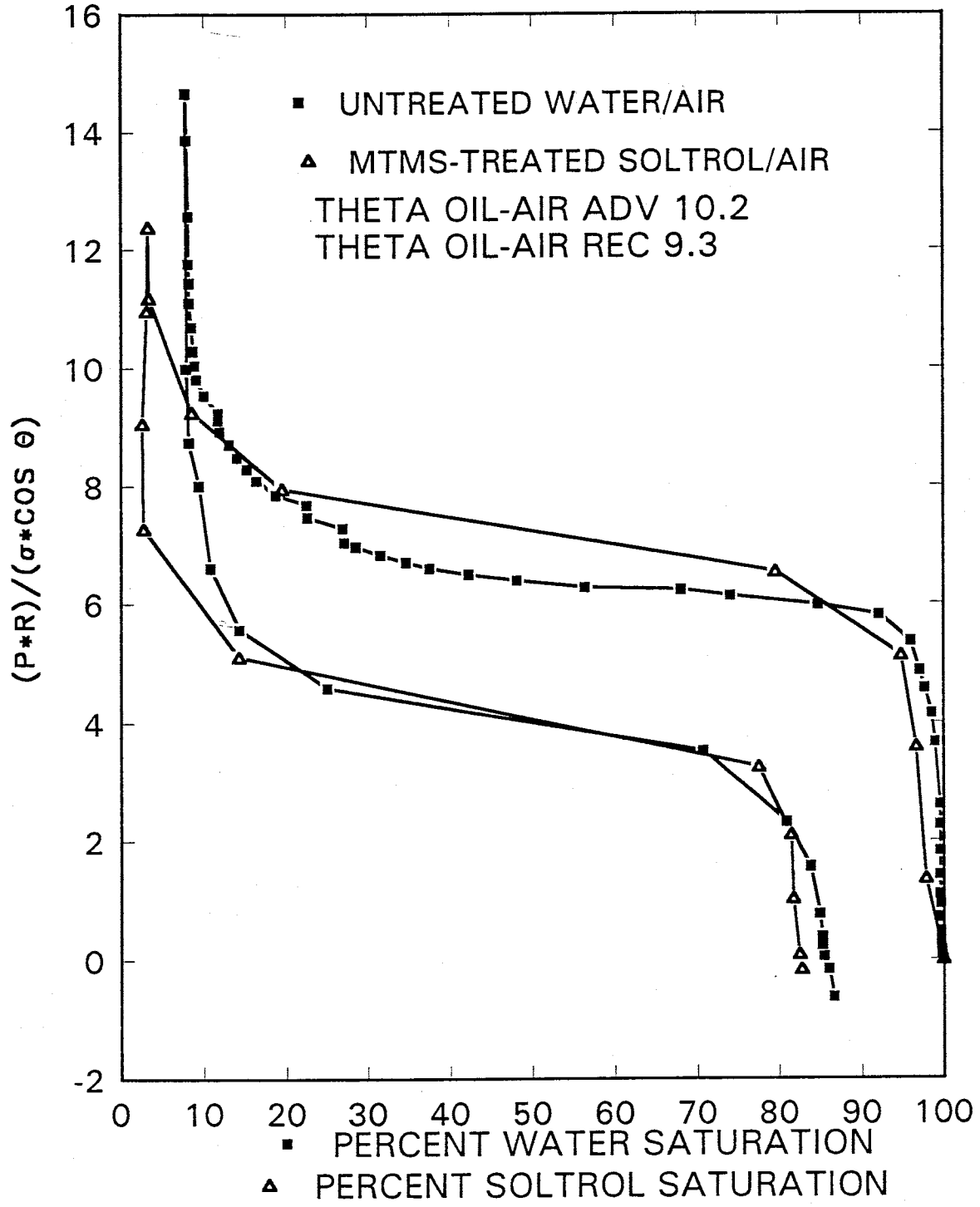

FIGURE 3.27: SCALED PRESSURE-SATURATION CURVE UNTREATED WATER-AIR VS. GC-18-TREATED SOLTROL-AIR

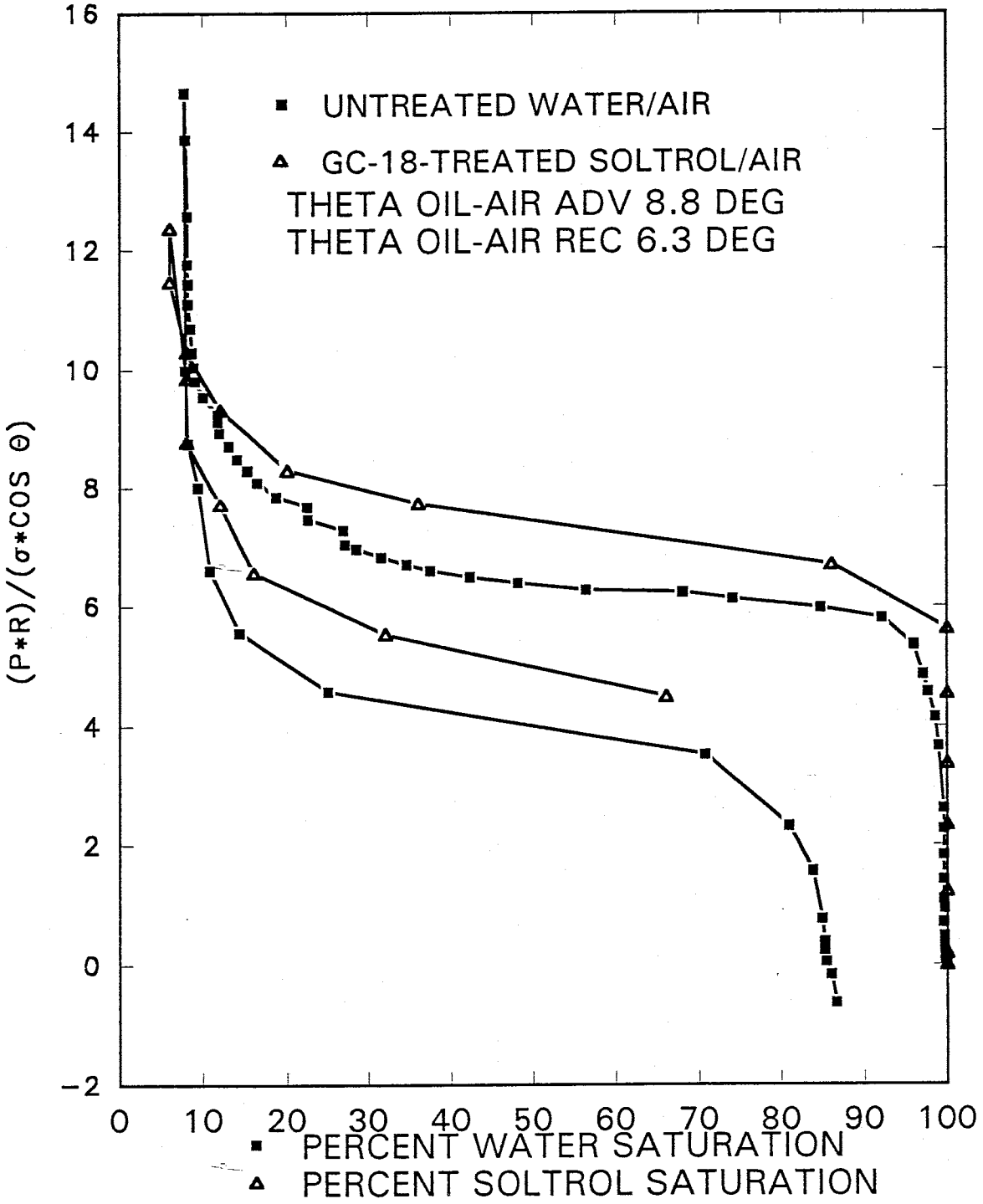

Figure 3.28 shows the results of the MTMS-treated water-air system (PB39). In this case the drainage curve for the MTMS-treated system was much higher on the capillary pressure axis than the untreated system. Although the imbibition curves match fairly well, this agreement may be coincidental.

The results of the MTMS-treated water-Soltrol system (PB35) are illustrated in Figure 3.29. The drainage curve for the MTMS-treated system is much higher than the untreated system. The imbibition curve is almost completely vertical, indicating that almost none of the drained fluid was able to imbibe.

Figure 3.30 shows the results of the GC-18-treated water-Soltrol system (PB27). The drainage curve of the GC-18-treated system is much higher than the untreated system.

Figure 3.31 shows the results of the GC-18-treated water-air system (PB28).

Figure 3.32 illustrates the results of an attempt to scale data obtained by Wei (1991) for a hydrophilic water-Soltrol system with 300 micron beads. The drainage curves are in good agreement. Wei's scaled imbibition curve is somewhat higher than that for the control system. However, overall the agreement is reasonable.

Several systems were scaled using the correction factor proposed by Desai, et al., (1992). Figure 3.33 shows the experimental and predicted curves for untreated water-

FIGURE 3.28: SCALED PRESSURE-SATURATION CURVE UNTREATED WATER-AIR VS. MTMS-TREATED WATER-AIR

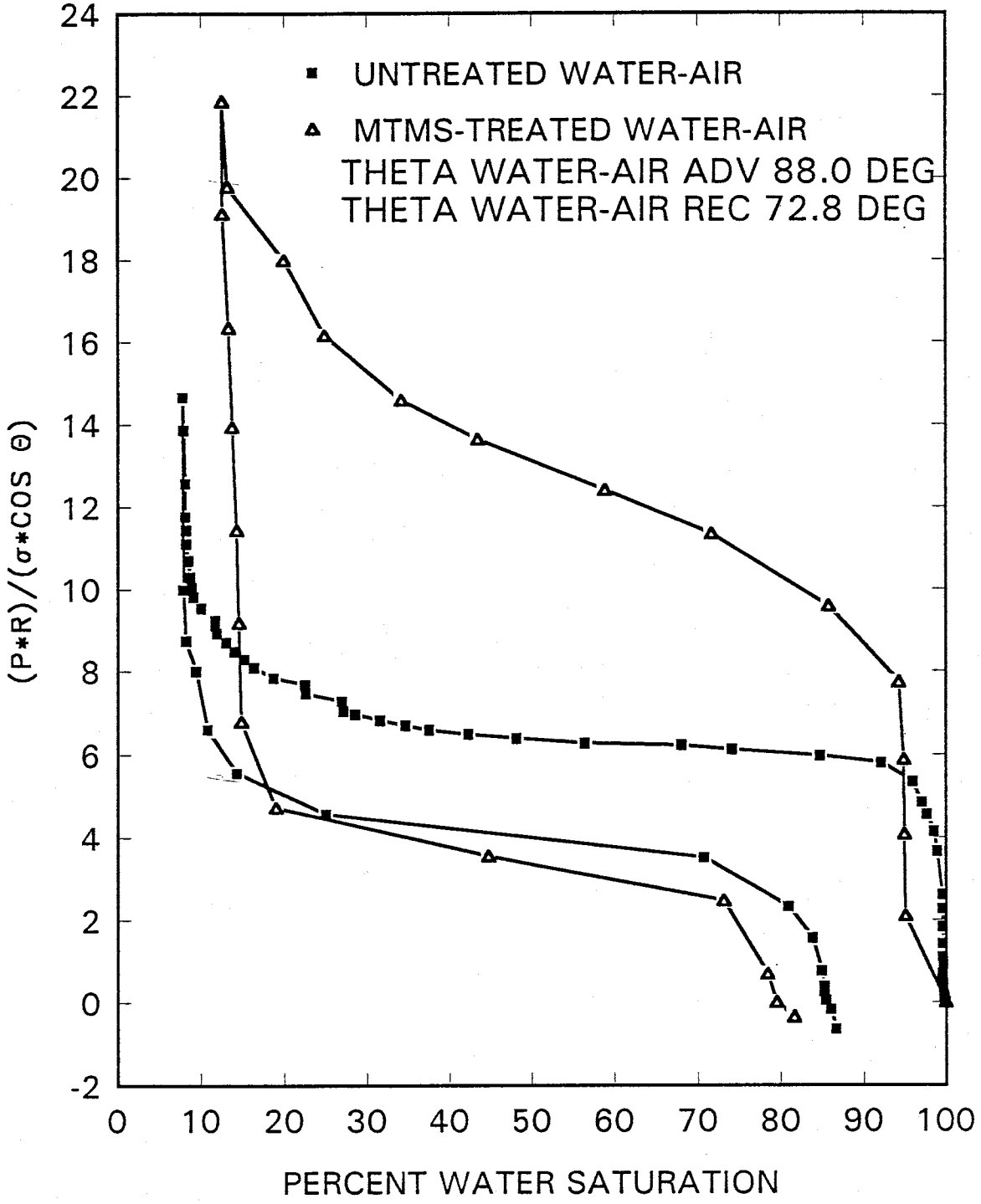

FIGURE 3.29: SCALED PRESSURE-SATURATION CURVE UNTREATED WATER-AIR VS. MTMS-TREATED WATER-SOLTROL

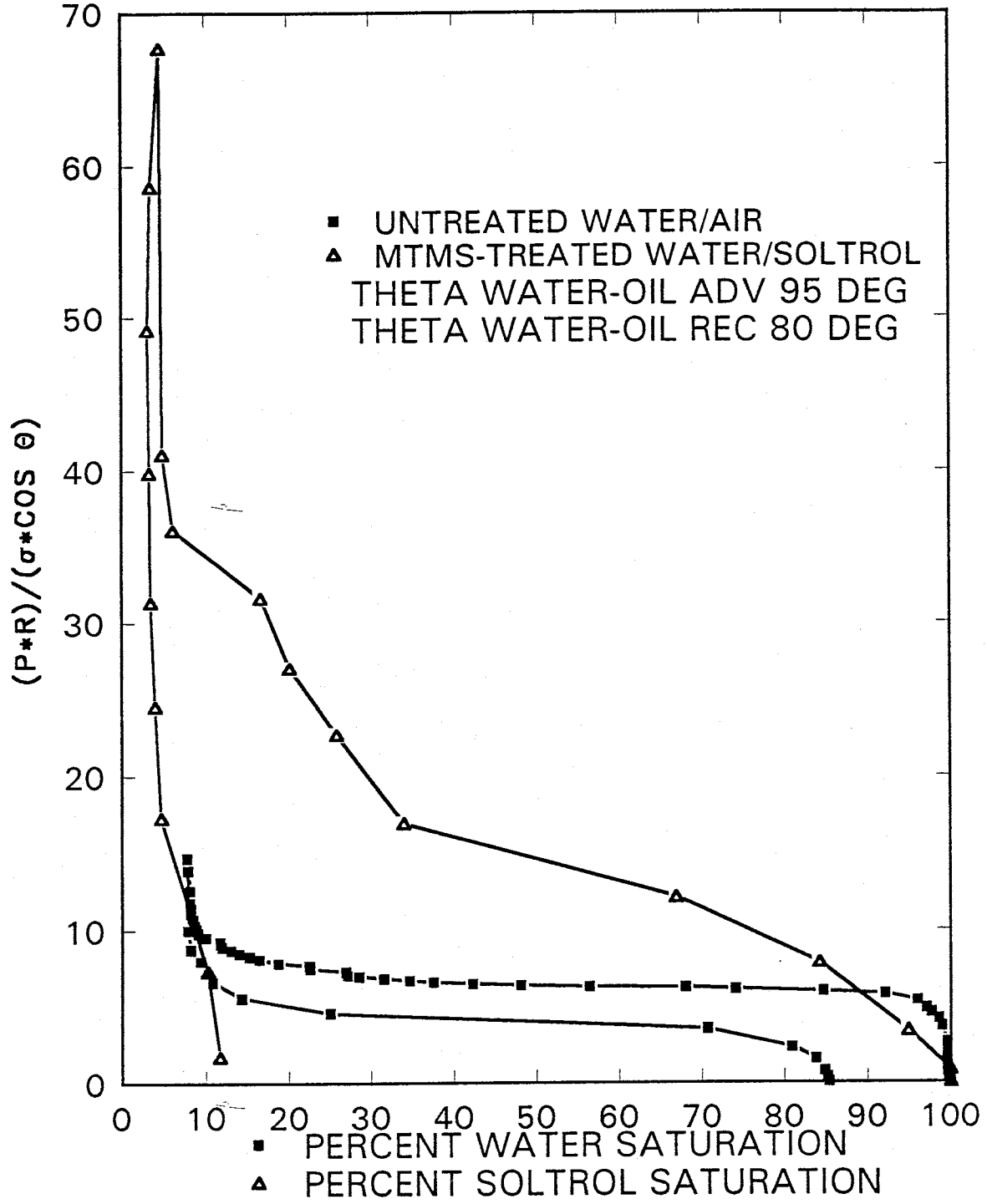

FIGURE 3.30: SCALED PRESSURE-SATURATION CURVE UNTREATED WATER-AIR VS. GC-18-TREATED WATER-SOLTROL

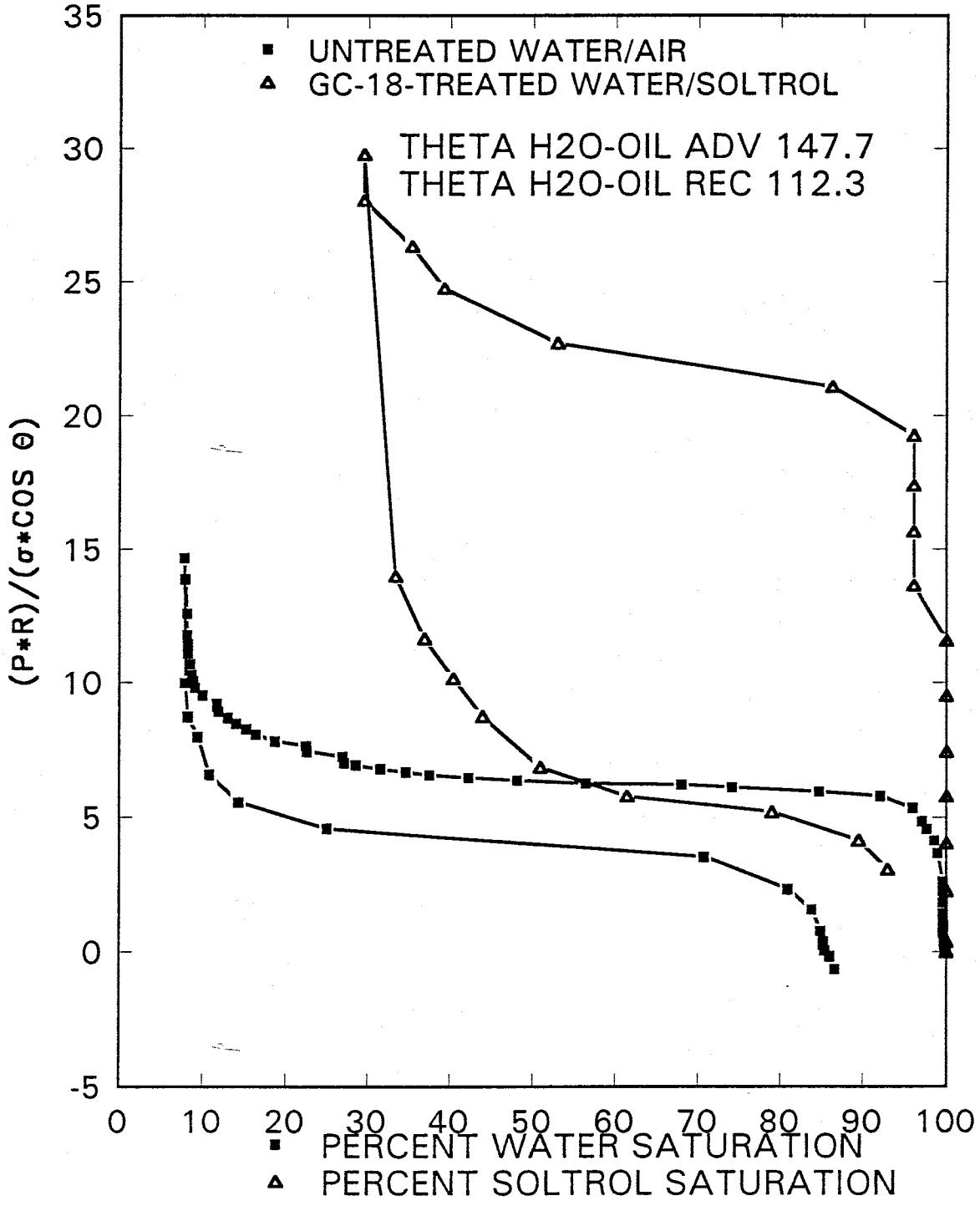

FIGURE 3.31: SCALED PRESSURE -SATURATION CURVE UNTREATED WATER-AIR VS. GC-18-TREATED WATER-AIR

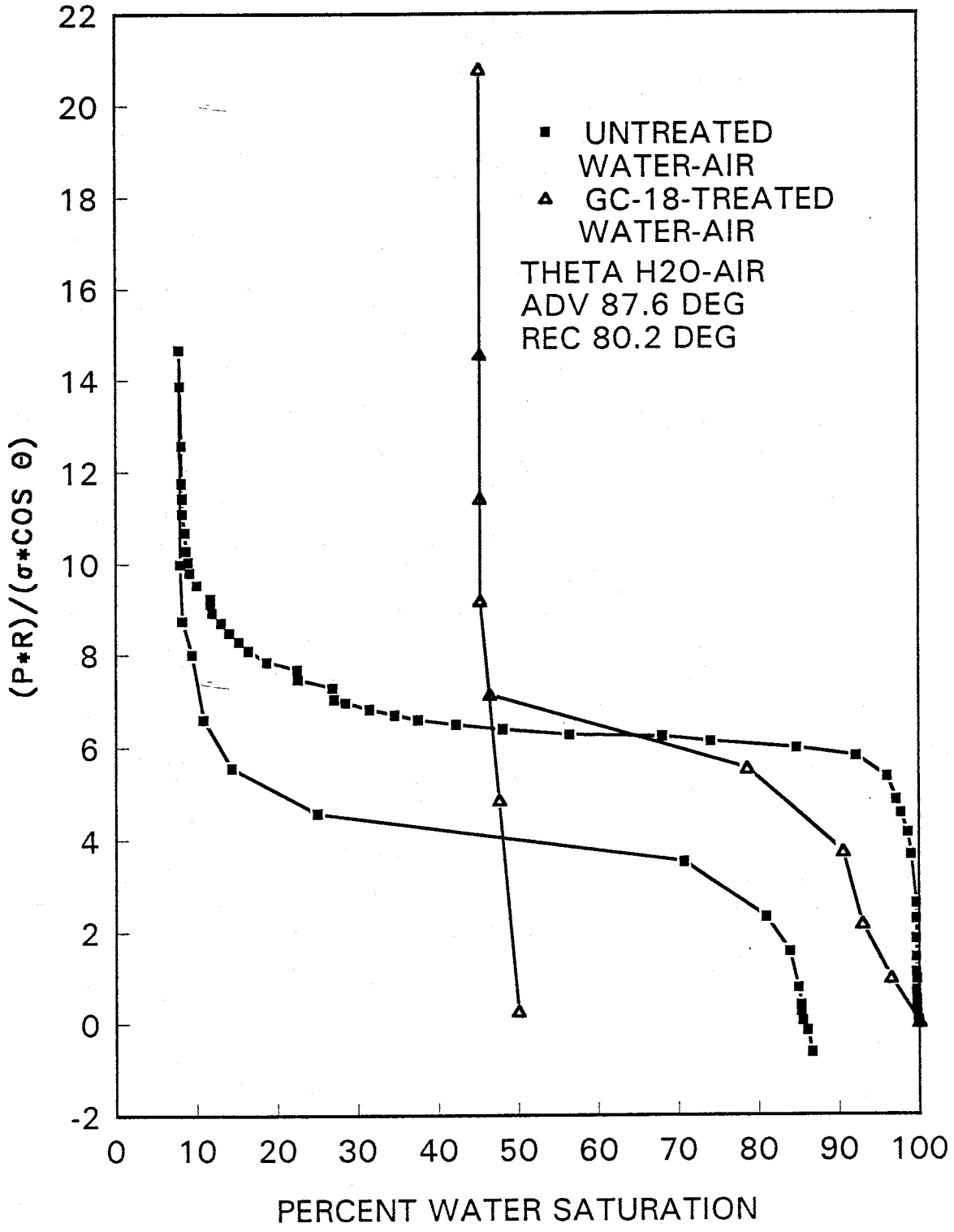

FIGURE 3.32: SCALED PRESSURE SATURATION CURVE
UNTREATED WATER-AIR (50 micron) VS. WEI'S
UNTREATED WATER-SOLTROL (300 micron)

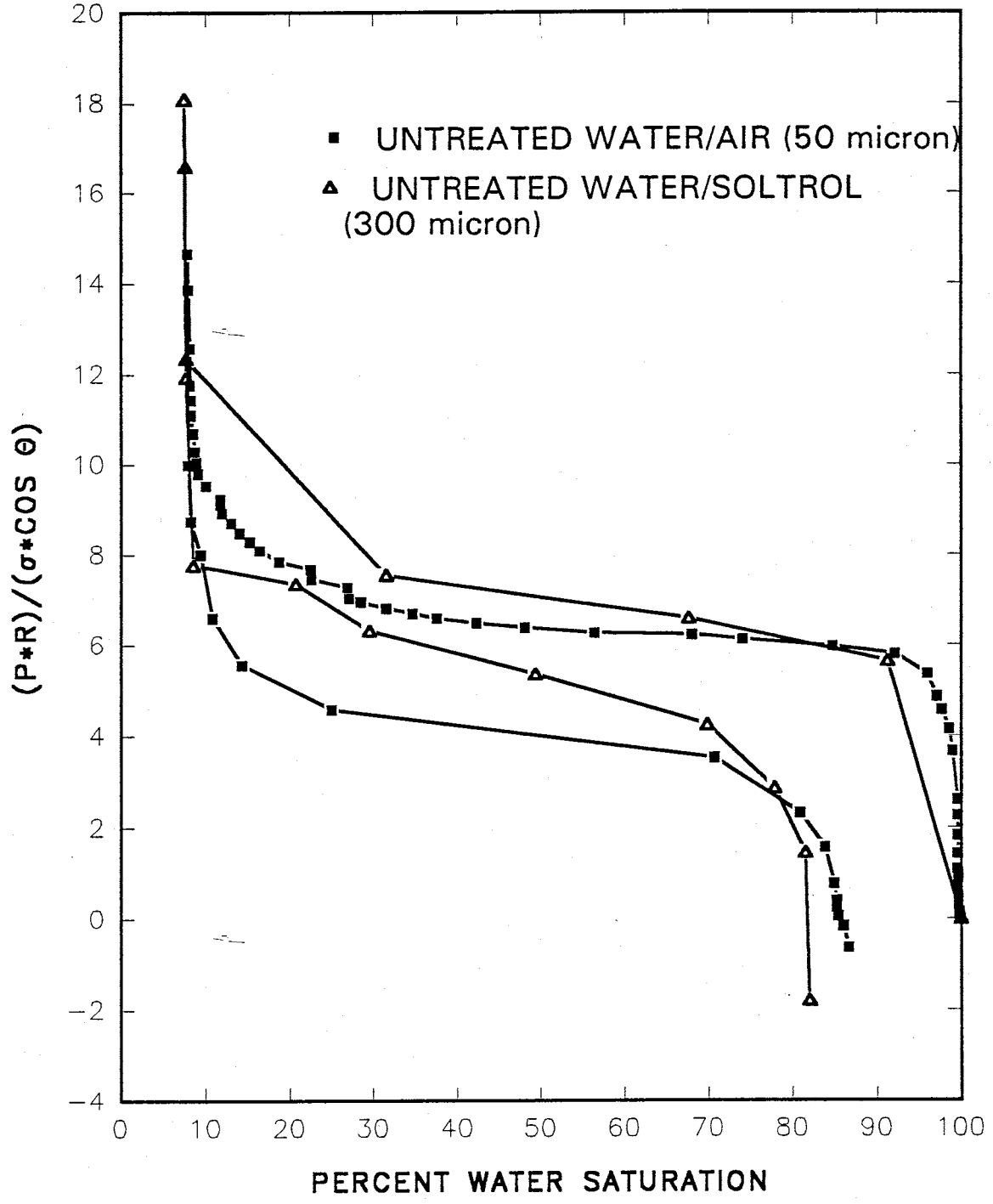

FIGURE 3.33: DESAI, et al., (1992) SCALING

UNTREATED WATER/SOLTROL SYSTEMS

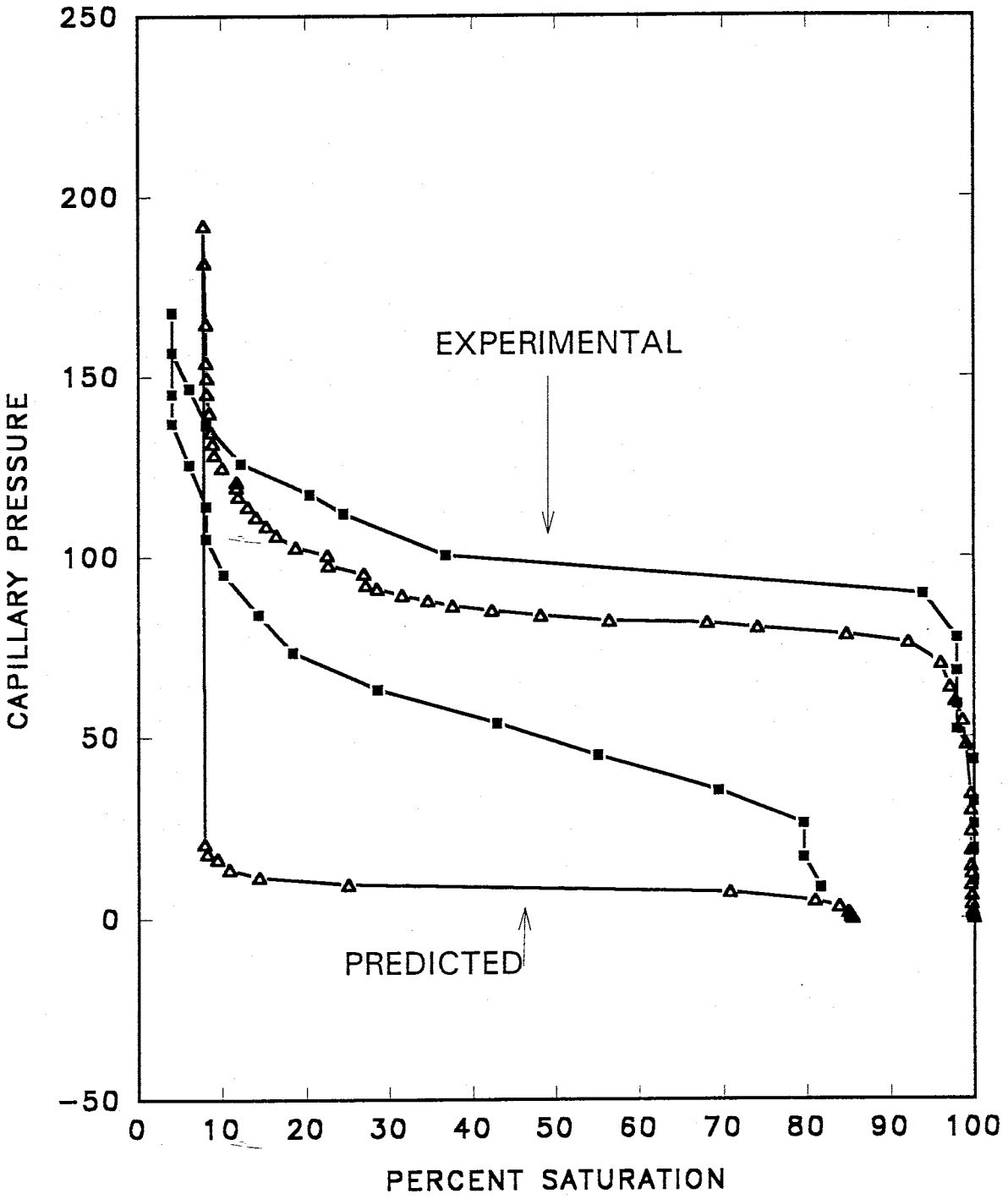

Soltrol systems. In this figure, the predicted drainage curve is somewhat lower than the experimental curve, and the predicted imbibition curve shows a significant departure from the experimental curve. This system was plotted again, this time the only correction factor was the ratio of interfacial tension of the systems. The results of this scaling attempt are shown in Figure 3.34. This appears to be a better match.

The experimental and predicted curves for the untreated Soltrol-air systems are shown in Figure 3.35. Again the experimental curves fall somewhat above the predicted curves.

Figure 3.36 shows the experimental and predicted curves for the MTMS-treated Soltrol-air systems. Here the experimental drainage curve is above the predicted curve, but the imbibition curves appear to be in fairly good agreement.

The experimental and predicted curves for the GC-18-treated Soltrol-air systems are shown in Figure 3.37. Once again the experimental curves fall above the predicted curves.

The capillary pressure-saturation results were also prepared using effective saturation and with the scaling factor: $P^*R/\sigma$. These results are presented in Figures 3.38 through 3.46. Figure 3.38 shows the results of PB6 and PB7, untreated water-air experiments. The results of PB24, the

FIGURE 3.34: SIMPLE SIGMA SCALING UNTREATED WATER-SOLTROL SYSTEMS

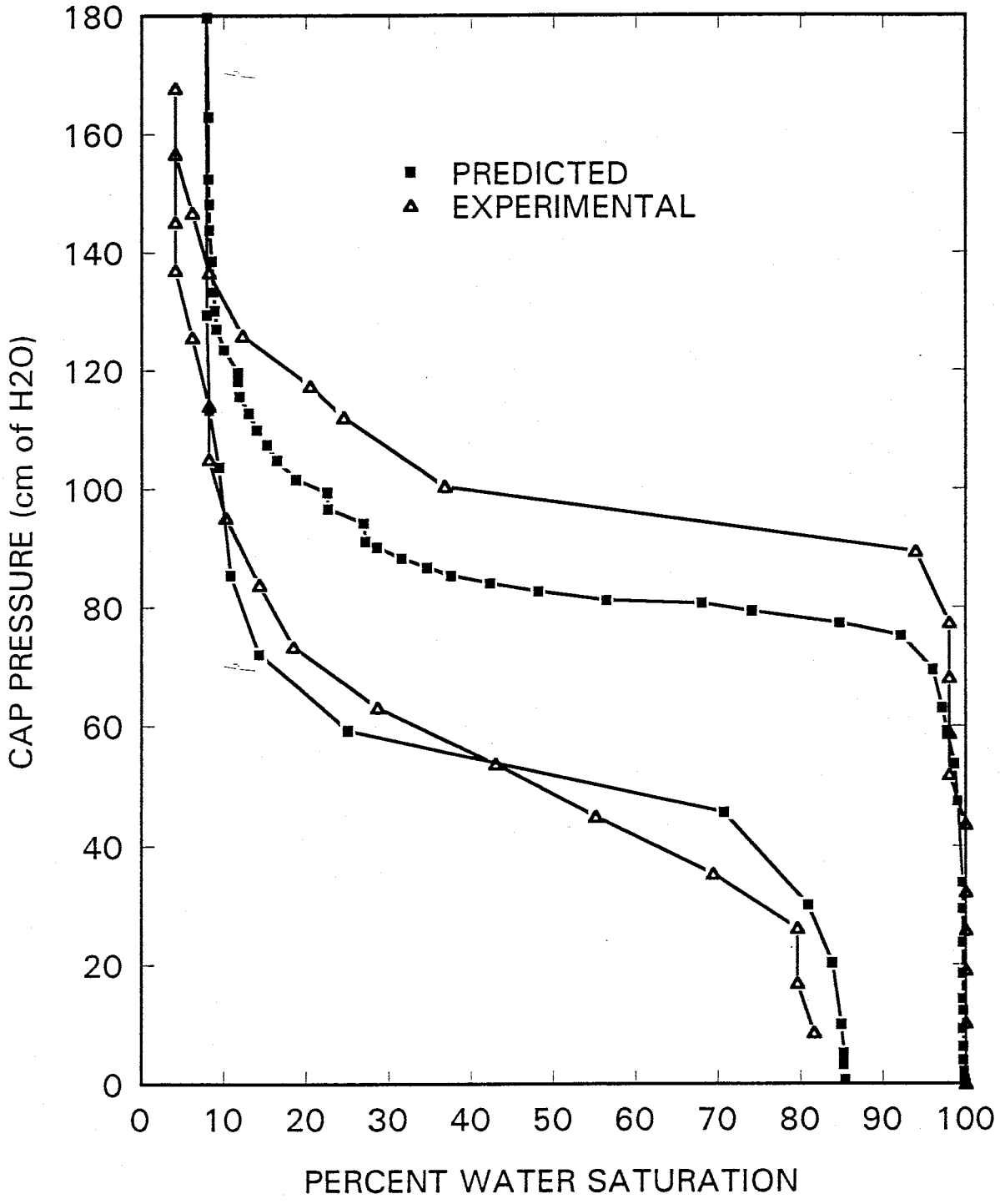

FIGURE 3.35: DESAI, et al., (1992) SCALING

UNTREATED SOLTROL/AIR SYSTEMS

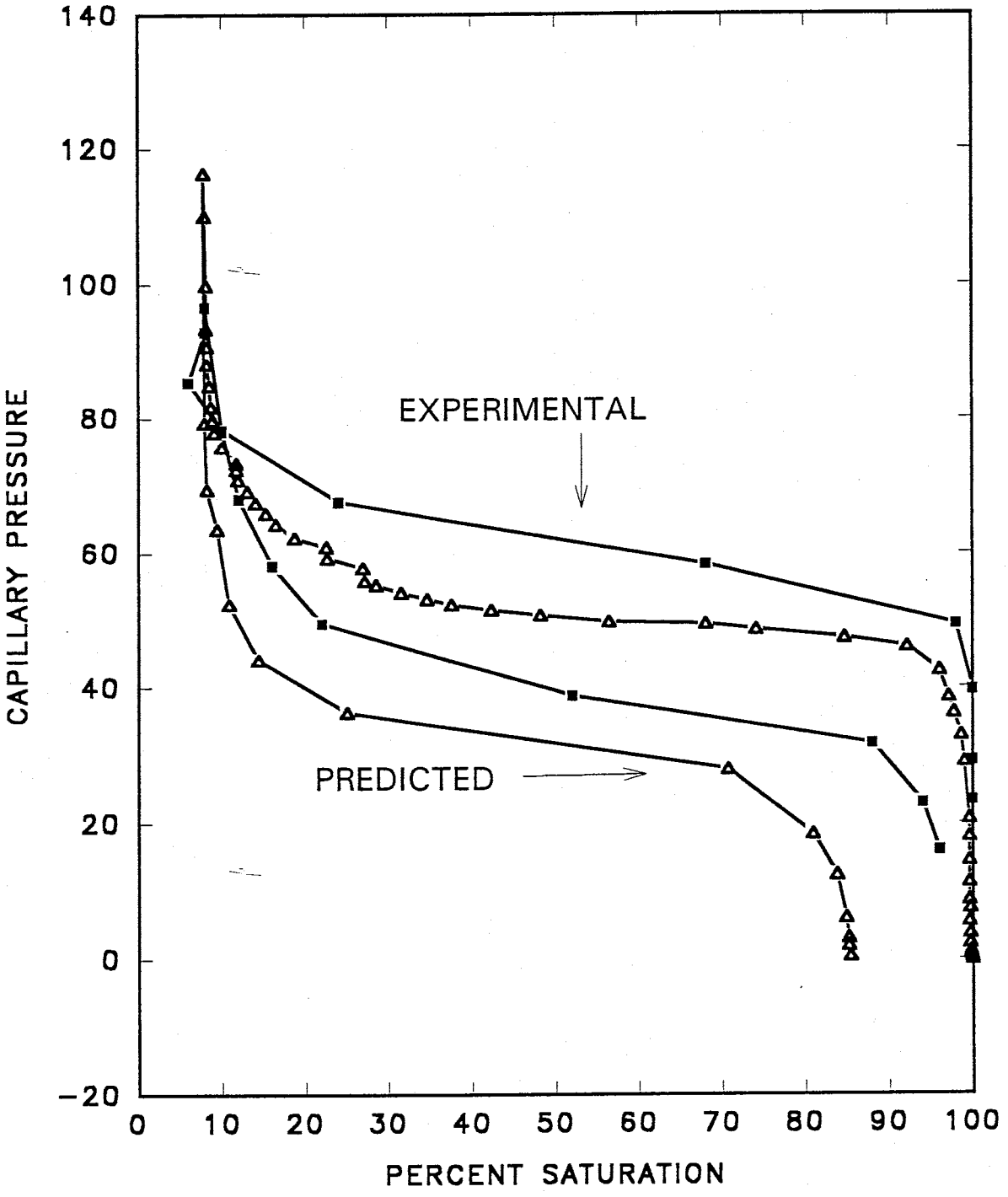

FIGURE 3.36: DESAI, et al., (1992) SCALING MTMS-TREATED SOLTROL/AIR SYSTEMS

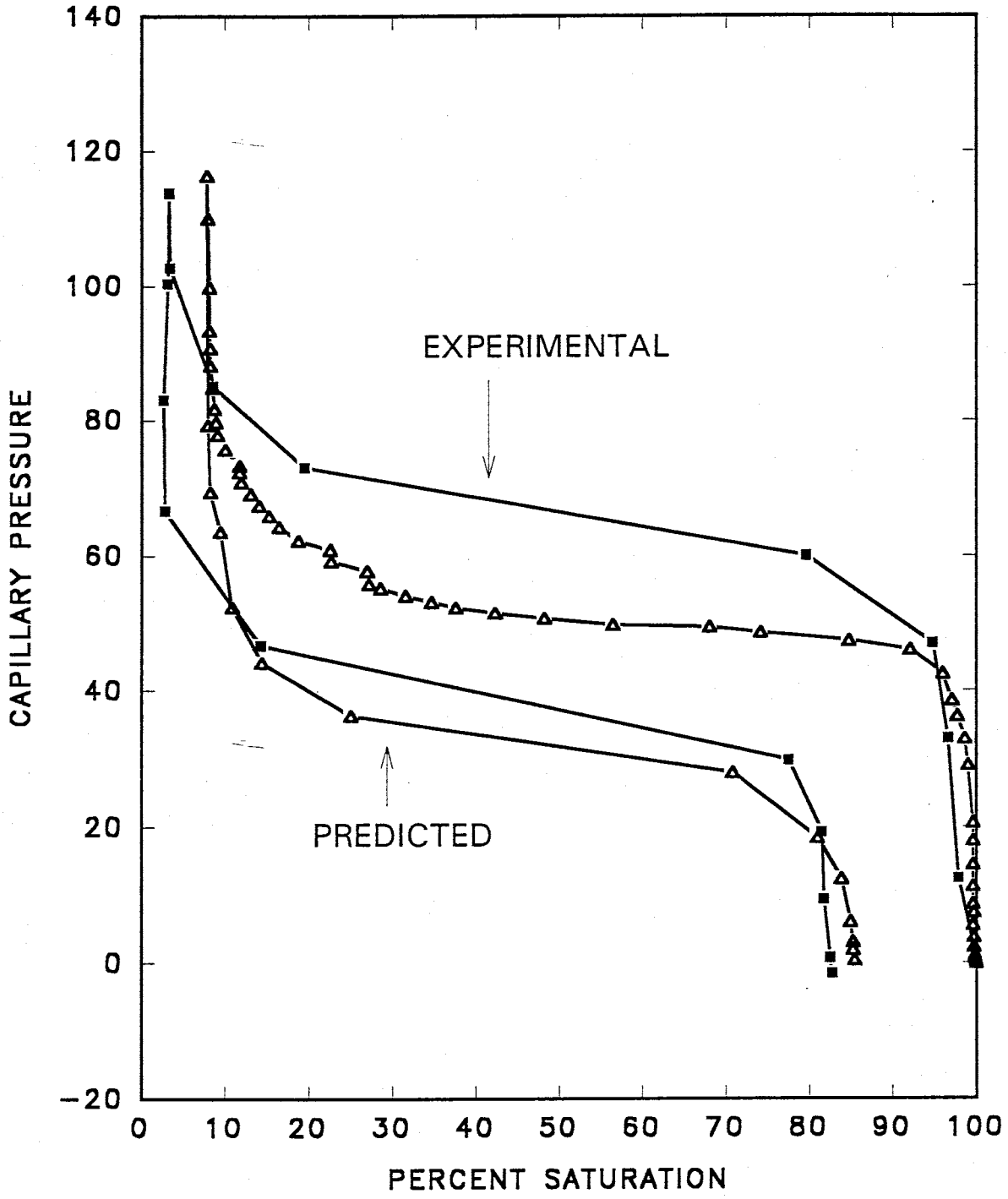

FIGURE 3.37: DESAI, et al., (1992) SCALING GC18-TREATED SOLTROL/AIR SYSTEMS

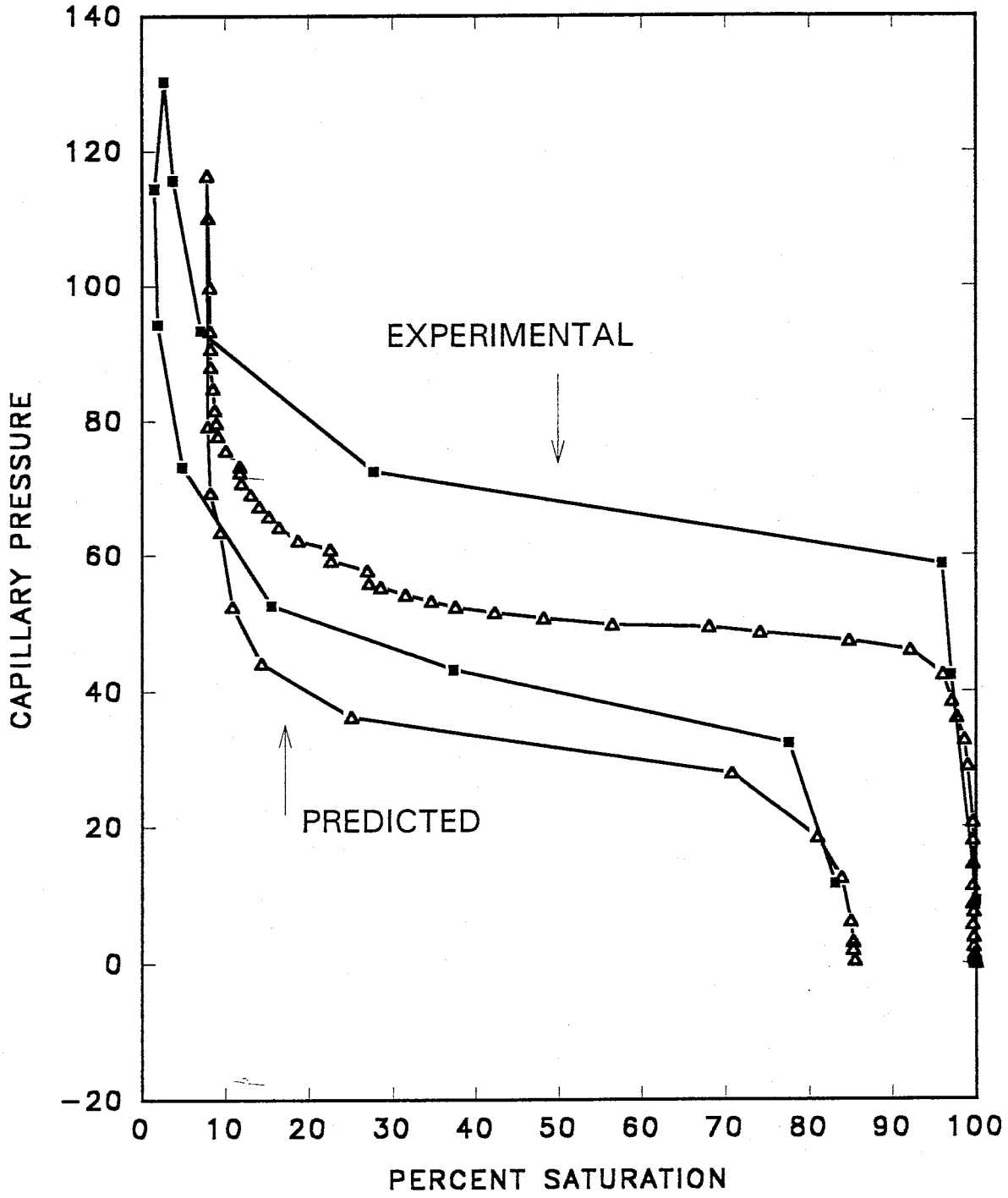

FIGURE 3.38: PB6 & PB7 UNTREATED WATER-AIR

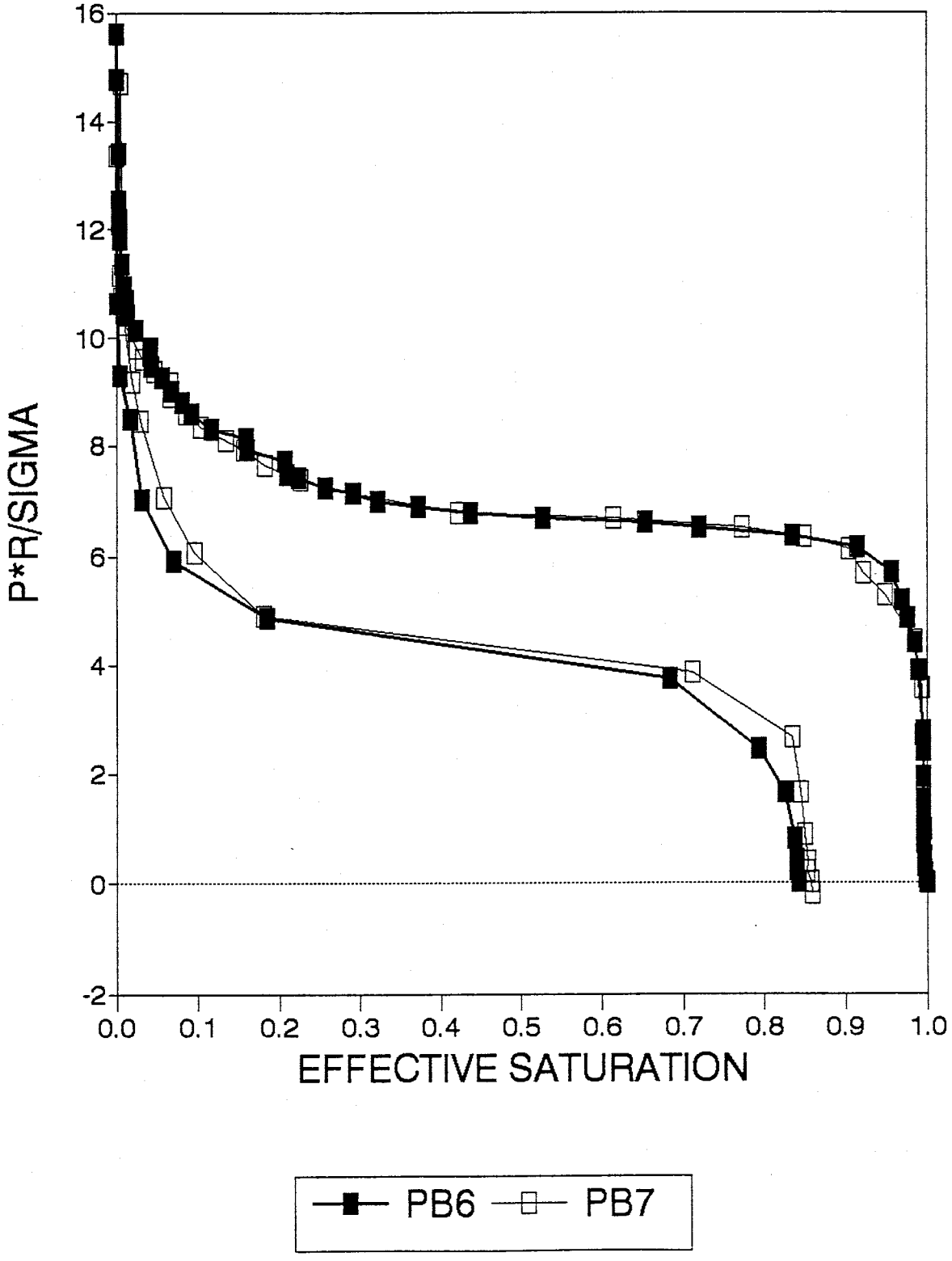

FIGURE 3.39: PB24 UNTREATED
WATER-SOLTROL (WATER SAT)

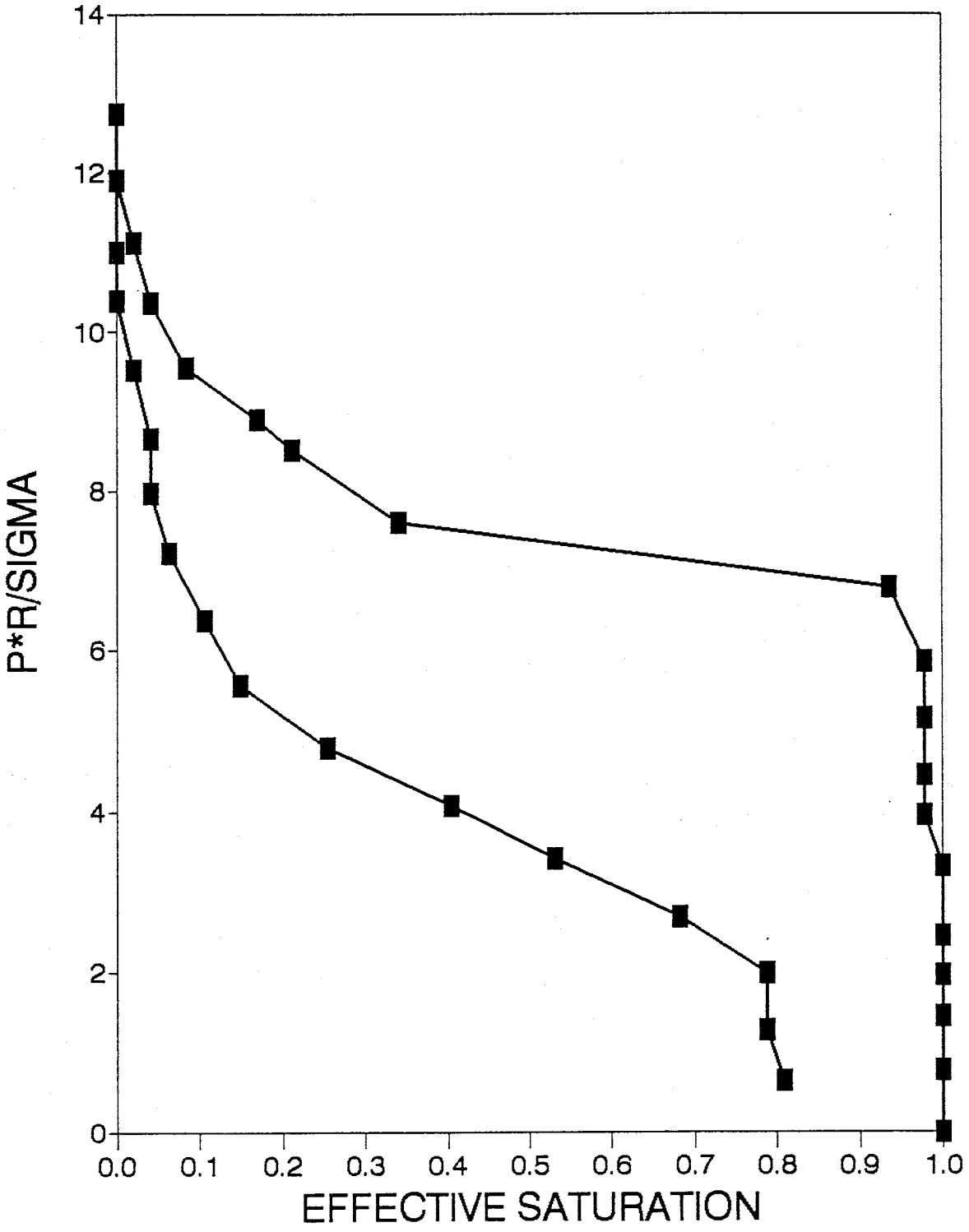

FIGURE 3.40: PB23 UNTREATED SOLTROL-AIR

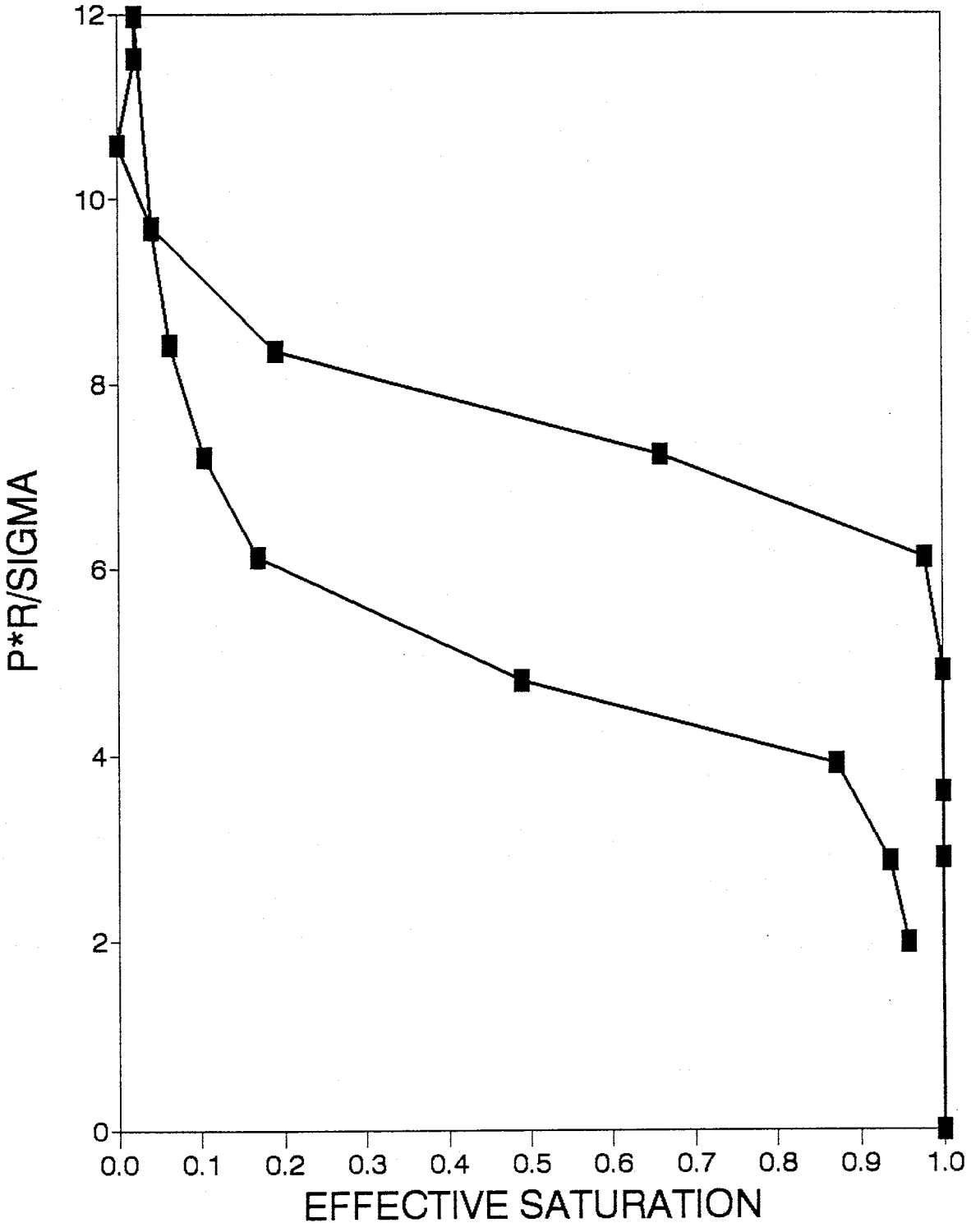

FIGURE 3.41: PB38 & PB39 MTMS-TREATED WATER-AIR

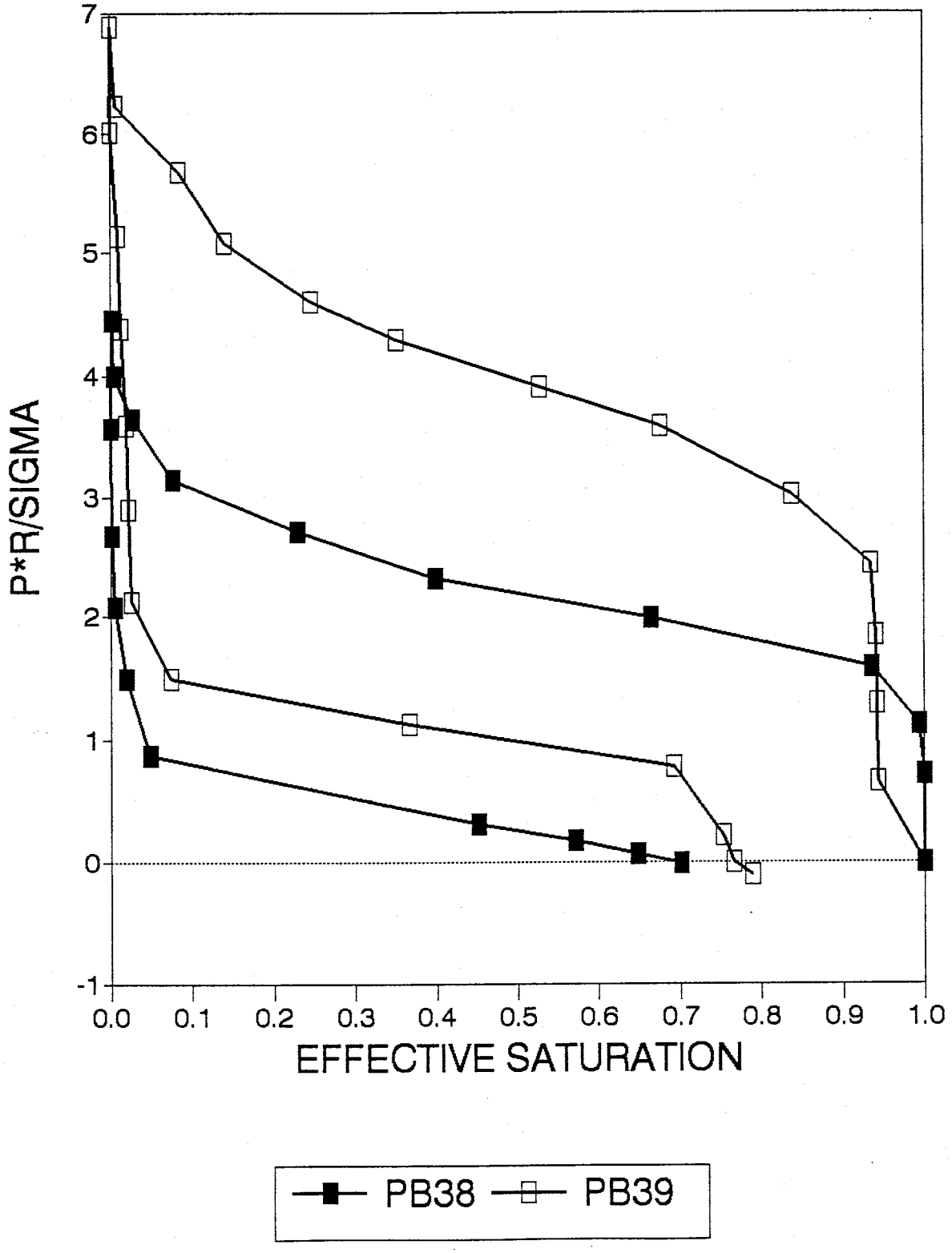

FIGURE 3.42: PB35 MTMS-TREATED WATER-SOLTROL (SOLTROL SAT)

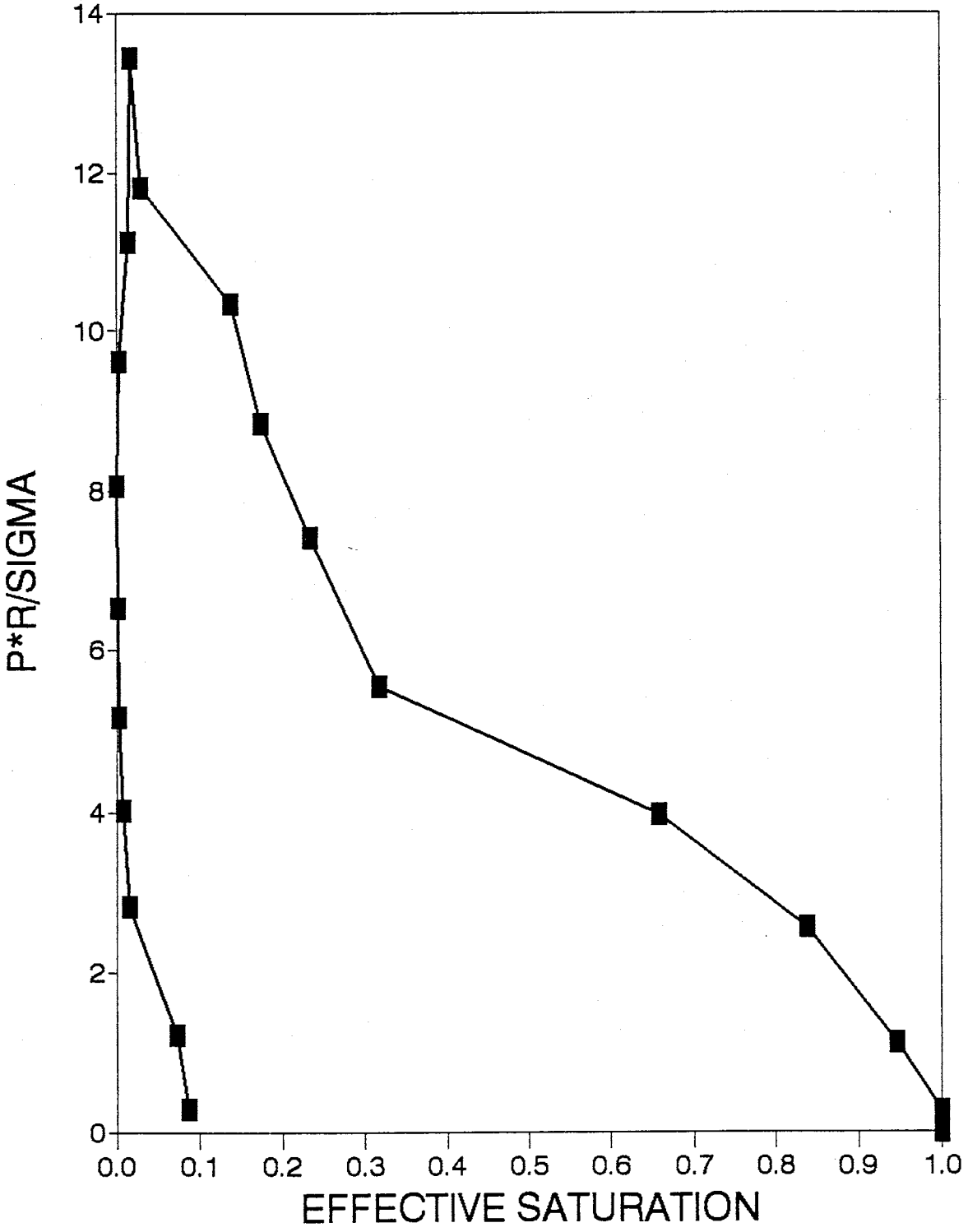

FIGURE 3.43: PB37 MTMS-TREATED SOLTROL-AIR

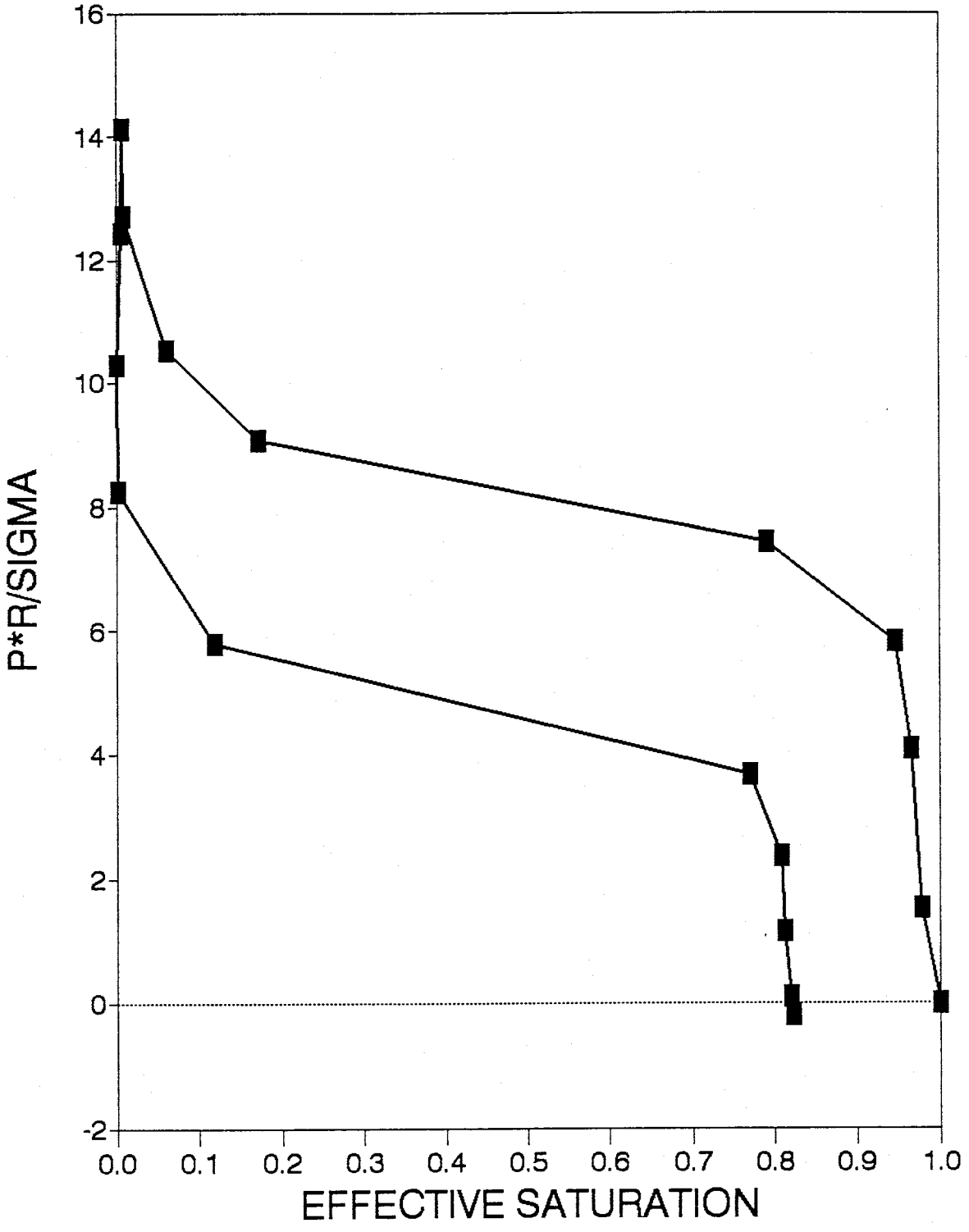

FIGURE 3.44: PB28 GC-18-TREATED WATER-AIR

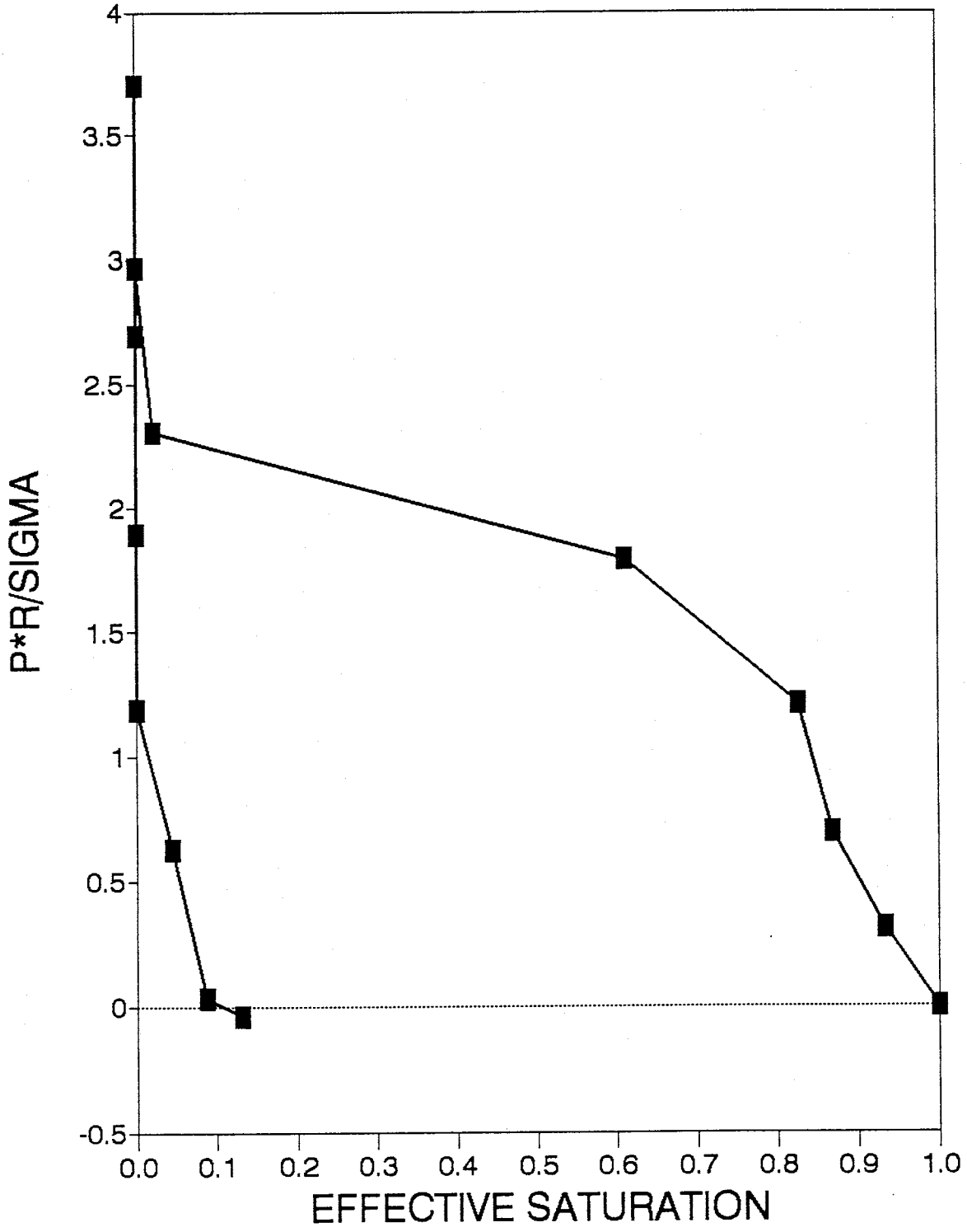

FIGURE 3.45: PB27 GC-18-TREATED WATER-SOLTROL (SOLTROL SAT)

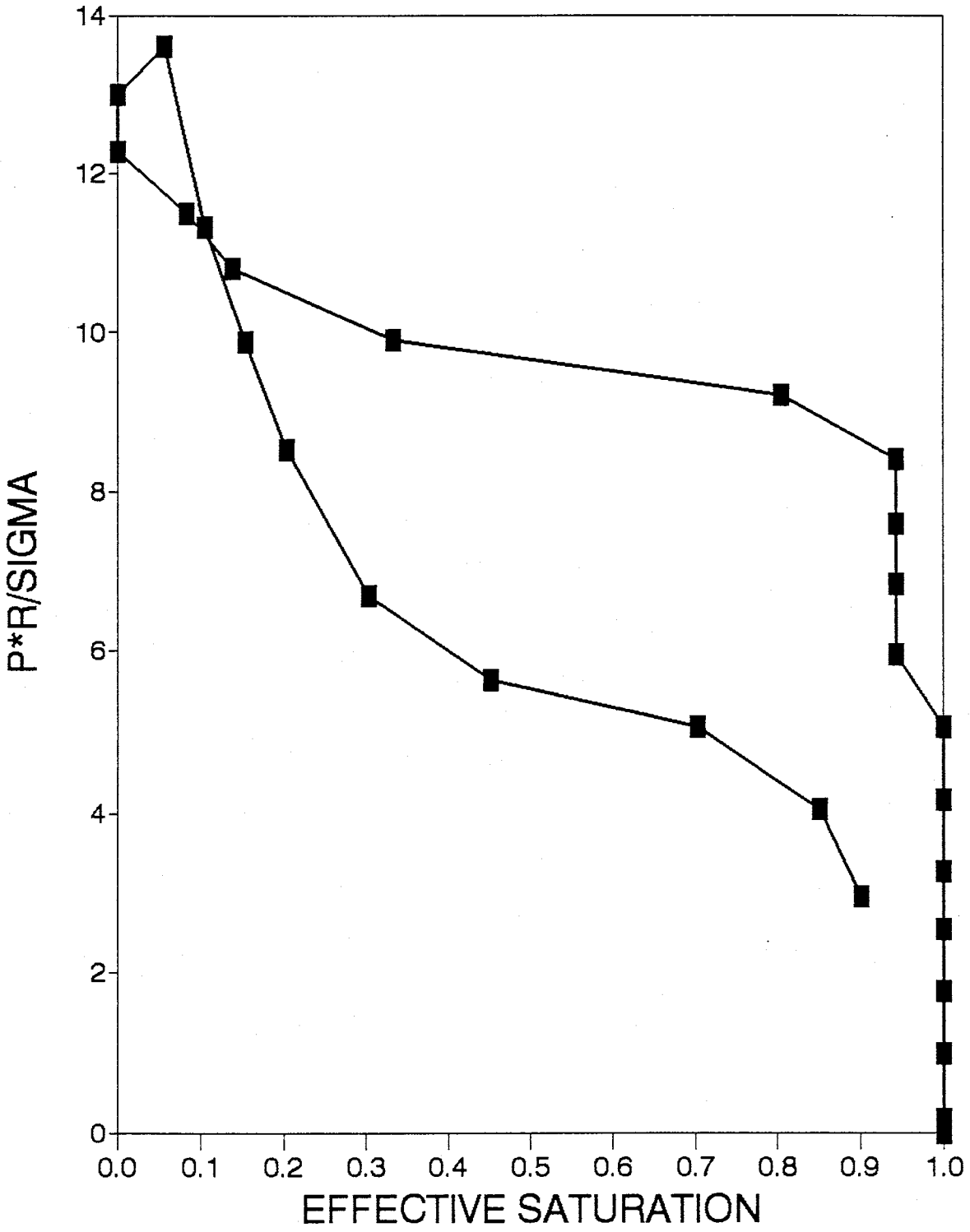

FIGURE 3.46: PB25 & PB30 GC-18-TREATED SOLTROL-AIR

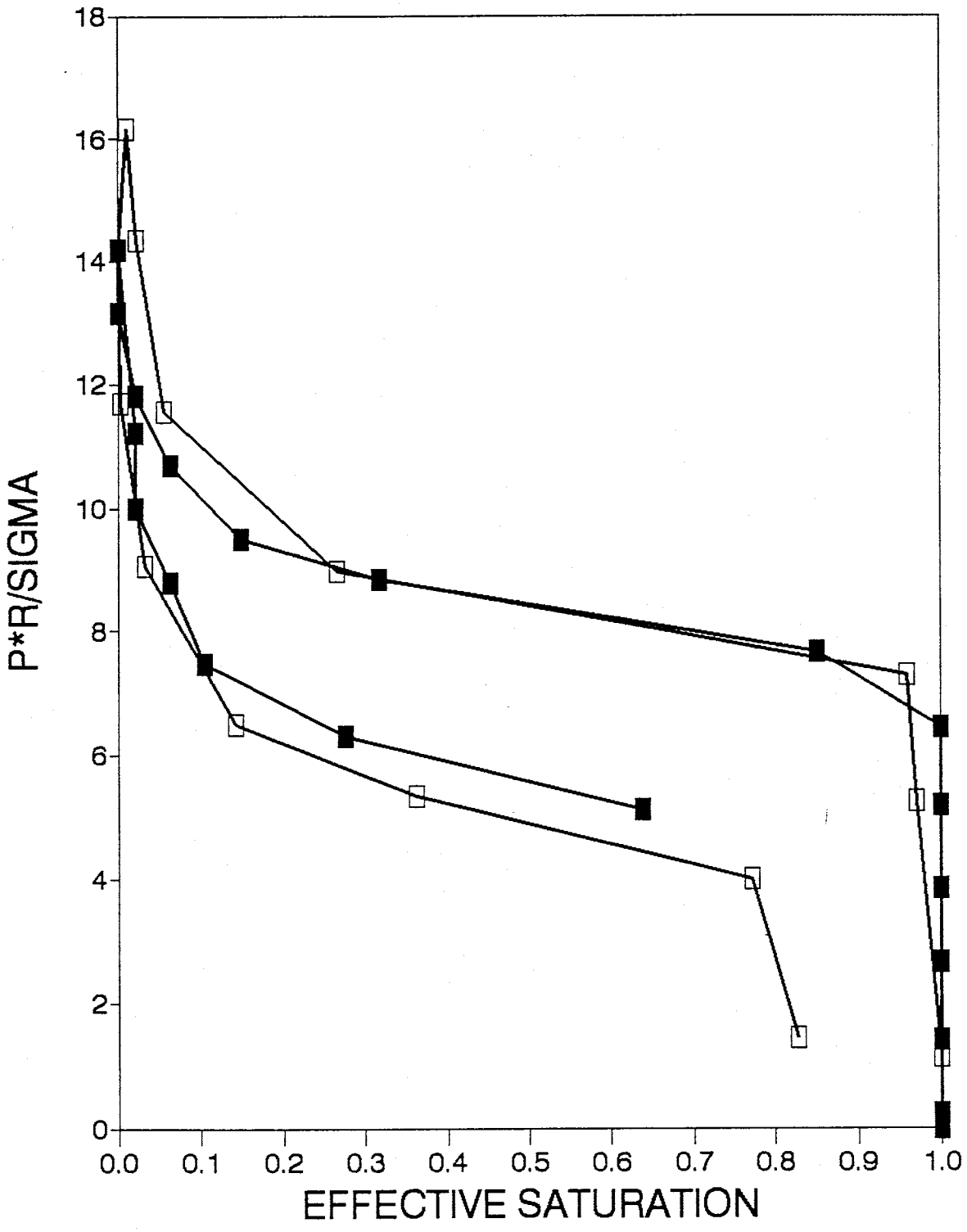

untreated water-Soltrol experiment are illustrated in Figure 3.39. Figure 3.40 presents the results of the untreated Soltrol-air experiment (PB23). The results of PB38 and PB39, the MTMS-treated water-air columns, are shown in Figure 3.41. Figure 3.42 shows the results of the MTMS-treated water-Soltrol experiment (PB35). The results of PB37, the MTMS-treated Soltrol-air column, are illustrated in Figure 3.43. Figure 3.44 shows the results of PB28, the GC-18-treated water-air column. PB27, the GC-18-treated water-Soltrol column, is shown in Figure 3.45. Finally, the results of columns PB25 and PB30, the GC-18-treated Soltrol-air experiments, are shown in Figure 3.46.

The results of the $Z$ factor calculations are shown graphically in Figures 3.47 through 3.54. Average $Z$ values for drainage and imbibition portions of each experiment are shown in Table 3.5. A plot of $Z$ values vs. contact angle is provided in Figure 3.55.

FIGURE 3.47: Z FACTOR PB24 UNTREATED WATER-SOLTROL (WATER SAT)

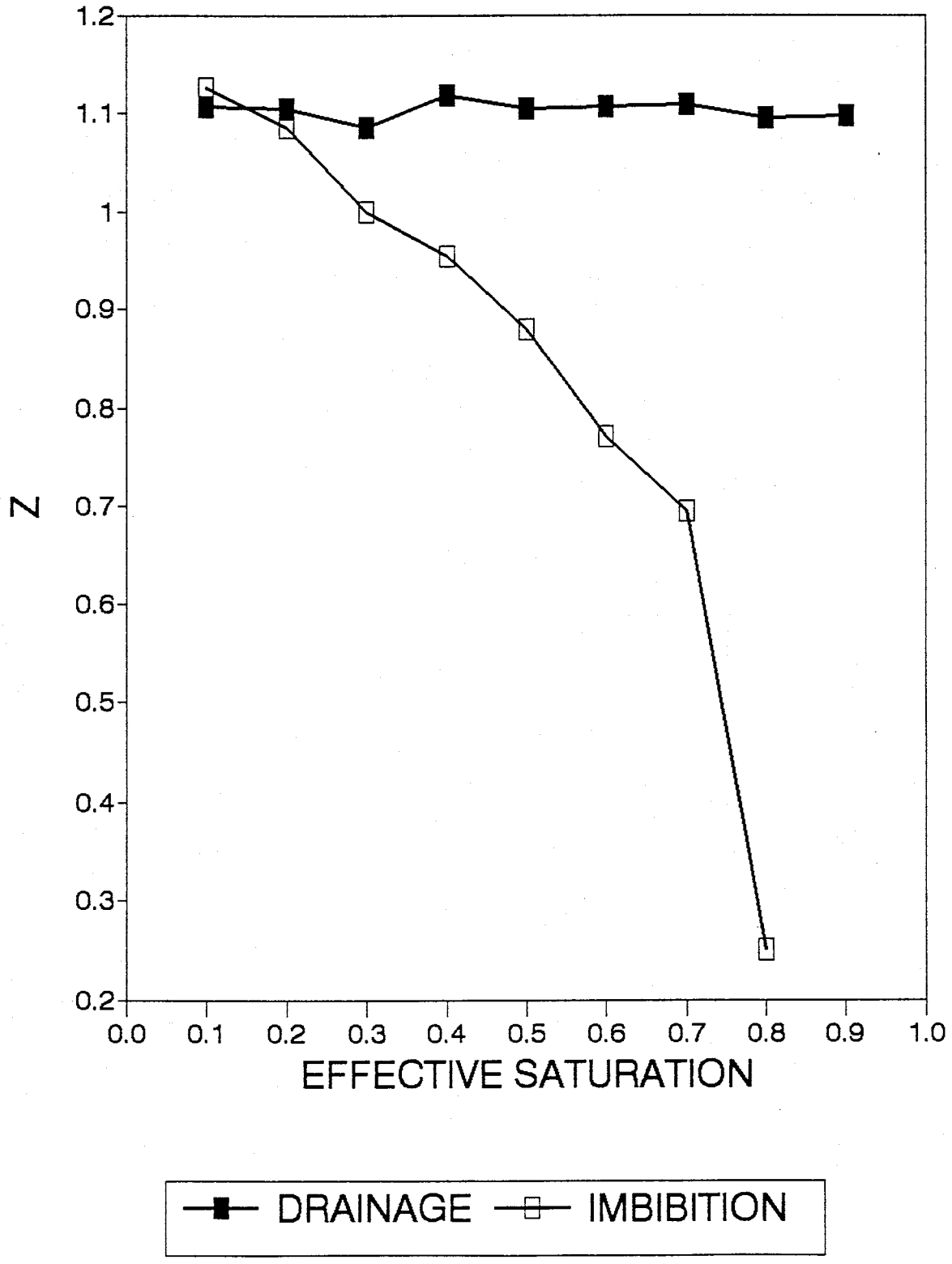

FIGURE 3.48: Z FACTOR PB23 UNTREATED SOLTROL-AIR

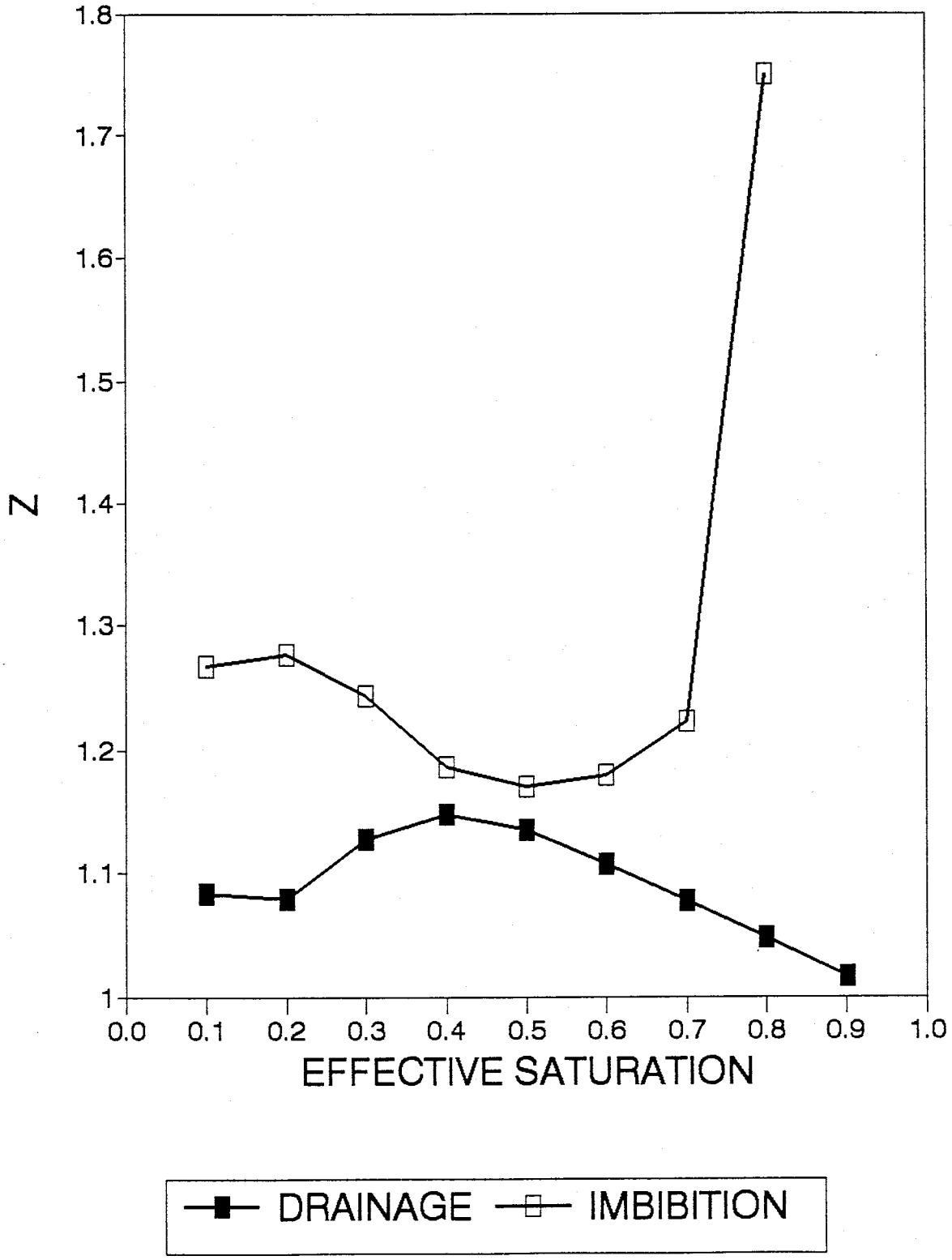

FIGURE 3.49: Z FACTOR PB38 & PB39
MTMS-TREATED WATER-AIR

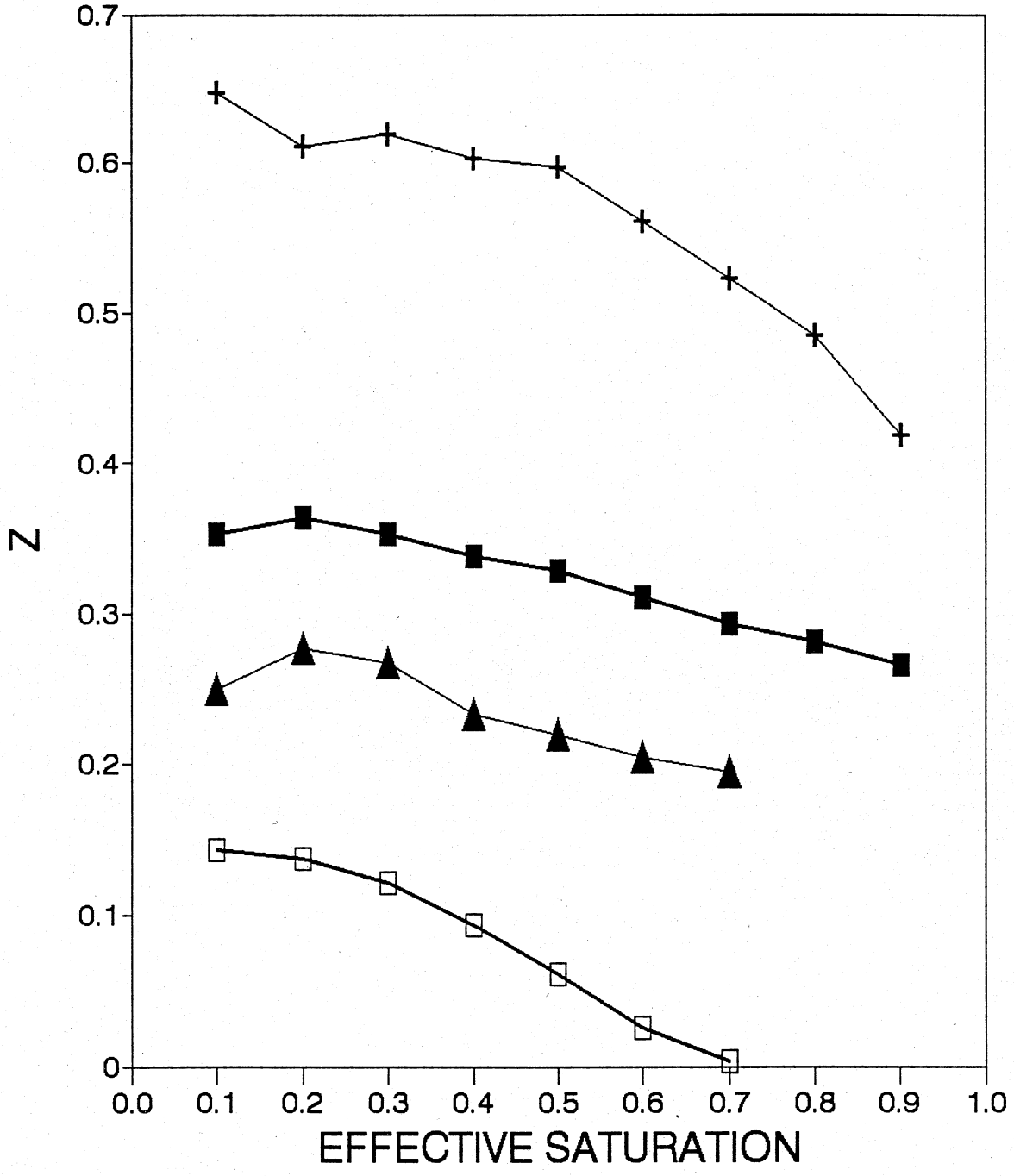

FIGURE 3.50: Z FACTOR PB35 MTMS-TREATED WATER-SOLTROL (SOLTROL SAT)

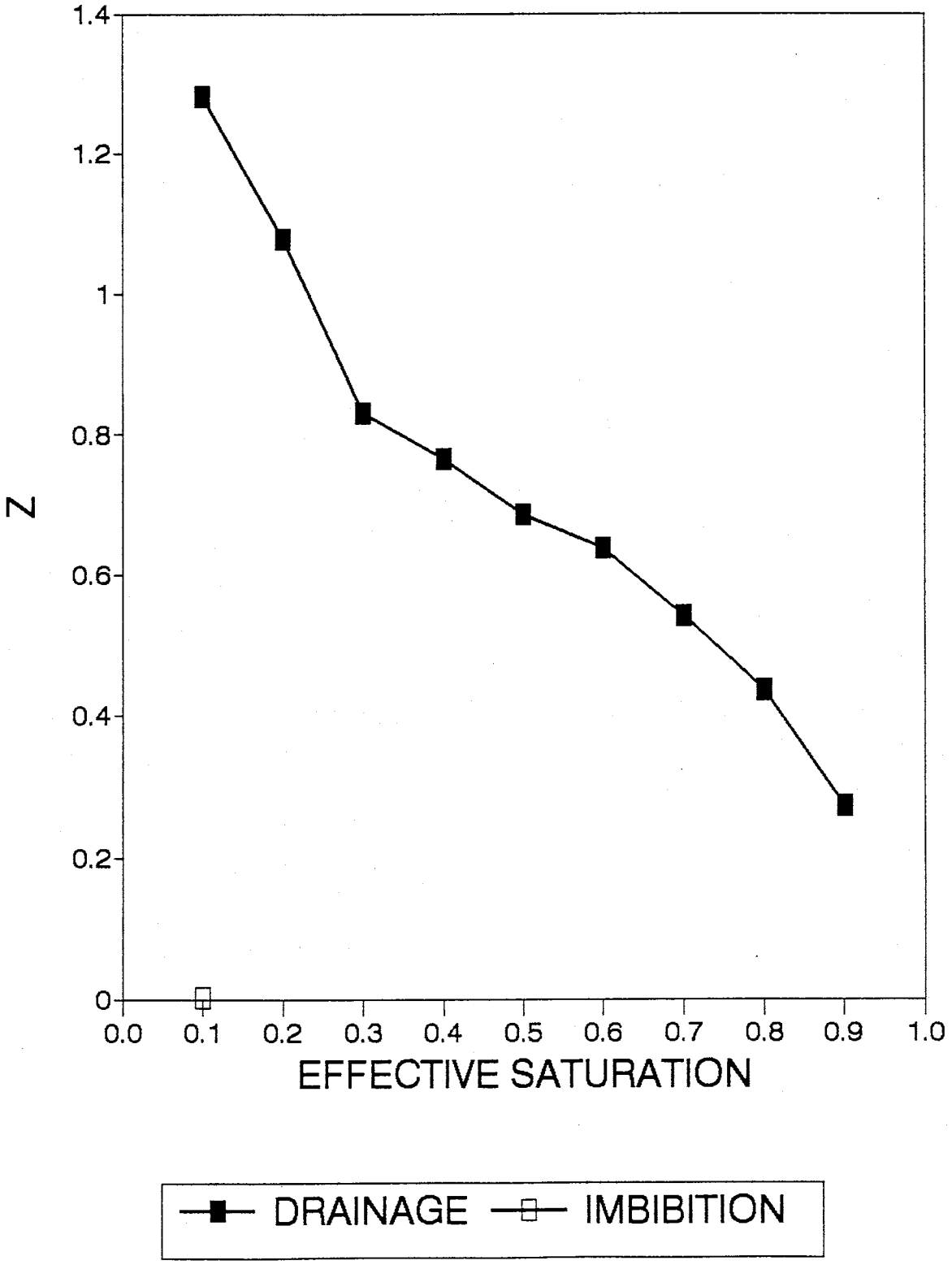

FIGURE 3.51: Z FACTOR PB37 MTMS-TREATED SOLTROL-AIR

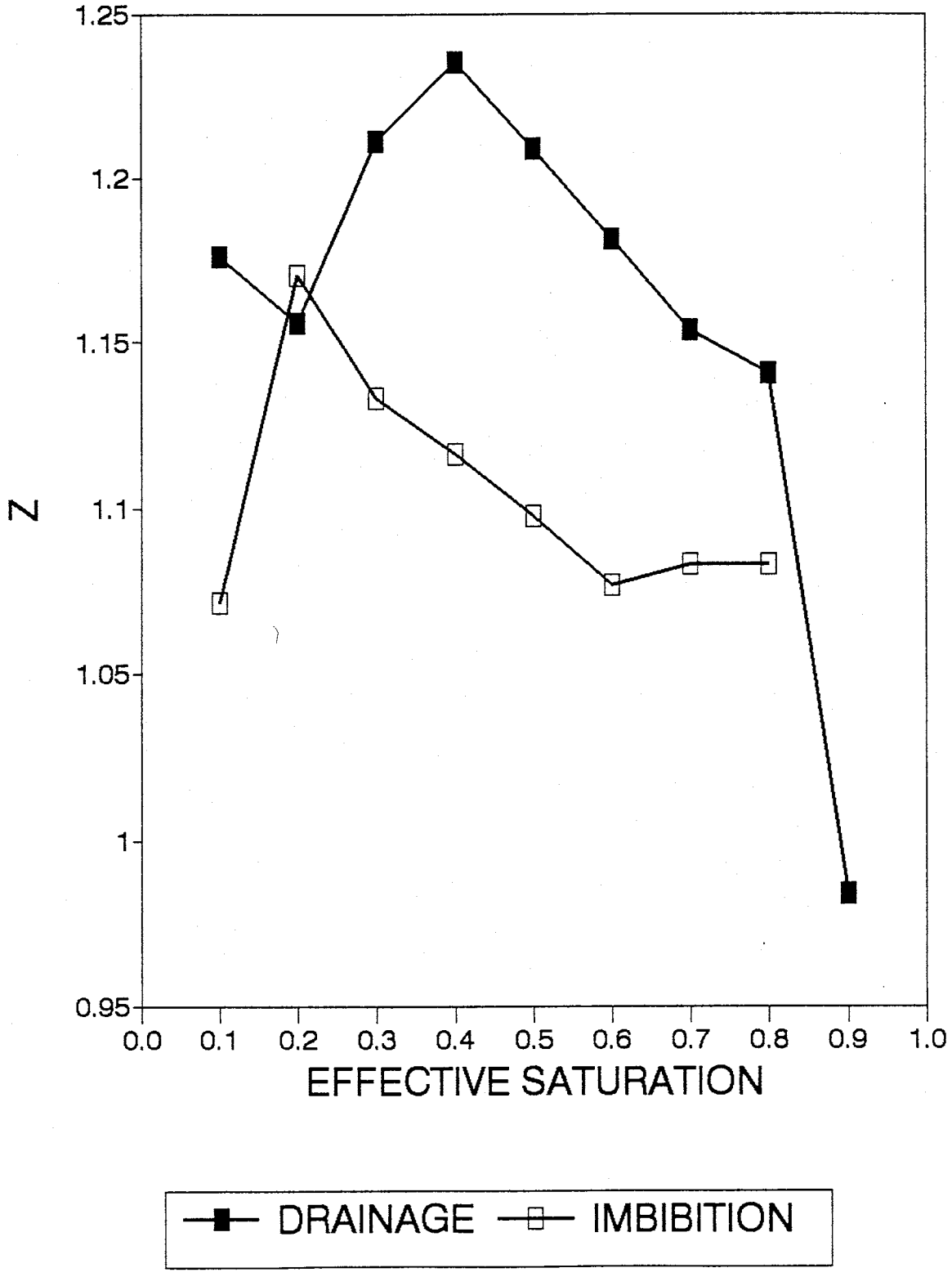

FIGURE 3.52: Z FACTOR PB28 GC18-TREATED WATER-AIR

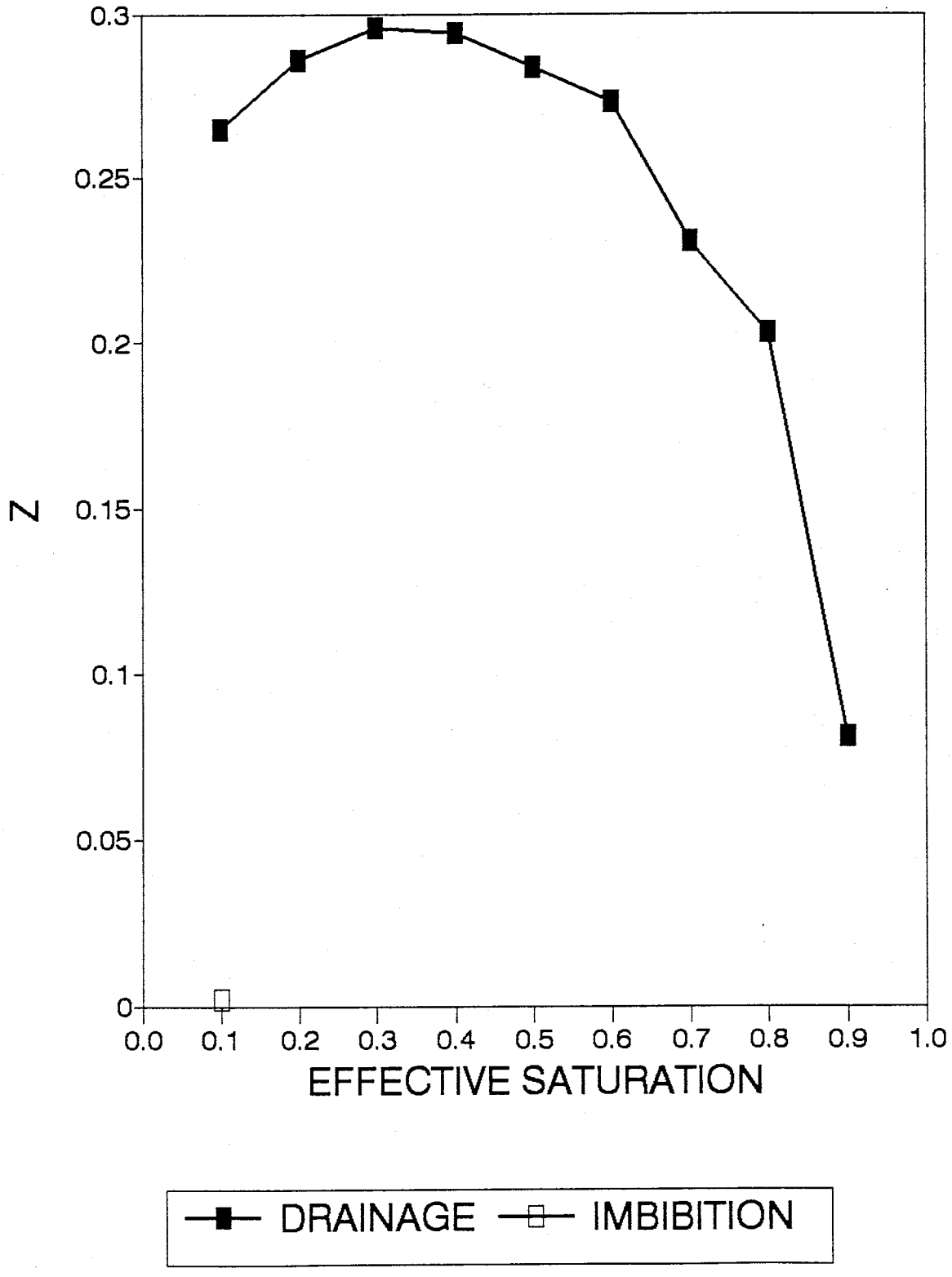

FIGURE 3.53: Z FACTOR PB27 GC18-TREATED WATER-SOLTROL (SOLTROL SAT)

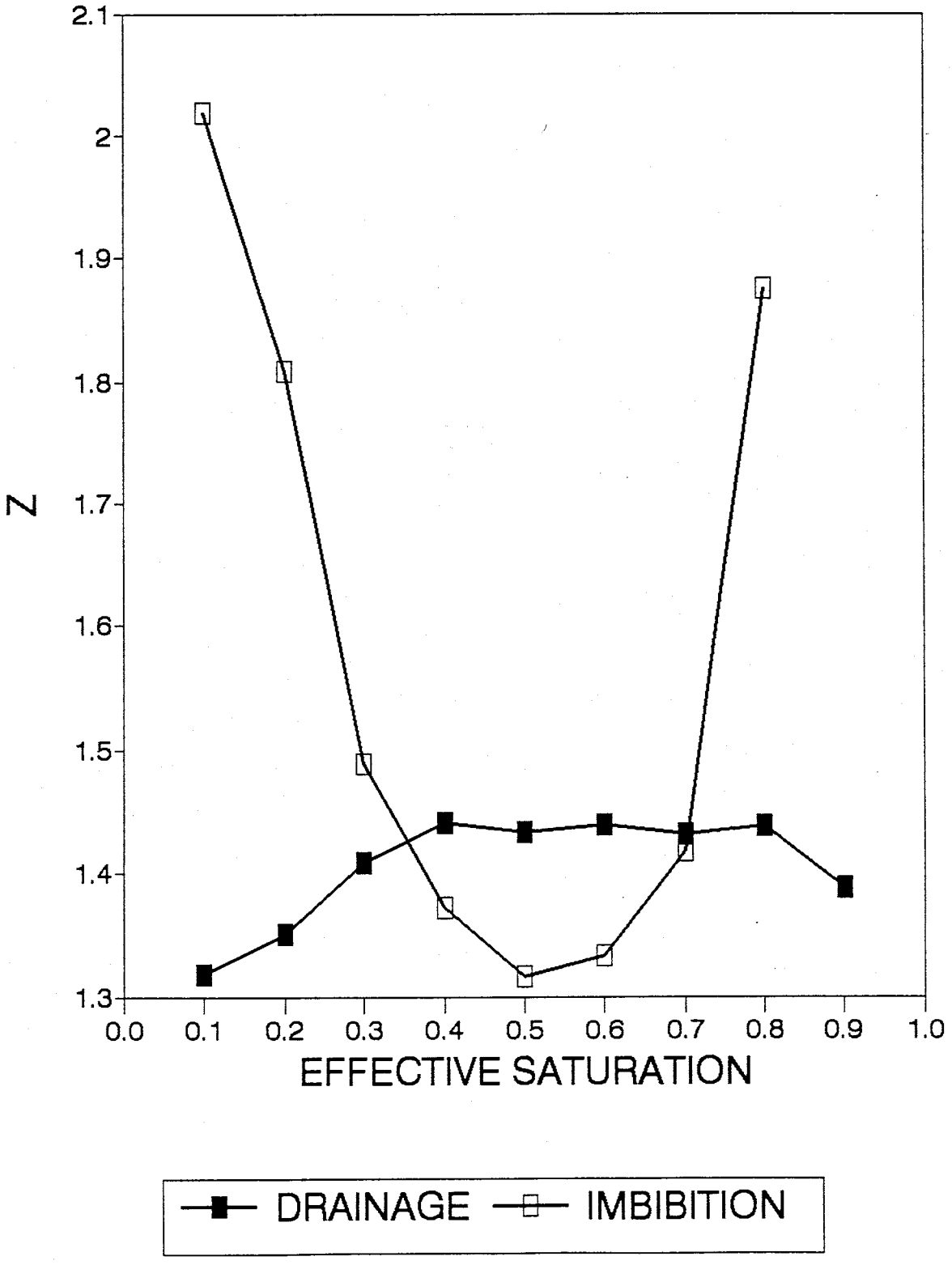

FIGURE 3.54: Z FACTOR PB25 & PB30
GC18-TREATED SOLTROL-AIR

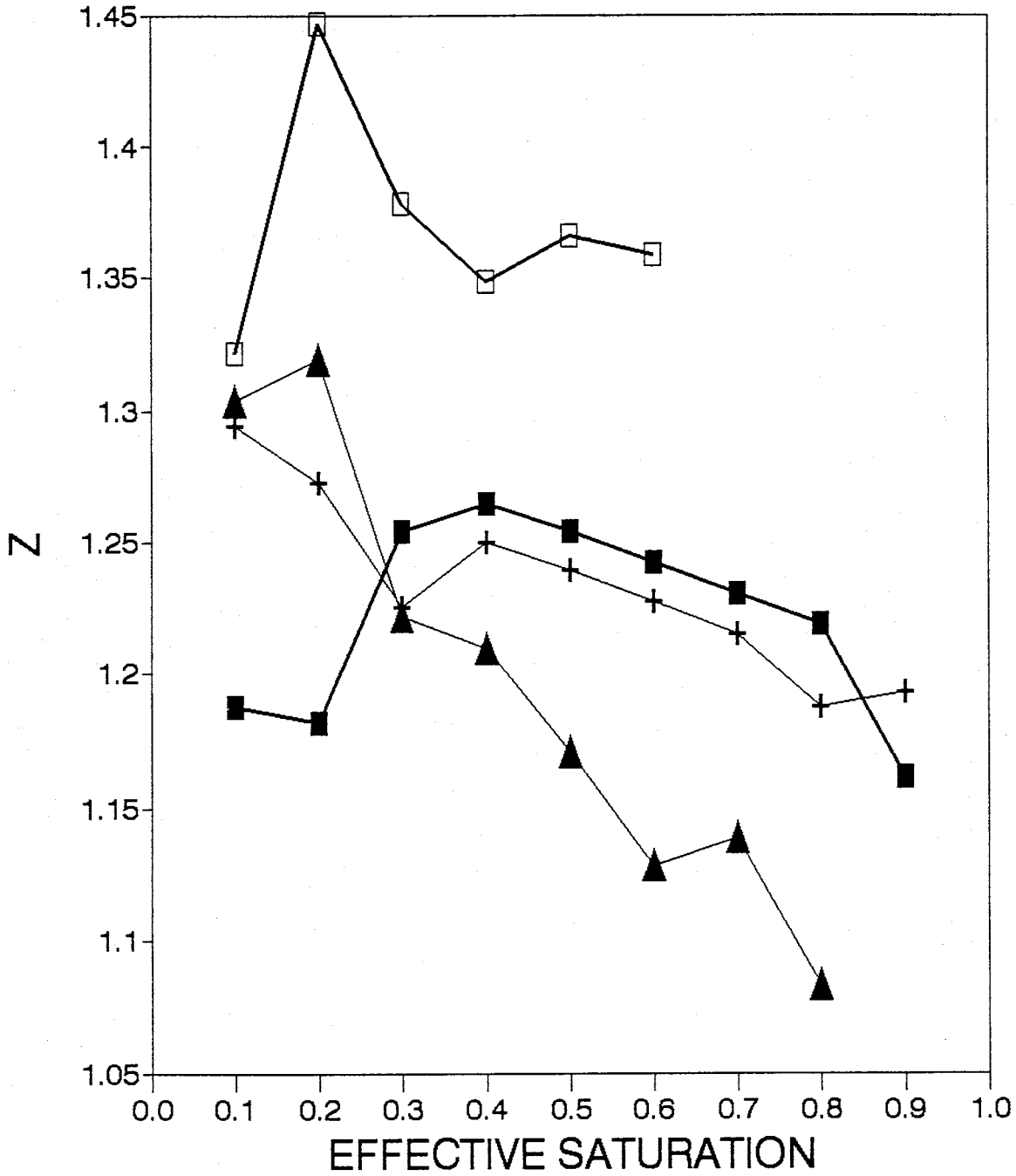

Table 3.5 Summary of *Z* values

| EXPERIMENT | FLUIDS | AVERAGE *Z* FOR DRAINAGE | AVERAGE *Z* FOR IMBIBITION |
|---|---|---|---|
| PB23 | UNTREATED SOLTROL-AIR | 1.1 | 1.3 |
| PB24 | UNTREATED WATER-SOLTROL (SAT WATER) | 1.1 | 0.8 |
| PB25 | GC-18-TREATED SOLTROL-AIR | 1.2 | 1.4 |
| PB27 | GC-18-TREATED WATER-SOLTROL (SAT SOLTROL) | 1.4 | 1.6 |
| PB28 | GC-18-TREATED WATER-AIR | 0.2 | 0.0 |
| PB30 | GC-18-TREATED SOLTROL-AIR | 1.2 | 1.2 |
| PB35 | MTMS-TREATED WATER-SOLTROL (SAT SOLTROL) | 0.7 | 0.0 |
| PB37 | MTMS-TREATED SOLTROL-AIR | 1.2 | 1.1 |
| PB38 | MTMS-TREATED WATER-AIR | 0.3 | 0.1 |
| PB39 | MTMS-TREATED WATER-AIR | 0.6 | 0.2 |

FIGURE 3.55: Z FACTOR VS. CONTACT ANGLE

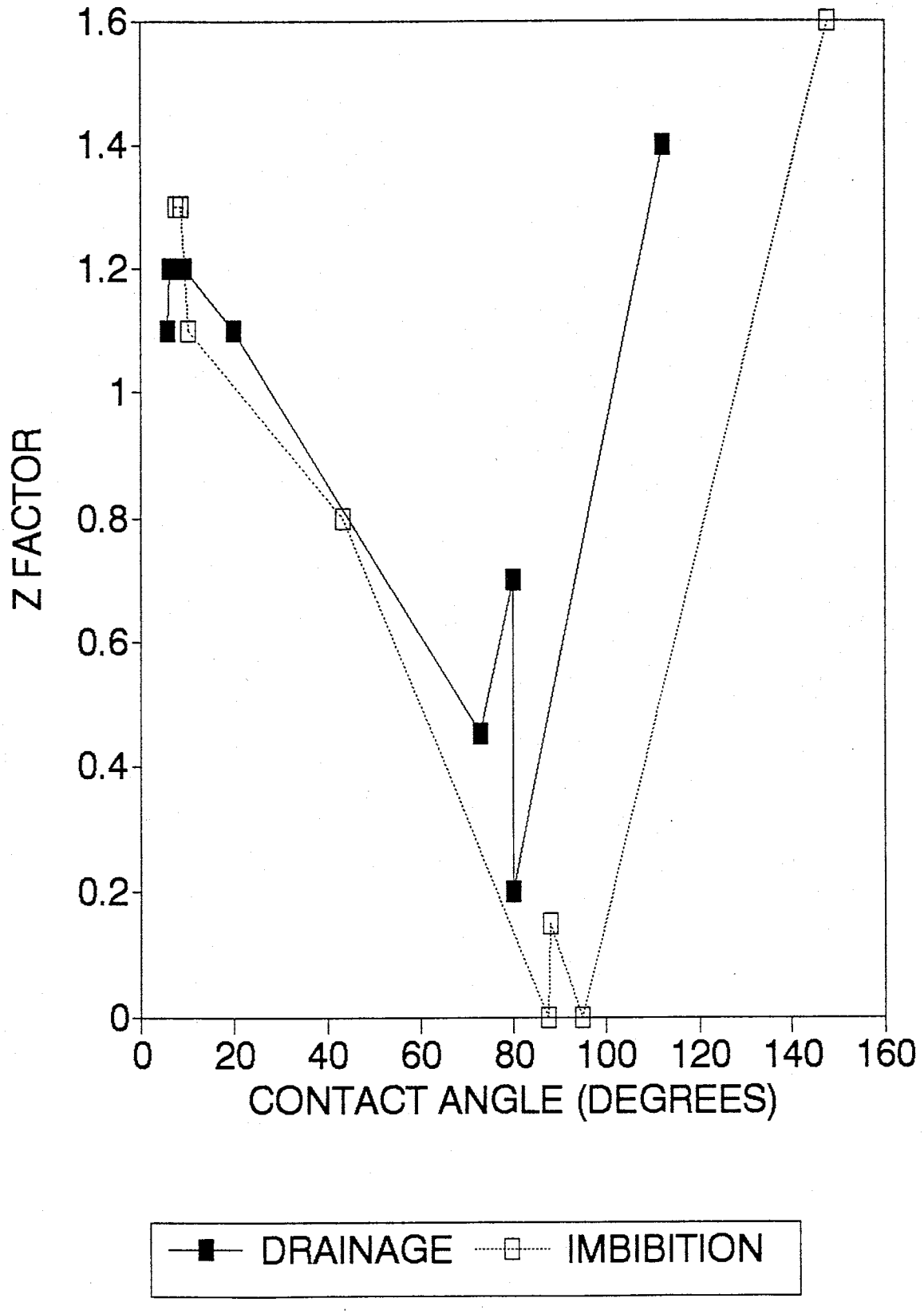

Discussion of the scaled capillary pressure-saturation results

These results indicate that the capillary tube model scaling procedure should probably not be used. Superficially it was relatively successful for the systems with contact angles below about 50°. However, this is not surprising since low contact angles (<20°) have a cosine near unity, and there was only one data point between about ten degrees and fifty degrees. In addition, the procedure appeared to work reasonably well for scaling different sizes of porous materials when the contact angle of the system is below 50°.

However, for systems with higher contact angles, the method did not work well. This failure may be attributed to a number of factors. Perhaps the most important factor is that the model does not consider the three dimensional geometry of the pore space which includes diverging and converging pores. In addition, the operative contact angle in the porous medium may not be close to that measured on the flat glass slides.

Therefore, use of the capillary tube model to scale capillary pressure-saturation curves (if it is used at all) should probably be limited to low (<50°) contact angle systems.

The Desai, et al., (1992) correction factor gave predicted results for four systems that were not in very

close agreement with the experimental results. The obvious problem with this scaling factor is that it corrects for roughness that probably is not present in these glass bead systems. The correction appears to have been appropriate for the silica sand systems used by Desai, et al., (1992), but they are not necessary for our smooth glass bead systems. Interestingly, however, if one were to leave out the roughness correction, the deviation between predicted and experimental results increases. The one attempt to scale with only the ratio of the interfacial tension (Leverett's (1941) function) appears to have worked well.

The plot of $Z$ factors versus contact angle has an interest shape. Values of $Z$ are above one for low contact angles. The $Z$ factors are near zero for the intermediate contact angles, and they increase again to near one for the higher contact angles. These experimental results can be compared with the calculations published by Melrose (1965). Of course, this is a relatively small data set from which to draw conclusions. More work in this area is needed to establish trends.

# CHAPTER 4

# SUMMARY, CONCLUSIONS AND RECOMMENDATIONS FOR FUTURE WORK

## SUMMARY AND CONCLUSIONS

### WETTABILITY ALTERATION TECHNIQUES

- From the contact angle results, MTMS appears to be a relatively stable treatment for rendering surfaces intermediate-wet.
- Based on this research, GC-18 is a suitable treatment for making surfaces hydrophobic.
- In general, the longer the functional carbon chain on an alkoxysilane, the more hydrophobic the substrate will become. Thus a methyl functional group with only one carbon will not be as hydrophobic as a functional group consisting of eighteen carbons, for example.

### CONTACT ANGLE MEASUREMENTS

- Advancing and receding contact angles were measured with the dynamic sessile drop method for the three fluid pairs using hydrophilic, hydrophobic, and intermediate-wet glass microscope slides. Advancing contact angles ranged from 6.5° for water and air on an untreated slide to 147.7° for water and Soltrol 130 on a slide treated with GC-18. Receding contact angles ranged from 4.5° for water and air on an untreated slide to 112.3° for water and Soltrol 130 on

a slide treated with GC-18.

SURFACE AND INTERFACIAL TENSION

- Surface and interfacial tension measurements were made for the three fluid combinations using the ring tensiometer method. The water-air surface tension was 70.7 dynes/cm. The Soltrol 130-air surface tension was 22.6 dynes/cm. The interfacial tension between water and Soltrol 130 was 36.9 dynes/cm. These results are in relatively good agreement with those reported by other researchers.

CAPILLARY PRESSURE-SATURATION

- Capillary pressure-saturation curves were measured for nine systems using a short column apparatus to determine whether the curves could be scaled using the capillary tube model. Three fluid combinations (water-air, water-Soltrol, and Soltrol-air) and three types of glass beads (untreated, GC-18-treated, and MTMS-treated) were used.
- Scaling capillary pressure-saturation curves with the capillary tube model was relatively successful for the systems with contact angles below about 50°. In addition, the procedure appeared to work reasonably well for scaling different sizes of porous materials when the contact angle of the system is below 50°.

However, for systems with higher contact angles, the

method did not work well. This failure may be attributed to a number of factors. Perhaps the most important factor is that the model, in assuming the porous medium can be likened to a bundle of capillary tubes, does not adequately account for diverging and converging pores. In addition, the operative contact angle in the porous medium may not be close to that measured on the flat glass slides.

- Scaling smooth glass beads with the correction factor used by Desai, et al., (1992) does not appear to work very well. The roughness correction it uses is probably not appropriate for glass bead systems.

## RECOMMENDATIONS FOR FUTURE WORK

### SURFACE WETTABILITY ALTERATION

- Attempt to observe the surfaces of hydrophilic (clean) and treated slides and glass beads under an electron microscope to learn more about the surface properties. These observations could be performed over time and in the presence of various fluids such as water, air, and Soltrol 130 to learn about the processes involved in treatment deterioration.

### CONTACT ANGLES AND INTERFACIAL TENSION

- Develop or obtain the software needed to use the computer imaging system to measure interfacial tension and

contact angles using the pendant drop method.

CAPILLARY PRESSURE-SATURATION

- Additional column studies could be done using glass beads with mixed wettability and using bead packs with a larger particle size distribution.
- Column studies could be performed using filtered Soltrol or with a pure organic phase such as decane.
- The short column apparatus used to measure capillary pressure-saturation curves required relatively long equilibrium times resulting in experiments that took several weeks to complete. In the future it would be desirable to design and build a dynamic system for measuring capillary pressure-saturation relationships. These systems are capable of obtaining complete drainage and imbibition curves for a sample in about one day. In addition, a data acquisition system could be installed to collect and store the results electronically.

SHORT COLUMNS

Refinements need to be made in the short column apparatus used for the displacement experiments. Key features that would be desirable in a redesigned apparatus are:

- The procedure used to glue filters onto endcaps used in frequently was unsuccessful and had to be repeated. Eliminate the need to glue the filters onto the fritted

glass disc. Hold the filters securely in place with o-rings to prevent leaks.

- Design the top endcap such that there is no need to thread the endcap inside the column. In other words, have a plate hold the porous media in the column directly. Tempe cells (Reginato and van Bavel, 1962) are set up this way on top and may provide ideas for redesigning the short columns. Tempe cells are available from Soil Moisture (Santa Barbara, CA).
- The current polycarbonate valves leak occasionally. A more robust valve that is still transparent would be desirable.

**REFERENCES**

Adamson, A.W. 1982. Physical chemistry of surfaces. 4th ed., John Wiley & Sons, New York.

Amott, E. 1959. Observations relating to the wettability of porous rocks. Trans. AIME 216:156-162.

Anderson, W.G. 1986b. Wettability literature survey - Part 2: Wettability measurement. J. Pet. Technol. 38(11):1246- 1262.

Andreas, J.M., E.A. Hauser, and W.B. Tucker. 1938. Boundary tension by pendant drops. J. Phys. Chem. 42:1001-1019.

Arkles, B., J.R. Steinmetz, J. Zazyczny and P. Mehta. 1991. Factors contributing to the stability of alkoxysilane in aqueous solution. In Silicon Compounds: Register and Review 5th Edition. Hüls America Inc. Piscataway, NJ.

Bowman, R.S. and J.L. Wilson. 1988. The effects of wetting on transport of organics. Unpublished research proposal to USGS.

Bowman, R.S., J.L. Wilson, M. Wei, R. Huddleston, D. Neel, and P. Burck. 1992. The effects of wetting on transport

of organics in groundwater. Technical completion report no. 268. New Mexico Water Resources Research Institute, Las Cruces, NM. 69p.

Calhoun, J.C., Jr., M. Lewis, Jr., and R.C. Newman. 1949. Experiments on the capillary properties of porous solids. Trans. AIME 186:189-196.

Corey, A.T. 1986. Mechanics of immiscible fluids in porous media. Littleton, Colorado: Water Resources Publications.

Dekker, L. 1992. Seminar at New Mexico Institute of Mining and Technology, Socorro, NM.

Demond, A.H. 1988. Capillarity in two-phase liquid flow of organic contaminants in groundwater. PhD. Thesis, Stanford University.

Demond, A.H., K.F. Hayes, and F.N. Desai. 1992. The influence of surfactant sorption on capillary pressure-saturation relationships for organic liquid-water systems, presented at Fall AGU Meeting, December, San Francisco, abstr. in EOS. Vol. 73, No. 27, p. 164.

Demond, A.H., and P.V. Roberts. 1991. Effect of interfacial

forces on two-phase capillary pressure-saturation relationships. Water Res. Res. 27(3):423-437.

Desai, F.N., A.H. Demond, and K.F. Hayes. 1992. The influence of surfactant sorption on capillary pressure-saturation relationships, Chapter 11, Colloid and Interfacial Aspects of Groundwater and Soil Cleanup. D.Sabatini and R. Knox (Eds), American Chemical Society, Washington, D.C., pp. 133-148.

Donaldson, E.C., R.D. Thomas, and P.B. Lorenz. 1969. Wettability determination and its effect on recovery efficiency. Soc. Petroleum Eng. J. (March 1969) pp. 13-20.

Dumore, J.M., and R.S. Schols. 1974. Drainage capillary functions and the influence of connate water. Soc. Petroleum Eng. J. 14:437-444.

du Nouy. 1919. Jour. Gen. Physiol. 1:521.

Fenimore, D.C., C.M. Davis, J.H. Whitford, and C.A. Harrington. 1976. Vapor phase silylation of laboratory glassware. Analytical Chemistry. 48(14):2289-2290.

Haines, W.B. 1930. Studies in the physical properties of

soils. V. The hysteresis effect in capillary properties, and the modes of moisture distribution associated herewith. Journ. Agric. Sci. 20:97-116.

Hillel, D. 1980. Fundamentals of soil physics. San Diego: Academic Press, Inc.

Hüls America. 1991. Silicon compounds register and review. Bristol, PA.

Jennings, H.Y. 1967. The effect of temperature and pressure on the interfacial tension of benzene-water and n-decane- water. J. Colloid Interf. Sci. 24:323-329.

Koorevaar, P., G. Menelik, and C. Dirksen. 1983. Elements of soil physics. Amsterdam: Elsevier Science Publishers.

Larson, R.G., and N.R. Morrow. 1981. Effects of sample size on capillary pressures in porous media. Powder Technology 30:123-138.

Lenhard, R.J., and J.C. Parker. 1987. Measurement and prediction of saturation-pressure relationships in three- phase porous media systems. J. Contaminant Hydrol. 1:407- 424.

Leverett, M.C. 1941. Capillary behavior in porous solids. Transactions of AIME. 142:152-169.

Mace, R.E. 1990. The effect of the fine fraction on the residual trapping of nonaqueous organic liquids in unconsolidated porous media in the saturated zone. Open file report, H 90-6, New Mexico Institute of Mining and Technology.

Mason, G., and N.R. Morrow. 1986. Meniscus displacement curvatures of a perfectly wetting liquid in capillary pore throats formed by spheres. J. Colloid Interface Sci. 109(1):46-56.

Mason, G., and N.R. Morrow. 1991. Capillary behavior of a perfectly wetting liquid in irregular triangular tubes. J. Colloid Interface Sci. 141(1):262-274.

Mason, G., M.D. Nguyen, and N.R. Morrow. 1983. Effect of contact angle on the meniscus between two equal contacting rods and a plate. J. Colloid Interface Sci. 95(2):494-501.

Melrose, J.C. 1965. Wettability as related to capillary action in porous media. Society of Petroleum Engineers Journal. 5:259-271.

Menawat, A., J. Henry, Jr., and R. Siriwardane. 1984. Control of surface energy of glass by surface reactions: contact angle and stability. J. Colloid Interface Sci. 101(1):110-119.

Morrow, N.R. 1975. Journal of Canadian Petroleum Technology. 14(4):42-53.

Morrow, N.R. 1976. Capillary pressure correlations for uniformly wetted porous media. J. Canadian Petroleum Technol. 15(4):49-69.

Morrow, N.R., and F.G. McCaffery. 1978. Displacement studies in uniformly wetted porous media. In Wetting, spreading and adhesion. Edited by J.F. Padday, 289-319. New York: Academic Press.

Morrow, N.R., and N. Mungan. 1981. Mouillabilite et capillarite en mileux poreux. Revue de L'Institut Francais du Petrole 26(7-8):629-650.

Purcell, W.R. 1949. Capillary pressures - their measurement using mercury and the calculation of permeability therefrom. Trans., AIME. 186:39.

Purcell, W.R. 1950. Interpretation of capillary pressure

data. Trans., AIME. 189:369.

Reginato, R.J. and C.H.M van Bavel. 1962. Soil Science Society of America Proceedings. 26(1):1-3.

Rotenberg, Y., L. Boruvka, and A.W. Neumann. 1983. J. Colloid Interface Sci. 93(169)

Takach, N.E., L.B. Bennett, C.B. Douglas, M.A. Andersen, and D.C. Thomas. 1988. Wettability alteration of model sandstone surfaces by vapor-phase treatment with organosilanes. Preprints, American Chemical Society. 33:525-529.

Wei, M. 1991. Wetting and non-aqueous phase liquid saturations in homogeneous porous media. Master's Thesis, New Mexico Institute of Mining and Technology, Socorro, New Mexico.

Wei, M., R.S. Bowman, J.L. Wilson, and N.R. Morrow. 1993. Wetting properties and stability of silane-treated glass exposed to water, air, and oil. J. Colloid Interf. Sci. Submitted for publication.

Wilson, J.L. 1988. The need for research: Physical processes-Land, the role of wetting in environmental

problems. Proc. Conf. on Fundamental Research Needs in Envr. Engineering. eds. R.G. Luthy and M.J. Small, Assoc. Environ. Engr. Professors, Washington, DC.

Wilson, J.L., S.H. Conrad, W.R. Mason, W.P. Peplinski, and E. Hagan. 1990. Laboratory investigation of residual liquid organics from spills, leaks, and the disposal of hazardous wastes in groundwater. EPA report: EPA/600/6-90/004.

# APPENDIX A

TABLE A1: Chemical Analysis of Glass Materials

| Typical Composition | Corning Glass Microslides (2947)[1] | Cataphote Glass Beads[2] |
|---|---|---|
| $SiO_2$ | 72.1% | 71-74% |
| $Fe_2O_3$ | 0.045% | 0-Trace |
| $Al_2O_3$ | 1.8% | 0.2-1.5% |
| CaO | 7.3% | 8.0-10.0% |
| MgO | 3.8% | 1.5-3.8% |
| $K_2O$ | 0.15% | 0-0.2% |
| $Na_2O$ | 14.0% | 12.0-15.0% |
| $SO_3$ | 0.3% | --- |

[1] From: Wei, M., 1991.

[2] From: Technical Data on the Chemical and Physical Properties of Standard Microbeads (Cataphote). The glass used to make glass beads is remelted soda-lime plate glass.

## APPENDIX B

This appendix contains the data from the contact angle experiments. The following list matches each contact angle measurement with the appropriate experiment number.

UNTREATED EXPERIMENTS

Water-Air.....Experiment 18
Water-Soltrol 130.....Experiment 31
Soltrol 130-Air.....Experiment 30

MTMS-TREATED EXPERIMENTS

Water-Air.....Experiment 34C
Water-Soltrol 130.....Experiment 33B
Soltrol 130-Air.....Experiment 38

GC-18-TREATED EXPERIMENTS

Water-Air.....Experiment 36
Water-Soltrol 130.....Experiment 37
Soltrol 130-Air.....Experiment 29B

GC-18 coverage experiment.....Experiment 8

GC-18 stability in water.....Experiment 29
GC-18 stability in air.....Experiment 29A

MTMS stability.....Experiments 33,34

NA stands for not applicable.
NR means not recorded.

TABLE B1: CAM08 WATER - AIR Contact Angle Measurement

| | |
|---|---|
| EXPERIMENT | CAM08 |
| FLUIDS | WATER - AIR |
| TREATMENT | GC-18 |
| STORAGE FLUID | AIR |

RESULTS:

| DATE 1991 | NUMBER OF GC-18 TREATMENTS | THETA ADVANCING (DEGREES) | THETA RECEDING (DEGREES) |
|---|---|---|---|
| JANUARY 18 | 0 | 39.9 ± 4.7 | 28.0 ± 3.5 |
| JANUARY 18 | 1 | 89.2 ± 4.0 | 70.9 ± 6.1 |
| JANUARY 18 | 2 | 91.9 ± 3.2 | 71.1 ± 4.3 |
| JANUARY 18 | 3 | 95.2 ± 3.0 | 77.4 ± 2.2 |
| JANUARY 19 | 4 | 97.5 ± 2.4 | 73.1 ± 1.6 |
| JANUARY 19 | 5 | 100.7 ± 3.3 | 72.6 ± 1.9 |
| JANUARY 19 | 6 | 100.8 ± 4.8 | 73.1 ± 3.3 |
| JANUARY 20 | 7 | 101.9 ± 5.4 | 70.2 ± 3.8 |
| JANUARY 20 | 8 | 99.7 ± 6.3 | 71.4 ± 3.9 |
| JANUARY 20 | 9 | 100.8 ± 3.9 | 73.2 ± 3.0 |
| JANUARY 20 | 10 | 102.0 ± 3.8 | 72.4 ± 3.5 |

TABLE B2: CAM18 WATER - AIR Contact Angle Measurement

| | |
|---|---|
| EXPERIMENT | CAM18 |
| FLUIDS | WATER - AIR |
| TREATMENT | UNTREATED |
| STORAGE FLUID | NA |

RESULTS:

| DATE 1991 | TIME | HOURS ELAPSED | THETA ADVANCING (DEGREES) | THETA RECEDING (DEGREES) |
|---|---|---|---|---|
| JULY 3 | NR | NA | 6.7 ± 0.7 | 4.5 ± 1.6 |

TABLE B3: CAM29 WATER - AIR Contact Angle Measurement

| | |
|---|---|
| EXPERIMENT | CAM29 |
| FLUIDS | WATER - AIR |
| TREATMENT | GC-18 |
| STORAGE FLUID | WATER WITH 1000 mg/L $NaN_3$ |

RESULTS:

| DATE 1991 | TIME | HOURS ELAPSED | THETA ADVANCING (DEGREES) | THETA RECEDING (DEGREES) |
|---|---|---|---|---|
| AUGUST 28 | 16:00 | 0.00 | 100.6 ± 2.4 | 73.6 ± 3.0 |
| SEPTEMBER 1 | 14:30 | 94.50 | 95.1 ± 3.0 | 69.2 ± 4.4 |
| SEPTEMBER 5 | 15:15 | 191.25 | 91.0 ± 0.9 | 66.1 ± 3.1 |
| SEPTEMBER 10 | 12:30 | 308.50 | 95.2 ± 1.8 | 72.8 ± 1.7 |
| SEPTEMBER 16 | 19:00 | 459.00 | 96.8 ± 2.0 | 75.0 ± 2.0 |
| SEPTEMBER 27 | 12:30 | 716.50 | 100.9 ± 1.9 | 74.6 ± 2.4 |
| OCTOBER 4 | 17:00 | 889.00 | 99.1 ± 2.9 | 73.1 ± 2.4 |

TABLE B4: CAM29A WATER - AIR Contact Angle Measurement

| | |
|---|---|
| EXPERIMENT | CAM29A |
| FLUIDS | WATER - AIR |
| TREATMENT | GC-18 |
| STORAGE FLUID | AIR |

RESULTS:

| DATE 1991 | TIME | HOURS ELAPSED | THETA ADVANCING (DEGREES) | THETA RECEDING (DEGREES) |
|---|---|---|---|---|
| AUGUST 28 | 16:00 | 0.00 | 100.6 ± 2.4 | 73.6 ± 3.0 |
| SEPTEMBER 1 | 15:00 | 95.00 | 95.1 ± 1.8 | 75.0 ± 2.4 |
| SEPTEMBER 5 | 15:00 | 191.00 | 96.5 ± 2.3 | 77.2 ± 1.6 |
| SEPTEMBER 10 | 12:00 | 308.00 | 94.8 ± 1.9 | 75.9 ± 2.1 |
| SEPTEMBER 16 | 18:30 | 458.50 | 95.7 ± 2.0 | 74.7 ± 2.9 |
| SEPTEMBER 27 | 12:15 | 716.25 | 97.4 ± 2.1 | 78.6 ± 3.7 |
| OCTOBER 4 | 17:15 | 889.25 | 98.1 ± 3.2 | 76.5 ± 3.9 |

TABLE B5: CAM29B SOLTROL - AIR Contact Angle Measurement

| | |
|---|---|
| EXPERIMENT | CAM29B |
| FLUIDS | SOLTROL - AIR |
| TREATMENT | GC-18 |
| STORAGE FLUID | NA |

RESULTS:

| DATE 1992 | TIME | HOURS ELAPSED | THETA ADVANCING (DEGREES) | THETA RECEDING (DEGREES) |
|---|---|---|---|---|
| MARCH 28 | NR | NA | 8.8 ± 1.9 | 6.3 ± 1.4 |

TABLE B6: CAM30 SOLTROL - AIR Contact Angle Measurement

| | |
|---|---|
| EXPERIMENT | CAM30 |
| FLUIDS | SOLTROL - AIR |
| TREATMENT | UNTREATED |
| STORAGE FLUID | NA |

RESULTS:

| DATE 1991 | TIME | HOURS ELAPSED | THETA ADVANCING (DEGREES) | THETA RECEDING (DEGREES) |
|---|---|---|---|---|
| OCTOBER 4 | NR | NA | 7.5 ± 2.5 | 5.7 ± 2.3 |

TABLE B7: CAM31 WATER - SOLTROL Contact Angle Measurement

| | |
|---|---|
| EXPERIMENT | CAM31 |
| FLUIDS | WATER - SOLTROL |
| TREATMENT | UNTREATED |
| STORAGE FLUID | NA |

RESULTS:

| DATE 1991 | TIME | HOURS ELAPSED | THETA ADVANCING (DEGREES) | THETA RECEDING (DEGREES) |
|---|---|---|---|---|
| OCTOBER 4 | NR | NA | 43.5 ± 3.0 | 19.9 ± 2.5 |

TABLE B8: CAM33A WATER - AIR Contact Angle Measurement

| | |
|---|---|
| EXPERIMENT | CAM33A |
| FLUIDS | WATER - AIR |
| TREATMENT | MTMS |
| STORAGE FLUID | AIR |

RESULTS:

| DATE 1992 | TIME | HOURS ELAPSED | THETA ADVANCING (DEGREES) | THETA RECEDING (DEGREES) |
|---|---|---|---|---|
| JUNE 18 | 11:30 | 0.00 | 80.2 ± 2.0 | 59.3 ± 4.1 |
| JUNE 19 | 16:15 | 28.75 | 88.4 ± 2.9 | 66.4 ± 3.4 |
| JUNE 21 | 20:00 | 80.50 | 88.5 ± 1.4 | 69.7 ± 2.8 |
| JUNE 25 | 14:00 | 170.50 | 89.0 ± 2.4 | 67.8 ± 1.9 |
| JULY 6 | 15:00 | 435.50 | 87.6 ± 1.5 | 70.6 ± 2.1 |
| JULY 13 | 14:30 | 603.00 | 88.0 ± 3.8 | 69.3 ± 3.9 |
| JULY 21 | 13:45 | 794.25 | 87.9 ± 2.6 | 69.2 ± 3.4 |
| JULY 30 | 11:15 | 1007.75 | 90.0 ± 1.3 | 74.7 ± 1.2 |

TABLE B9: CAM33B WATER - SOLTROL Contact Angle Measurement

| | |
|---|---|
| EXPERIMENT | CAM33B |
| FLUIDS | WATER - SOLTROL 130 |
| TREATMENT | MTMS |
| STORAGE FLUID | WATER WITH 1000 mg/L $NaN_3$ |

RESULTS:

| DATE 1992 | TIME | HOURS ELAPSED | THETA ADVANCING (DEGREES) | THETA RECEDING (DEGREES) |
|---|---|---|---|---|
| JUNE 18 | 12:15 | 0.00 | 107.3 ± 2.5 | 92.2 ± 1.4 |
| JUNE 19 | 16:45 | 28.50 | 101.3 ± 2.7 | 80.3 ± 5.3 |
| JUNE 21 | 20:15 | 80.00 | 101.2 ± 2.6 | 74.0 ± 6.4 |
| JUNE 25 | 15:00 | 170.75 | 99.3 ± 2.5 | 75.4 ± 2.5 |
| JULY 6 | 18:00 | 437.75 | 94.6 ± 2.1 | 80.0 ± 5.7 |
| JULY 13 | 15:45 | 603.50 | 93.0 ± 2.3 | 74.0 ± 4.2 |
| JULY 21 | 15:15 | 795.00 | 96.5 ± 3.3 | 76.8 ± 4.4 |
| JULY 30 | 12:00 | 1007.75 | 89.4 ± 1.9 | 64.3 ± 3.9 |

TABLE B10: CAM33C WATER - AIR Contact Angle Measurement

| | |
|---|---|
| EXPERIMENT | CAM33C |
| FLUIDS | WATER - AIR |
| TREATMENT | MTMS |
| STORAGE FLUID | SOLTROL 130 |

RESULTS:

| DATE 1992 | TIME | HOURS ELAPSED | THETA ADVANCING (DEGREES) | THETA RECEDING (DEGREES) |
|---|---|---|---|---|
| JUNE 18 | 11:30 | 0.00 | 80.2 ± 2.0 | 59.3 ± 4.1 |
| JUNE 19 | 17:15 | 29.25 | 89.4 ± 1.3 | 70.0 ± 4.2 |
| JUNE 25 | 14:30 | 169.00 | 85.5 ± 2.6 | 66.7 ± 2.4 |
| JULY 6 | 17:30 | 436.00 | 80.6 ± 2.0 | 64.4 ± 4.6 |
| JULY 13 | 15:30 | 602.00 | 83.0 ± 2.0 | 60.2 ± 3.8 |
| JULY 21 | 15:00 | 793.50 | 80.2 ± 1.3 | 64.7 ± 2.6 |
| JULY 30 | 11:45 | 1006.25 | 85.0 ± 1.9 | 63.8 ± 2.1 |

TABLE B11: CAM33D WATER - AIR Contact Angle Measurement

| | |
|---|---|
| EXPERIMENT | CAM33D |
| FLUIDS | WATER - AIR |
| TREATMENT | MTMS |
| STORAGE FLUID | WATER WITH 1000 mg/L $NaN_3$ |

RESULTS:

| DATE 1992 | TIME | HOURS ELAPSED | THETA ADVANCING (DEGREES) | THETA RECEDING (DEGREES) |
|---|---|---|---|---|
| JUNE 18 | 11:30 | 0.00 | 80.2 ± 2.0 | 59.3 ± 4.1 |
| JUNE 19 | 16:30 | 29.00 | 79.6 ± 3.5 | 62.1 ± 4.7 |
| JUNE 21 | 20:05 | 80.50 | 75.5 ± 3.9 | 56.9 ± 3.8 |
| JUNE 25 | 14:15 | 170.75 | 76.0 ± 2.9 | 56.9 ± 1.8 |
| JULY 6 | 17:00 | 437.75 | 69.9 ± 4.1 | 58.7 ± 5.0 |
| JULY 13 | 15:00 | 603.50 | 75.3 ± 3.9 | 52.4 ± 2.1 |
| JULY 21 | 14:00 | 794.50 | 69.5 ± 2.0 | 55.8 ± 2.1 |
| JULY 30 | 11:30 | 1007.00 | 70.7 ± 1.9 | 52.4 ± 2.6 |

TABLE B12: CAM34A WATER - AIR Contact Angle Measurement

| | |
|---|---|
| EXPERIMENT | CAM34A |
| FLUIDS | WATER - AIR |
| TREATMENT | MTMS |
| STORAGE FLUID | AIR |

RESULTS:

| DATE 1992 | TIME | HOURS ELAPSED | THETA ADVANCING (DEGREES) | THETA RECEDING (DEGREES) |
|---|---|---|---|---|
| JULY 23 | 12:00 | 0.00 | 86.2 ± 2.8 | 59.6 ± 5.0 |
| JULY 29 | 10:00 | 142.00 | 88.5 ± 4.2 | 65.6 ± 4.9 |
| AUGUST 12 | 14:15 | 482.25 | 86.6 ± 3.0 | 72.1 ± 4.6 |
| AUGUST 26 | 14:45 | 818.75 | 89.9 ± 1.8 | 75.5 ± 3.3 |
| SEPTEMBER 9 | 10:30 | 1150.50 | 89.0 ± 1.6 | 73.4 ± 1.8 |

TABLE B13: CAM34B WATER - SOLTROL Contact Angle Measurement

| | |
|---|---|
| EXPERIMENT | CAM34B |
| FLUIDS | WATER - SOLTROL 130 |
| TREATMENT | MTMS |
| STORAGE FLUID | WATER WITH 1000 mg/L $NaN_3$ |

RESULTS:

| DATE 1992 | TIME | HOURS ELAPSED | THETA ADVANCING (DEGREES) | THETA RECEDING (DEGREES) |
|---|---|---|---|---|
| JULY 23 | 15:30 | 0.00 | 133.9 ± 5.0 | 100.1 ± 4.9 |
| JULY 29 | 11:00 | 139.50 | 103.9 ± 2.1 | 81.3 ± 3.9 |
| AUGUST 12 | 15:30 | 480.00 | 95.4 ± 1.5 | 67.4 ± 3.9 |
| AUGUST 26 | 15:30 | 816.00 | 96.1 ± 3.9 | 76.0 ± 6.4 |
| SEPTEMBER 9 | 14:00 | 1150.50 | 93.5 ± 2.3 | 69.9 ± 3.9 |

TABLE B14: CAM34C WATER - AIR Contact Angle Measurement

| | |
|---|---|
| EXPERIMENT | CAM34C |
| FLUIDS | WATER - AIR |
| TREATMENT | MTMS |
| STORAGE FLUID | SOLTROL 130 |

RESULTS:

| DATE 1992 | TIME | HOURS ELAPSED | THETA ADVANCING (DEGREES) | THETA RECEDING (DEGREES) |
|---|---|---|---|---|
| JULY 23 | 12:30 | 0.00 | 88.0 ± 1.6 | 72.8 ± 2.6 |
| JULY 29 | 10:45 | 142.25 | 86.4 ± 3.4 | 69.1 ± 3.1 |
| AUGUST 12 | 15:00 | 482.75 | 85.3 ± 2.8 | 73.3 ± 4.1 |
| AUGUST 26 | 15:15 | 819.00 | 86.7 ± 1.4 | 73.9 ± 1.9 |
| SEPTEMBER 9 | 13:45 | 1153.50 | 82.4 ± 3.0 | 66.2 ± 5.6 |

TABLE B15: CAM34D WATER - AIR Contact Angle Measurement

| | |
|---|---|
| EXPERIMENT | CAM34D |
| FLUIDS | WATER - AIR |
| TREATMENT | MTMS |
| STORAGE FLUID | WATER WITH 1000 mg/L $NaN_3$ |

RESULTS:

| DATE 1992 | TIME | HOURS ELAPSED | THETA ADVANCING (DEGREES) | THETA RECEDING (DEGREES) |
|---|---|---|---|---|
| JULY 23 | 12:15 | 0.00 | 88.6 ± 1.8 | 75.0 ± 2.2 |
| JULY 29 | 10:30 | 142.25 | 84.4 ± 4.0 | 61.4 ± 5.6 |
| AUGUST 12 | 14:30 | 482.25 | 82.3 ± 6.8 | 55.4 ± 6.7 |
| AUGUST 26 | 15:00 | 818.75 | 77.5 ± 3.1 | 56.0 ± 2.8 |
| SEPTEMBER 9 | 13:30 | 1153.25 | 83.4 ± 4.7 | 58.2 ± 5.9 |

TABLE B16: CAM36 WATER - AIR Contact Angle Measurement

| | |
|---|---|
| EXPERIMENT | CAM36 |
| FLUIDS | WATER - AIR |
| TREATMENT | GC-18 |
| STORAGE FLUID | NA |

RESULTS:

| DATE 1992 | TIME | TEMPERATURE | THETA ADVANCING (DEGREES) | THETA RECEDING (DEGREES) |
|---|---|---|---|---|
| JULY 24 | 1600 | 23.0° C | 87.6 ± 1.9 | 80.2 ± 4.1 |

TABLE B17: CAM37 WATER - SOLTROL Contact Angle Measurement

| | |
|---|---|
| EXPERIMENT | CAM37 |
| FLUIDS | WATER - SOLTROL |
| TREATMENT | GC-18 |
| STORAGE FLUID | NA |

RESULTS:

| DATE 1992 | TIME | TEMPERATURE | THETA ADVANCING (DEGREES) | THETA RECEDING (DEGREES) |
|---|---|---|---|---|
| JULY 24 | 1800 | 23.5° C | 147.7 ± 9.0 | 112.3 ± 7.9 |

TABLE B18: CAM38 SOLTROL - AIR Contact Angle Measurement

| | |
|---|---|
| EXPERIMENT | CAM38 |
| FLUIDS | SOLTROL - AIR |
| TREATMENT | MTMS |
| STORAGE FLUID | NA |

RESULTS:

| DATE 1992 | TIME | TEMPERATURE | THETA ADVANCING (DEGREES) | THETA RECEDING (DEGREES) |
|---|---|---|---|---|
| SEPTEMBER 1 | 2000 | 19.0° C | 10.2 ± 2.6 | 9.3 ± 3.0 |

## Appendix C

Appendix C contains the data from the surface and interfacial tension measurements.

TABLE C1: STM 101 WATER - AIR Surface Tension Measurement

| | |
|---|---|
| EXPERIMENT | STM 101 |
| FLUIDS | WATER - AIR |
| DATE | JULY 14, 1992 |
| TIME | 11:30 |
| TEMPERATURE | 21.5 DEGREES C |

Water was ultrapure.

RESULTS:

| MEASUREMENT NUMBER | APPARENT SURFACE TENSION (DYNES / CM) | TIME |
|---|---|---|
| 1 | 75.7 | NA |
| 2 | 75.8 | NA |
| 3 | 75.7 | NA |
| 4 | 75.6 | NA |
| 5 | 75.5 | NA |
| 6 | 75.5 | NA |
| 7 | 75.6 | NA |
| 8 | 75.4 | NA |
| 9 | 75.3 | NA |
| 10 | 75.5 | NA |

STATISTICS:

| | |
|---|---|
| AVERAGE | 75.6 DYNES PER CM |
| SAMPLE STANDARD DEVIATION | 0.2 |
| CORRECTION FACTOR | 0.9 |
| TRUE SURFACE TENSION | 70.7 DYNES PER CM |

TABLE C2: STM 102 WATER - AIR Surface Tension Measurement

| | |
|---|---|
| EXPERIMENT | STM 102 |
| FLUIDS | WATER - AIR |
| DATE | JULY 14, 1992 |
| TIME | 15:00 |
| TEMPERATURE | 21.5 DEGREES C |

Water was ultrapure and degassed.

RESULTS:

| MEASUREMENT NUMBER | APPARENT SURFACE TENSION (DYNES / CM) | TIME |
|---|---|---|
| 1 | 75.9 | NA |
| 2 | 75.3 | NA |
| 3 | 75.3 | NA |
| 4 | 74.9 | NA |
| 5 | 74.8 | NA |
| 6 | 74.9 | NA |
| 7 | 74.7 | NA |
| 8 | 74.5 | NA |
| 9 | 74.5 | NA |
| 10 | 74.8 | NA |

STATISTICS:

| | |
|---|---|
| AVERAGE | 75.0 DYNES / CM |
| SAMPLE STANDARD DEVIATION | 0.4 DYNES / CM |
| CORRECTION FACTOR | 0.9 |
| TRUE SURFACE TENSION | 70.1 DYNES / CM |

TABLE C3: STM 103 WATER - AIR Surface Tension Measurement

| | |
|---|---|
| EXPERIMENT | STM 103 |
| FLUIDS | WATER - AIR |
| DATE | JULY 14, 1992 |
| TIME | 15:30 |
| TEMPERATURE | 21.5 DEGREES C |

Water was ultrapure, degassed and contained 1000 mg/L $NaN_3$ as a bactericide.

RESULTS:

| MEASUREMENT NUMBER | APPARENT SURFACE TENSION (DYNES / CM) | TIME |
|---|---|---|
| 1 | 67.4 | 15:38 |
| 2 | 68.6 | 15:39 |
| 3 | 69.0 | 15:40 |
| 4 | 69.8 | 15:41 |
| 5 | 70.0 | 15:42 |
| 6 | 70.8 | 15:43 |
| 7 | 70.9 | 15:44 |
| 8 | 71.3 | 15:45 |
| 9 | 72.2 | 15:47 |
| 10 | 72.0 | 15:48 |

STATISTICS:

| | |
|---|---|
| AVERAGE | 70.2 DYNES / CM |
| SAMPLE STANDARD DEVIATION | 1.5 DYNES / CM |
| CORRECTION FACTOR | 0.9 |
| TRUE SURFACE TENSION | 65.3 DYNES / CM |

TABLE C4: STM 104 SOLTROL 130 - AIR Surface Tension Measurement

| | |
|---|---|
| EXPERIMENT | STM 104 |
| FLUIDS | SOLTROL 130 - AIR |
| DATE | JULY 14, 1992 |
| TIME | 16:50 |
| TEMPERATURE | 21.5 DEGREES C |

Regular Soltrol 130 Lot E-833

RESULTS:

| MEASUREMENT NUMBER | APPARENT SURFACE TENSION (DYNES / CM) | TIME |
|---|---|---|
| 1 | 25.9 | 16:50 |
| 2 | 25.7 | 16:51 |
| 3 | 25.8 | 16:52 |
| 4 | 25.8 | 16:56 |
| 5 | 25.7 | 16:57 |
| 6 | 25.7 | 16:58 |
| 7 | 25.7 | 17:00 |
| 8 | 25.7 | 17:01 |
| 9 | 25.7 | 17:03 |
| 10 | 25.8 | 17:04 |

STATISTICS:

| | |
|---|---|
| AVERAGE | 25.8 DYNES / CM |
| SAMPLE STANDARD DEVIATION | 0.1 DYNES / CM |
| CORRECTION FACTOR | 0.9 |
| TRUE SURFACE TENSION | 22.7 DYNES / CM |

TABLE C5: STM 105 SOLTROL 130 - AIR Surface Tension Measurement

| | |
|---|---|
| EXPERIMENT | STM 105 |
| FLUIDS | SOLTROL 130 - AIR |
| DATE | JULY 14, 1992 |
| TIME | 17:09 |
| TEMPERATURE | 21.5 DEGREES C |

Degassed Regular Soltrol 130 Lot E-833

RESULTS:

| MEASUREMENT NUMBER | APPARENT SURFACE TENSION (DYNES / CM) | TIME |
|---|---|---|
| 1 | 25.6 | 17:09 |
| 2 | 25.9 | 17:10 |
| 3 | 25.6 | 17:11 |
| 4 | 25.5 | 17:12 |
| 5 | 25.6 | 17:13 |
| 6 | 25.7 | 17:14 |
| 7 | 25.7 | 17:15 |
| 8 | 25.6 | 17:17 |
| 9 | 25.7 | 17:18 |
| 10 | 25.7 | 17:19 |

STATISTICS:

| | |
|---|---|
| AVERAGE | 25.7 DYNES / CM |
| SAMPLE STANDARD DEVIATION | 0.1 DYNES / CM |
| CORRECTION FACTOR | 0.9 |
| TRUE SURFACE TENSION | 22.6 DYNES / CM |

TABLE C6: STM 106 WATER - SOLTROL 130 Interfacial Tension Measurement

| | |
|---|---|
| EXPERIMENT | STM 106 |
| FLUIDS | WATER - SOLTROL 130 |
| DATE | JULY 17, 1992 |
| TIME | 12:00 |
| TEMPERATURE | (NOT RECORDED) |

RESULTS:

| MEASUREMENT NUMBER | APPARENT SURFACE TENSION (DYNES / CM) | TIME |
|---|---|---|
| 1 | 41.3 | 12:12 |
| 2 | 41.0 | 12:14 |
| 3 | 40.7 | 12:16 |
| 4 | 41.2 | 12:17 |
| 5 | 41.1 | 12:19 |
| 6 | 40.5 | 12:20 |
| 7 | 40.5 | 12:22 |
| 8 | 40.6 | 12:23 |
| 9 | 40.2 | 12:24 |
| 10 | 40.2 | 12:25 |

NOTE: In this experiment only measurement number 1 is valid. Measurements 2 through 10 are not considered valid because the ring becomes "contaminated" with oil after the first measurement. The additional measurements were performed to determine the extent of the change in the surface tension given this contamination.

STATISTICS:

| | |
|---|---|
| AVERAGE | (NOT APPLICABLE) DYNES / CM |
| SAMPLE STANDARD DEVIATION | (NOT APPLICABLE) DYNES / CM |
| CORRECTION FACTOR FOR NO. 1 | 0.9 |
| TRUE SURFACE TENSION FOR NO. 1 | 37.2 DYNES / CM |

TABLE C7: STM 107 WATER - SOLTROL 130 Interfacial Tension Measurement

| | |
|---|---|
| EXPERIMENT | STM 107 |
| FLUIDS | WATER - SOLTROL 130 |
| DATE | JULY 17, 1992 |
| TIME | 17:00 |
| TEMPERATURE | (NOT RECORDED) |

RESULTS:

| MEASUREMENT NUMBER | APPARENT SURFACE TENSION (DYNES / CM) | TIME |
|---|---|---|
| 1 | 41.1 | 17:27 |
| 2 | 40.6 | 17:28 |
| 3 | 40.2 | 17:30 |
| 4 | 40.1 | 17:31 |
| 5 | 39.8 | 17:33 |
| 6 | 39.9 | 17:34 |
| 7 | 40.0 | 17:37 |
| 8 | 39.6 | 17:38 |
| 9 | 39.4 | 17:40 |
| 10 | 39.4 | 17:41 |

NOTE: In this experiment only measurement number 1 is valid. Measurements 2 through 10 are not considered valid because the ring becomes "contaminated" with oil after the first measurement. The additional measurements were performed to determine the extent of the change in the surface tension given this contamination.

STATISTICS:

| | |
|---|---|
| AVERAGE | (NOT APPLICABLE) DYNES / CM |
| SAMPLE STANDARD DEVIATION | (NOT APPLICABLE) DYNES / CM |
| CORRECTION FACTOR FOR NO. 1 | 0.9 |
| TRUE SURFACE TENSION FOR NO. 1 | 37.3 DYNES / CM |

TABLE C8: STM 108 WATER - SOLTROL 130 Interfacial Tension Measurement

| | |
|---|---|
| EXPERIMENT | STM 108 |
| FLUIDS | WATER - SOLTROL 130 |
| DATE | JULY 20, 1992 |
| TIME | 14:30 |
| TEMPERATURE | 22.5 DEGREES C |

RESULTS:

| MEASUREMENT NUMBER | APPARENT SURFACE TENSION (DYNES / CM) | TIME |
|---|---|---|
| 1 | 40.2 | 14:35 |
| 2 | 40.5 | 14:36 |
| 3 | 40.7 | 14:38 |
| 4 | 40.6 | 14:39 |
| 5 | 40.6 | 14:41 |
| 6 | 41.0 | 14:42 |
| 7 | 40.8 | 14:43 |
| 8 | 40.6 | 14:44 |
| 9 | 41.0 | 14:45 |
| 10 | 40.6 | 14:47 |

NOTE: In this experiment only measurement number 1 is valid. Measurements 2 through 10 are not considered valid because the ring becomes "contaminated" with oil after the first measurement. The additional measurements were performed to determine the extent of the change in the surface tension given this contamination.

STATISTICS:

| | |
|---|---|
| AVERAGE | (NOT APPLICABLE) DYNES / CM |
| SAMPLE STANDARD DEVIATION | (NOT APPLICABLE) DYNES / CM |
| CORRECTION FACTOR FOR NO. 1 | 0.9 |
| TRUE SURFACE TENSION FOR NO. 1 | 36.1 DYNES / CM |

TABLE C9: STM 109 WATER - AIR Surface Tension Measurement

| | |
|---|---|
| EXPERIMENT | STM 109 |
| FLUIDS | WATER - AIR |
| DATE | JULY 22, 1992 |
| TIME | 16:45 |
| TEMPERATURE | 26.0 DEGREES C |

Water was ultrapure.

RESULTS:

| MEASUREMENT NUMBER | APPARENT SURFACE TENSION (DYNES / CM) | TIME |
|---|---|---|
| 1 | 74.7 | 16:52 |
| 2 | 74.5 | 16:55 |
| 3 | 74.9 | 16:57 |
| 4 | 74.5 | 16:59 |
| 5 | 74.4 | 17:01 |
| 6 | 74.4 | 17:03 |
| 7 | 74.4 | 17:05 |
| 8 | 74.2 | 17:07 |
| 9 | 74.4 | 17:09 |
| 10 | 74.3 | 17:10 |

STATISTICS:

| | |
|---|---|
| AVERAGE | 74.5 DYNES / CM |
| SAMPLE STANDARD DEVIATION | 0.2 DYNES / CM |
| CORRECTION FACTOR | 0.9 |
| TRUE SURFACE TENSION | 69.6 DYNES / CM |

## APPENDIX D

This appendix contains the data from the capillary pressure-saturation experiments. The following list matches each capillary pressure-saturation experiment with the appropriate experiment number. Each experiment give the capillary pressure in centimeters, the percent saturation and the column $P*R/(\sigma*\theta)$ is the scaled capillary pressure which is dimensionless.

| UNTREATED EXPERIMENTS | EXPERIMENT | TABLE |
|---|---|---|
| Water-Air..... | 6, 7 | D1, D2 |
| Water-Soltrol 130..... | 24 | D4 |
| Soltrol 130-Air..... | 23 | D3 |
| **MTMS-TREATED EXPERIMENTS** | | |
| Water-Air..... | 38, 39 | D11, D12 |
| Water-Soltrol 130..... | 35 | D9 |
| Soltrol 130-Air..... | 37 | D10 |
| **GC-18-TREATED EXPERIMENTS** | | |
| Water-Air..... | 28 D7 | |
| Water-Soltrol 130..... | 27 | D6 |
| Soltrol 130-Air..... | 25, 30 | D5, D8 |

Wei's (1991) Results

| UNTREATED | | |
|---|---|---|
| Water-Soltrol 130..... | MW14 | D13 |

Haines (1930) Results

| UNTREATED | | |
|---|---|---|
| Water-Air..... | | D14 |

TABLE D1: PB06 UNTREATED WATER-AIR

| CAPILLARY PRESSURE (cm of H2O) | PERCENT WATER SATURATION | P*R/(σ*θ) |
|---|---|---|
| 0.0 | 100.0 | 0.0 |
| 1.3 | 99.9 | 0.052361 |
| 2.3 | 99.8 | 0.092639 |
| 3.9 | 99.8 | 0.157083 |
| 7.5 | 99.7 | 0.302083 |
| 11.9 | 99.7 | 0.479306 |
| 17.55 | 99.6 | 0.706875 |
| 23.4 | 99.7 | 0.9425 |
| 27.2 | 99.6 | 1.095556 |
| 35.4 | 99.6 | 1.425833 |
| 45.45 | 99.6 | 1.830625 |
| 56.35 | 99.6 | 2.269653 |
| 64.8 | 99.6 | 2.61 |
| 91.0 | 99.0 | 3.665278 |
| 103.0 | 98.6 | 4.148611 |
| 113.35 | 97.7 | 4.565486 |
| 120.6 | 97.1 | 4.8575 |
| 132.9 | 96.0 | 5.352917 |
| 144.0 | 92.1 | 5.8 |
| 148.2 | 84.7 | 5.969167 |
| 152.0 | 74.1 | 6.122222 |
| 154.6 | 68.0 | 6.226944 |
| 155.6 | 56.4 | 6.267222 |
| 158.5 | 48.1 | 6.384028 |
| 161.05 | 42.2 | 6.486736 |
| 163.6 | 37.5 | 6.589444 |
| 166.2 | 34.6 | 6.694167 |
| 169.2 | 31.5 | 6.815 |
| 172.7 | 28.5 | 6.955972 |
| 174.6 | 27.1 | 7.0325 |
| 180.6 | 26.9 | 7.274167 |
| 185.2 | 22.6 | 7.459444 |
| 190.45 | 22.5 | 7.670903 |
| 194.6 | 18.7 | 7.838056 |
| 200.8 | 16.4 | 8.087778 |
| 205.8 | 15.2 | 8.289167 |
| 210.6 | 14.0 | 8.4825 |
| 216.0 | 13.0 | 8.7 |
| 221.5 | 11.9 | 8.921528 |
| 226.3 | 11.7 | 9.114861 |
| 229.2 | 11.7 | 9.231667 |
| 236.65 | 10 | 9.531736 |
| 243.4 | 9.1 | 9.803611 |
| 249.3 | 8.9 | 10.04125 |

TABLE D1: PB06 UNTREATED WATER-AIR (CONTINUED)

| CAPILLARY PRESSURE (cm of H2O) | PERCENT WATER SATURATION | P*R/(σ*θ) |
|---|---|---|
| 255.4 | 8.7 | 10.28694 |
| 265.4 | 8.5 | 10.68972 |
| 275.5 | 8.2 | 11.09653 |
| 283.8 | 8.2 | 11.43083 |
| 292.0 | 8.1 | 11.76111 |
| 312.1 | 8.1 | 12.57069 |
| 344.2 | 7.9 | 13.86361 |
| 363.9 | 7.8 | 14.65708 |
| 247.9 | 7.9 | 9.984861 |
| 216.9 | 8.2 | 8.73625 |
| 198.6 | 9.4 | 7.999167 |
| 163.75 | 10.8 | 6.595486 |
| 138.0 | 14.3 | 5.558333 |
| 113.5 | 25.0 | 4.571528 |
| 87.4 | 70.7 | 3.520278 |
| 57.6 | 80.9 | 2.32 |
| 38.8 | 83.8 | 1.562778 |
| 19.0 | 84.9 | 0.765278 |
| 9.7 | 85.2 | 0.390694 |
| 6.2 | 85.2 | 0.249722 |
| 1.3 | 85.4 | 0.052361 |

TABLE D2: PB07 UNTREATED WATER-AIR

| CAPILLARY PRESSURE (cm of H2O) | PERCENT WATER SATURATION | $P*R/(\sigma*\theta)$ |
|---|---|---|
| 0.0 | 100.0 | .0 |
| 20.5 | 99.6 | 0.825694 |
| 42.2 | 99.6 | 1.699722 |
| 62.65 | 99.5 | 2.523403 |
| 83.7 | 99.5 | 3.37125 |
| 104.1 | 98.6 | 4.192917 |
| 123.7 | 95.2 | 4.982361 |
| 132.5 | 92.8 | 5.336806 |
| 142.6 | 91.1 | 5.743611 |
| 147.6 | 86.0 | 5.945 |
| 152.1 | 78.9 | 6.12625 |
| 156.2 | 64.3 | 6.291389 |
| 158.7 | 46.6 | 6.392083 |
| 166.3 | 34.7 | 6.698194 |
| 172.6 | 28.6 | 6.951944 |
| 178.4 | 24.6 | 7.185556 |
| 185.1 | 22.2 | 7.455417 |
| 189.6 | 20.1 | 7.636667 |
| 195.1 | 17.4 | 7.858194 |
| 200.6 | 15.7 | 8.079722 |
| 208.0 | 13.8 | 8.377778 |
| 213.7 | 13.8 | 8.607361 |
| 218.6 | 12.1 | 8.804722 |
| 224.05 | 10.8 | 9.024236 |
| 229.1 | 10.1 | 9.227639 |
| 239.1 | 8.7 | 9.630417 |
| 250.4 | 8.2 | 10.08556 |
| 260.3 | 8.1 | 10.48431 |
| 282.15 | 8.0 | 11.36438 |
| 311.85 | 7.7 | 12.56063 |
| 342.5 | 8.2 | 13.79514 |
| 243.7 | 8.5 | 9.815694 |
| 214.8 | 9.6 | 8.651667 |
| 197.7 | 10.6 | 7.962917 |
| 164.6 | 13.1 | 6.629722 |
| 141.3 | 16.6 | 5.69125 |
| 113.95 | 24.5 | 4.589653 |
| 89.7 | 73.4 | 3.612917 |
| 61.8 | 84.6 | 2.489167 |
| 38.6 | 85.6 | 1.554722 |
| 20.5 | 86.1 | 0.825694 |
| 9.0 | 86.5 | 0.3625 |
| 5.0 | 86.4 | 0.201389 |
| 0.7 | 86.8 | 0.028194 |
| -3.75 | 87 | -0.15104 |

TABLE D3: PB23 UNTREATED SOLTROL-AIR

| CAPILLARY PRESSURE (cm of SOLTROL) | PERCENT SOLTROL SATURATION | P*R/(σ*θ) |
|---|---|---|
| 0.0 | 100.00 | 0.0 |
| 23.4 | 100.00 | 2.513333 |
| 29.2 | 100.00 | 3.136296 |
| 39.6 | 100.00 | 4.253333 |
| 49.35 | 98.00 | 5.300556 |
| 58.3 | 68.00 | 6.261852 |
| 67.45 | 24.00 | 7.24463 |
| 78.2 | 10.00 | 8.399259 |
| 85.3 | 6.00 | 9.161852 |
| 92.9 | 8.00 | 9.978148 |
| 96.6 | 8.00 | 10.37556 |
| 78.0 | 10.00 | 8.377778 |
| 67.95 | 12.00 | 7.298333 |
| 58.1 | 16.00 | 6.24037 |
| 49.5 | 22.00 | 5.316667 |
| 38.75 | 52.00 | 4.162037 |
| 31.7 | 88.00 | 3.404815 |
| 23.0 | 94.00 | 2.47037 |
| 16.0 | 96.00 | 1.718519 |

TABLE D4: PB24 UNTREATED WATER-SOLTROL

| CAPILLARY PRESSURE (cm of H2O) | PERCENT WATER SATURATION | P*R/(σ*θ) |
|---|---|---|
| 0.0 | 100.00 | 0.0 |
| 10.1 | 100.00 | 0.666 |
| 19.0 | 100.00 | 1.252 |
| 25.8 | 100.00 | 1.7 |
| 32.2 | 100.00 | 2.122 |
| 43.6 | 100.00 | 2.874 |
| 51.9 | 97.96 | 3.421 |
| 58.8 | 97.96 | 3.875 |
| 68.0 | 97.96 | 4.482 |
| 77.3 | 97.96 | 5.095 |
| 89.4 | 93.88 | 5.892 |
| 100.4 | 36.73 | 6.617 |
| 112.0 | 24.49 | 7.382 |
| 117.3 | 20.41 | 7.731 |
| 125.9 | 12.24 | 8.298 |
| 136.6 | 8.16 | 9.003 |
| 146.7 | 6.12 | 9.669 |
| 156.7 | 4.08 | 10.33 |
| 167.7 | 4.08 | 11.05 |
| 145.1 | 4.08 | 9.563 |
| 137.0 | 4.08 | 9.03 |
| 125.6 | 6.12 | 8.278 |
| 114.0 | 8.16 | 7.51 |
| 105.0 | 8.16 | 6.92 |
| 95.15 | 10.20 | 6.271 |
| 83.85 | 14.29 | 5.526 |
| 73.3 | 18.37 | 4.831 |
| 63.0 | 28.57 | 4.152 |
| 53.7 | 42.86 | 3.539 |
| 44.9 | 55.10 | 2.959 |
| 35.3 | 69.39 | 2.327 |
| 26.1 | 79.59 | 1.72 |
| 16.8 | 79.59 | 1.107 |
| 8.5 | 81.63 | 0.56 |

TABLE D5: PB25 GC-18-TREATED SOLTROL-AIR

| CAPILLARY PRESSURE (cm SOLTROL) | PERCENT SOLTROL SATURATION | P*R/(σ*θ) |
|---|---|---|
| 0.0 | 100.00 | 0.0 |
| 1.8 | 100.00 | 0.195 |
| 11.4 | 100.00 | 1.232 |
| 21.6 | 100.00 | 2.334 |
| 31.2 | 100.00 | 3.371 |
| 42.0 | 100.00 | 4.539 |
| 52.0 | 100.00 | 5.619 |
| 61.9 | 86.00 | 6.689 |
| 71.5 | 36.00 | 7.726 |
| 76.7 | 20.00 | 8.288 |
| 86.2 | 12.00 | 9.315 |
| 95.3 | 8.00 | 10.3 |
| 106.1 | 6.00 | 11.47 |
| 114.4 | 6.00 | 12.36 |
| 90.6 | 8.00 | 9.847 |
| 80.6 | 8.00 | 8.76 |
| 70.9 | 12.00 | 7.706 |
| 60.3 | 16.00 | 6.554 |
| 50.9 | 32.00 | 5.532 |
| 41.3 | 66.00 | 4.489 |

TABLE D6: PB27 GC-18-TREATED WATER-SOLTROL

| CAPILLARY PRESSURE (cm of H2O) | PERCENT WATER SATURATION | P*R/(σ*θ) |
|---|---|---|
| 0.0 | 100.00 | 0.0 |
| 2.2 | 100.00 | 0.382 |
| 13.0 | 100.00 | 2.258 |
| 23.2 | 100.00 | 4.03 |
| 33.3 | 100.00 | 5.784 |
| 42.9 | 100.00 | 7.451 |
| 54.8 | 100.00 | 9.518 |
| 66.6 | 100.00 | 11.57 |
| 78.5 | 96.08 | 13.63 |
| 90.1 | 96.08 | 15.65 |
| 100.0 | 96.08 | 17.37 |
| 110.8 | 96.08 | 19.25 |
| 121.2 | 86.27 | 21.05 |
| 130.6 | 52.94 | 22.68 |
| 142.4 | 39.22 | 24.73 |
| 151.5 | 35.29 | 26.31 |
| 161.5 | 29.41 | 28.04 |
| 171.3 | 29.41 | 29.75 |
| 179.2 | 33.33 | 13.97 |
| 149.3 | 36.84 | 11.64 |
| 130.2 | 40.35 | 10.15 |
| 112.3 | 43.86 | 8.757 |
| 88.1 | 50.88 | 6.87 |
| 74.2 | 61.40 | 5.786 |
| 66.7 | 78.95 | 5.201 |
| 53.1 | 89.47 | 4.14 |
| 39.0 | 92.98 | 3.041 |

TABLE D7: PB28 GC-18-TREATED WATER-AIR

| CAPILLARY PRESSURE (cm of H2O) | PERCENT WATER SATURATION | P*R/(σ*θ) |
|---|---|---|
| 0.0 | 100.00 | 0.0 |
| 7.3 | 96.43 | 0.967091 |
| 16.3 | 92.86 | 2.159396 |
| 28.2 | 90.48 | 3.735888 |
| 41.8 | 78.57 | 5.537592 |
| 53.8 | 46.43 | 7.127332 |
| 69.25 | 45.24 | 9.174121 |
| 86.2 | 45.24 | 11.41963 |
| 62.9 | 45.24 | 20.78843 |
| 44.0 | 45.24 | 14.54199 |
| 27.8 | 45.24 | 9.187891 |
| 14.7 | 47.62 | 4.858345 |
| 0.8 | 50.00 | 0.2644 |
| -0.8 | 52.38 | -0.2644 |

TABLE D8: PB30 GC-18-TREATED SOLTROL-AIR

| CAPILLARY PRESSURE (cm SOLTROL) | PERCENT SOLTROL SATURATION | P*R/(σ*θ) |
|---|---|---|
| 0.0 | 100.00 | 0.0 |
| 9.1 | 100.00 | 1.207 |
| 42.4 | 97.05 | 5.623 |
| 58.7 | 95.94 | 7.785 |
| 72.5 | 27.70 | 9.615 |
| 93.4 | 7.04 | 12.39 |
| 115.6 | 3.72 | 15.33 |
| 130.3 | 2.61 | 17.28 |
| 114.4 | 1.51 | 15.26 |
| 94.3 | 1.87 | 12.58 |
| 73.2 | 4.83 | 9.764 |
| 52.5 | 15.52 | 7.003 |
| 43.2 | 37.29 | 5.762 |
| 32.4 | 77.50 | 4.322 |
| 11.6 | 83.03 | 1.547 |

TABLE D9: PB35 MTMS-TREATED WATER-SOLTROL

| CAPILLARY PRESSURE (cm of H2O) | PERCENT WATER SATURATION | P*R/(σ*θ) |
|---|---|---|
| 0.0 | 100.00 | 0.0 |
| 3.5 | 100.00 | 0.811827 |
| 14.6 | 94.86 | 3.386477 |
| 33.8 | 84.24 | 7.839926 |
| 52.2 | 66.89 | 12.10781 |
| 73.0 | 33.95 | 16.93238 |
| 97.7 | 25.81 | 22.66156 |
| 116.4 | 20.14 | 26.99904 |
| 136.3 | 16.60 | 31.61485 |
| 155.5 | 6.15 | 36.0683 |
| 176.95 | 4.91 | 41.04364 |
| 146.45 | 4.56 | 67.67977 |
| 126.75 | 3.50 | 58.5757 |
| 106.4 | 3.14 | 49.17124 |
| 86.2 | 3.32 | 39.83609 |
| 67.8 | 3.50 | 31.3328 |
| 53.0 | 4.03 | 24.49319 |
| 37.4 | 4.74 | 17.28387 |
| 15.8 | 10.23 | 7.301744 |
| 3.7 | 11.64 | 1.709902 |

TABLE D10: PB37 MTMS-TREATED SOLTROL-AIR

| CAPILLARY PRESSURE (cm SOLTROL) | PERCENT SOLTROL SATURATION | $P*R/(\sigma*\theta)$ |
|---|---|---|
| 0.0 | 100.00 | 0.0 |
| 12.5 | 97.85 | 1.36 |
| 33.0 | 96.65 | 3.592 |
| 47.0 | 94.76 | 5.115 |
| 60.0 | 79.54 | 6.53 |
| 73.0 | 19.46 | 7.945 |
| 85.0 | 8.54 | 9.251 |
| 102.7 | 3.39 | 11.18 |
| 113.8 | 3.30 | 12.39 |
| 100.4 | 3.13 | 10.96 |
| 83.0 | 2.61 | 9.058 |
| 66.6 | 2.78 | 7.268 |
| 46.7 | 14.22 | 5.096 |
| 29.8 | 77.48 | 3.252 |
| 19.3 | 81.43 | 2.106 |
| 9.4 | 81.69 | 1.026 |
| 0.8 | 82.46 | 0.087 |
| -1.5 | 82.72 | -0.16 |

TABLE D11: PB38 MTMS-TREATED WATER-AIR

| CAPILLARY PRESSURE (cm of H2O) | PERCENT WATER SATURATION | P*R/(σ*θ) |
|---|---|---|
| 0.0 | 100.00 | 0.0 |
| 16.7 | 100.00 | 1.945 |
| 26.1 | 99.46 | 3.039 |
| 36.9 | 93.99 | 4.297 |
| 46.3 | 68.38 | 5.391 |
| 53.9 | 43.31 | 6.276 |
| 63.2 | 27.34 | 7.359 |
| 73.1 | 12.89 | 8.512 |
| 84.8 | 8.28 | 9.875 |
| 93.0 | 6.06 | 10.83 |
| 103.5 | 5.85 | 12.05 |
| 82.9 | 5.63 | 9.653 |
| 62.4 | 5.85 | 7.266 |
| 48.6 | 6.17 | 5.659 |
| 34.8 | 7.58 | 4.052 |
| 20.5 | 10.29 | 2.387 |
| 7.3 | 48.24 | 0.85 |
| 3.9 | 59.56 | 0.454 |
| 1.5 | 66.76 | 0.175 |
| -0.2 | 71.79 | -0.02 |

TABLE D12: PB39 MTMS-TREATED WATER-AIR

| CAPILLARY PRESSURE (cm of H2O) | PERCENT WATER SATURATION | P*R/(σ*Θ) |
|---|---|---|
| 0.0 | 100.00 | 0.0 |
| 15.4 | 95.05 | 2.098 |
| 30.0 | 94.93 | 4.086 |
| 43.2 | 94.86 | 5.884 |
| 56.8 | 94.25 | 7.737 |
| 70.3 | 85.71 | 9.575 |
| 83.2 | 71.60 | 11.33 |
| 91.0 | 58.79 | 12.39 |
| 100.1 | 43.32 | 13.63 |
| 107.1 | 34.10 | 14.59 |
| 118.6 | 24.81 | 16.15 |
| 132.1 | 19.93 | 17.99 |
| 145.2 | 13.18 | 19.78 |
| 160.5 | 12.50 | 21.86 |
| 140.4 | 12.56 | 19.12 |
| 120.0 | 13.30 | 16.34 |
| 102.3 | 13.74 | 13.93 |
| 83.9 | 14.29 | 11.43 |
| 67.4 | 14.54 | 9.18 |
| 49.8 | 14.85 | 6.783 |
| 34.7 | 19.00 | 4.726 |
| 26.1 | 44.62 | 3.555 |
| 18.1 | 73.08 | 2.465 |
| 5.1 | 78.34 | 0.695 |
| 0.1 | 79.46 | 0.014 |
| -2.5 | 81.56 | -0.34 |

TABLE D13: MW14 UNTREATED WATER-SOLTROL

| CAPILLARY PRESSURE (cm of H2O) | PERCENT WATER SATURATION | $P*R/(\sigma*\theta)$ |
|---|---|---|
| 0.00 | 100 | 0 |
| 16.22 | 91.2 | 5.642272 |
| 18.95 | 67.6 | 6.591927 |
| 21.69 | 31.5 | 7.545061 |
| 35.48 | 7.6 | 12.34204 |
| 47.65 | 7.5 | 16.57548 |
| 52.00 | 7.4 | 18.08867 |
| 26.43 | 7.6 | 11.91788 |
| 17.21 | 8.5 | 7.760377 |
| 16.29 | 20.7 | 7.345528 |
| 14.00 | 29.5 | 6.312916 |
| 11.88 | 49.3 | 5.35696 |
| 9.41 | 69.8 | 4.243181 |
| 6.36 | 77.8 | 2.867867 |
| 3.23 | 81.5 | 1.45648 |
| -4 | 82 | -1.80369 |

TABLE D14: HAINES (UNTREATED) WATER-AIR

| SCALED CAPILLARY PRESSURE | PERCENT WATER SATURATION |
|---|---|
| 0 | 100 |
| 4.2 | 98 |
| 6.1 | 94.5 |
| 7.4 | 30 |
| 10.2 | 10 |
| 11.2 | 8 |
| 7.3 | 16 |
| 4.9 | 33.5 |
| 3.2 | 87 |
| 0 | 88 |

Note: These are selected points from Haines (1930). Since these results were not tabulated, the values above are estimated from Figure 6 with a ruler. In some cases the values are substantiated within the text. The imbibition values appear to be the important ones, but are not the only ones shown on that figure.

This thesis is accepted on behalf of the faculty of the Institute by the following committee:

Adviser

5/4/93

Date